Available online at www.sciencedirect.com
ScienceDirect
Chemical Geology 247 (2008) 352–383
CHEMICAL GEOLOGY INCLUDING ISOTOPE GEOSCIENCE
www.elsevier.com/locate/chemgeo

# Zircon U–Pb and Hf isotopic study of gneissic rocks from the Chinese Altai: Progressive accretionary history in the early to middle Palaeozoic

Min Sun [a,*], Chao Yuan [b], Wenjiao Xiao [c], Xiaoping Long [a,b], Xiaoping Xia [a], Guochun Zhao [a], Shoufa Lin [d], Fuyuan Wu [c], A. Kröner [e]

[a] *Department of Earth Sciences, The University of Hong Kong, Pokfulam Road, Hong Kong, China*
[b] *Key Laboratory of Isotope Geochronology and Geochemistry, Guangzhou Institute of Geochemistry, Chinese Academy of Sciences, Guangzhou 510640, China*
[c] *State Key Laboratory of Lithospheric Evolution, Institute of Geology and Geophysics, Chinese Academy of Sciences, Beijing 100029, China*
[d] *Department of Earth Sciences, University of Waterloo, Waterloo, Ontario, Canada N2L 3G1*
[e] *Department of Geosciences, University of Mainz, 55099 Mainz, Germany*

Received 15 June 2007; received in revised form 14 October 2007; accepted 28 October 2007

Editor: S.L. Goldstein

**Abstract**

Gneissic rocks in the Chinese Altai Mountains have been interpreted as either Paleozoic metasedimentary rocks or Precambrian basement. This study reports geochemical and geochronological data for banded paragneisses and associated gneissic granitoids collected along a NE–SW traverse in the northwestern Chinese Altai. Petrological and geochemical data suggest that the protoliths of the banded gneisses were possibly immature sediments with significant volcanic input and that the gneissic granitoids were derived from I-type granites formed in a subduction environment. Three types of morphological features can be recognized in zircons from the banded gneisses and are interpreted to correlate with different sources. Zircons from five samples of banded paragneiss cluster predominantly between 466 and 528 Ma, some give Neoproterozoic ages, and a few yield discordant Paleoproterozoic to Archean ages. Zircon Hf isotopic compositions indicate that both juvenile/mantle and crust materials were involved in the generation of the source rocks from which these zircons were derived. In contrast, zircons occur ubiquitously as elongated euhedral prismatic crystals in the four samples of the gneissic granitoids, and define single populations for each sample with mean ages between 380 and 453 Ma. The general absence of Precambrian inheritance and positive zircon $\varepsilon$Hf values for these granitoids suggest insignificant crustal contribution to the generation of the precursor magmas. Our data can be interpreted in terms of a progressive accretionary history in early to middle Palaeozoic times, and the Chinese Altai may possibly represent a magmatic arc built on a continental margin dominated by Neoproterozoic rocks.


*Keywords:* U–Pb age; Hf isotope; Gneiss; Zircon; Altaids

## 1. Introduction

The Central Asian Orogenic Belt (CAOB or Altaids or Altaid collage) is the largest Phanerozoic orogenic

* Corresponding author. Tel.: +852 28592194 or 62746604; fax: +852 25176912.
*E-mail address:* minsun@hku.hk (M. Sun).

0009-2541/$ - see front matter © 2007 Elsevier B.V. All rights reserved.
doi:10.1016/j.chemgeo.2007.10.026

belt in the world, extending from the Urals in the west to the Pacific in the east and from Siberia in the north to the Tianshan in the south (Zonenshain et al., 1990; Mossakovsky et al., 1993; Şengör et al., 1993; Jahn et al., 2000a,b; Şengör and Natl'in, 2004; Windley et al., 2007). About 5.3 million km$^2$ of crustal materials were added to Asia along this belt, now found as fragments of island arcs, ophiolites, accretionary prisms, seamounts, and micro-continents, which were distributed in the Paleo-Asian Ocean, a long-lived ocean existed for 800 Ma from the late Mesoproerotoic to the Mesozoic (Khain et al., 2002; 2003; Windley et al., 2007; Kröner et al., in press, and references cited therein). In addition, voluminous granitoids from juvenile sources were emplaced in this region (Jahn, 2004 and references therein). Thus, this belt provides an excellent opportunity to study an accretionary orogen formed by continuous, long-lived subduction. However, unraveling the tectonic evolution of the CAOB is difficult because of the allochthonous nature of many terranes and their complicated amalgamation history. The tectonic settings of these terranes are controversial, thus leading to several competing models. For example, Şengör et al. (1993) proposed a single arc chain model that reconstructed the entire CAOB by oroclinally bending of the single Kipchak–Tuva–Mongol arc. In contrast, Didenko et al. (1994) and Mossakovsky et al. (1993) viewed the CAOB as a mosaic of exotic, and mostly unrelated arc terranes and microcontinents, a scenario similar to the present-day SW Pacific archipelago, which is in the process of becoming amalgamated to form an extensive new orogenic belt.

The Chinese Altai lies in the southern part of the CAOB and contains blocks of ophiolites, volcanic rocks, high-grade metamorphic rocks, and sedimentary sequences (Fig. 1). This varied assemblage makes the Chinese Altai not only an excellent natural laboratory in which to test the different models outlined above, but

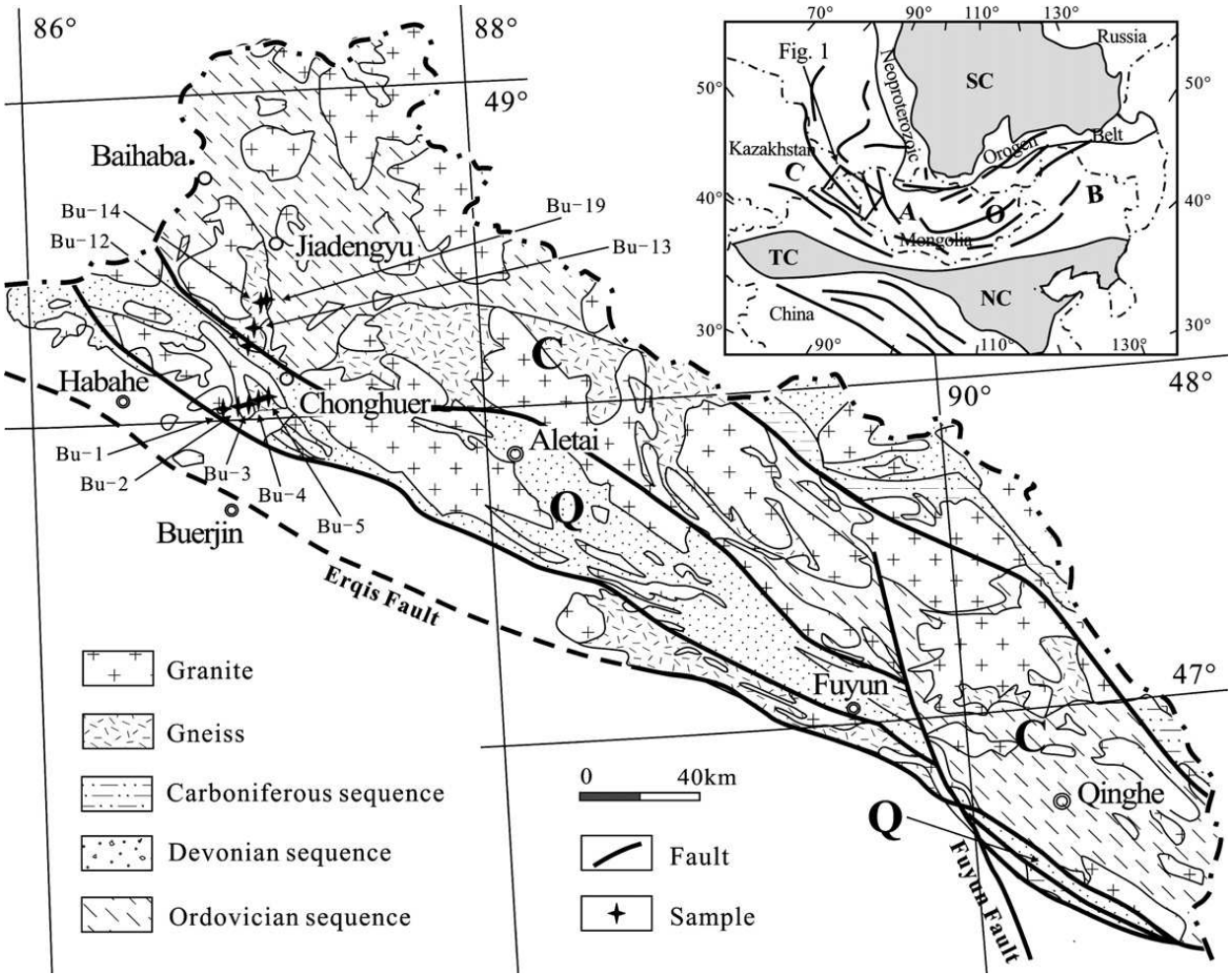


Fig. 1. Simplified geologic map of the Chinese Altai (He et al., 1990; Li et al., 1996; Windley et al., 2002). C — Central Domain, Q — Qiongkuer Domain. Inset figure shows the extension of the CAOB. The Chinese Atlai is represented by a box. SC — Siberia Craton, TC — Tarim Craton, NC — North China Craton.

also to study accretionary orogenic processes in general. Although the tectonic subdivision of the Chinese Altai is reasonably well understood (He et al., 1990; Windley et al., 2002), precise geochronological data are rare and firm tectonic constraints have not been provided. Consequently, the tectonic setting of the Chinese Altai has long been controversial, being variously envisaged as an island arc (Şengör and Natal'in, 1996), a passive continental margin (He et al., 1990), or a Precambrian micro-continent (e.g. Li et al., 2006). The high-grade metamorphic rocks within this region are a key element in understanding the tectonic history of the Chinese Altai. These rocks were previously considered to be the metamorphic equivalents of early Paleozoic sedimentary rocks (Habahe Group), but were re-assigned in the early 1990s as the Paleo-to Meso-proterozoic Kemuqi and Neoproterozoic Fuyun Groups (e.g. Li et al., 1996; Chen et al., 2003), and thus were interpreted to represent the Proterozoic basement of the Chinese Altai (e.g. He et al., 1990, 1994; Windley et al., 2002) or a Precambrian microcontinent (Li et al., 2006).

The Precambrian ages for these high-grade metamorphic rocks are based on Sm–Nd whole rock isotopic data (Hu et al., 2001, 2002; Wang et al., 2002), and Nd model ages (e.g. Hu et al., 2000), as well as on xenocrystic zircon dates for associated granitoids (e.g. Windley et al., 2002). Thus, it is imperative to obtain more reliable geochronological data for the high-grade metamorphic rocks in order to test the controversial tectonic models and to correctly understand the accretionary history of this part of the CAOB. This paper reports zircon U–Pb and Hf isotopic data for banded gneisses and gneissic granitoids collected along a NE–SW traverse in the northwestern part of the Chinese Altai. These results shed light on the evolutionary history of the Chinese Altai.

## 2. Geological background

The Chinese Altai, in northernmost Xinjiang Province, is situated between the south Siberian Sanyan block to the north and the Junggar block to the south. Based on recent geological investigations the region has been divided into six NW–SE trending terranes (e.g. Windley et al., 2002; Xiao et al., 2004). This study focuses on two adjacent tectonic domains, namely the Central Altai and Qiongkuer Domains (Fig. 1). *The Central Altai Domain* (Terranes 2 and 3 of Windley et al., 2002) contains low-grade quartzose-feldspathic clastic turbidites and pyroclastic rocks of the Habahe Group (He et al., 1990; Li et al., 2006). These rocks are isoclinally folded with steep axial planes and metamorphosed to low greenschist-facies schist and phyllite (Windley et al., 2002). This group was originally assigned to the middle to late Ordovician, but recent workers favor a Sinian (Vendian) to middle Ordovician age (e.g. BGMRX, 1993; Chen and Jahn, 2002; Windley et al., 2002; Li et al., 2006), and consider it to be a passive continental margin deposit (e.g. He et al., 1990; Li and Poliyangsiji, 2001; Li et al., 2006). However, new data do not support this interpretation since whole-rock geochemical data indicate formation in an active continental margin and detrital zircons from this group have dominant U–Pb ages between 460 and 570 Ma (Long et al., 2006; 2007). *The Qiongkuer Domain* (Terrane 4 of Windley et al., 2002) consists of late Silurian to early Devonian island arc-type volcanic and pyroclastic rocks (Kangbutiebao Formation) and the overlying middle Devonian turbiditic sandstone-shale sequence (Altai Formation) that is considered to be a fore-arc basin deposit (Windley et al., 2002). These two terranes are separated by nearly vertical, NE-dipping fault zones composed of highly deformed rocks with inverted metamorphic gradients (Windley et al., 2002).

High-grade gneissic rocks crop out extensively in these two terranes (Fig. 1) and are currently assigned to the Kemuqi and Fuyun Groups (Chen et al., 2003). The former group consists of coarse-and fine-grained gneiss, migmatite, amphibolite and mica schist, whereas the latter is composed of amphibolite, hornblende gneiss and sericite schist (Li et al., 1996). Their presumed Precambrian age is widely accepted by many workers (e.g. Chen et al., 2003) and led to the proposal of an Altai-Mongolia Precambrian microcontinent (Li et al., 2006). However, the above interpretation is not supported by SHRIMP zircon U–Pb data for high-grade metamorphic rocks from the southeastern part of the Chinese Altai (281±3 Ma and 279±6 Ma for Qinghe gneiss and Fuyun granulite, respectively; Chen et al., 2006; Hu et al., 2006). In order to firmly constrain the nature and age of the high-grade metamorphic rocks, banded gneisses and associated gneissic granitoids were collected from the Buerjin–Hanasi traverse for this study (Fig. 1).

## 3. Sample description

The rocks in the study area include intensely deformed, banded gneisses, gneissic granitoids and mylonites. Samples used in this study were collected near the road between Buerjin and Jiadengyu. The banded gneisses are generally dark-grey in color, variably migmatized and their prominent leucosomes form folded banding (Fig. 2a and b). The leucosomes


Fig. 2. Field photos of banded paragneisses (a and b) and gneissic granitoids (c and d) in the Chinese Altai.

were avoided during sampling. The banded gneisses are made of coarse to medium-grained quartz, plagioclase, K-feldspar, and biotite. Minor minerals are mainly sillimanite, garnet, tourmaline and zircon (Table 1). The mineral compositions of the gneisses suggest that their protoliths were either feldspathic sandstones or highly deformed granitoids.

The gneissic granitoids also have well-developed foliations, but can be distinguished from the banded gneisses by their more massive structure, uniform mineralogical compositions and occasionally preserved intrusive relationships (Fig. 2c and d). The gneissic granitoids have light grey color, and are mainly composed of coarse to medium-grained quartz, Na-rich plagioclase, K-feldspar, biotite and muscovite (Table 1). Granitic texture is apparent in some thin sections, and the plagioclase phenocrysts may be surrounded by oriented, recrystallized, fine-grained quartz. A fine-gained mylonite sample (Bu-2, Table 1) has granitic compositions and anhedral recrystallized quartz is locally stretched by deformation. Plagioclase laths show simple or polysynthetic twinning and K-feldspar typically possesses Carlsbad twinning. The mylonite is in sharp contact with the surrounding coarse-grained gneiss, and its fabric is concordant with that of the gneiss (Strike N40°W, Dip 68°NE).

## 4. Analytical methods

### 4.1. Major and trace element analysis

Major oxides were determined by wavelength-dispersive X-ray fluorescence spectrometry (XRF) on fused glass beads using a Philips PW2400 spectrometer at the University of Hong Kong. Matrix correction followed the procedure of Norrish and Hutton (1969), and G2 and G3 (granites) were used as reference materials. The accuracies of the XRF analyses are estimated to be ca.1% (relative) for $SiO_2$, ca. 2% (relative) for other major oxides present in concentrations greater than 0.5 wt.% and ca. 5% (relative) for MnO and $P_2O_5$. The trace elements, including REE, were determined by inductively coupled plasma mass spectrometry (ICP–MS) of nebulized solutions using a VG Plasma-Quad Excell ICP–MS at

Table 1
General description of banded gneiss and gneissic granitoid in the Chinese Altai

| Banded gneisses | BU-4 | BU-5 | BU-13 | BU-14 | BU-19 |
|---|---|---|---|---|---|
| Rock name | Coarse grained gneiss | Medium-grained gneiss | Coarse grained gneiss | Coarse grained gneiss | Coarse grained schist |
| GPS coordinates | 48° 03′ 12.3″ N<br>87° 00′ 02.1″ E | 48° 03′ 13.5″ N<br>87° 00′ 04.0″ E | 48° 16′ 11.4″ N<br>87° 03′ 58.0″ E | 48° 19′ 14.8″ N<br>87° 06′41.0″ E | 48° 21′ 21.1″ N<br>87° 08′13.4″ E |
| Color and Structure | Dark-grey | Dark-grey, with light reddish bands n the weathered surface | Dark-grey, slightly migmatized, quartz shows undulatory extinction | Dark-grey, alternating quartz-feldspar and biotite-amphibole bands | Dark-grey, with minor folded leucosome veins and augen structure |
| Major minerals (modal %) | | | | | |
| Quartz | 30 | 30 | 50 | 40 | 45 |
| plagioclase | 25 | 35 | 20 | 30 | 30 |
| K-feldspar | 15 | 15 | 10 | 18 | 10 |
| Minor minerals | Sillimanite, garnet, tourmaline, zircon | Sillimanite parallel to the foliation | Sillimanite and tourmaline | Blue–green amphibole | Biotite and muscovite |

| Gneissic granitoids: | BU-1 | BU-2 | BU-3 | BU-12 |
|---|---|---|---|---|
| Rock name | Coarse grained leucogranite | Fine-grained mylonite | Medium-grained granite | Coarse grained granodiorite |
| GPS coordinates | 48° 02′ 02.3″ N;<br>86° 52′51.8″ E | 48° 02′ 27.2″ N;<br>86° 57′36.4″ E | 48° 02′ 58.9″ N;<br>86° 58′10.4″ E | 48° 13′ 33.9″ N;<br>87° 01′28.0″ E |
| Major minerals (modal %) | | | | |
| Quartz | 35 | 50 | 40 | 30 |
| plagioclase | 50 | 25 | 45 | 40 |
| K-feldspar | 10 | 10 | 12 | 15 |
| Minor phases | Biotite and muscovite | Biotite, garnet | Biotite | biotite |

the University of Hong Kong after a 2-day closed beaker digestion using a mixture of HF and $HNO_3$ acids in high-pressure "bombs" (Qi and Gregoire, 2000). Two multi-element solutions were prepared for external calibration, with one containing Li, Be, V, Cr, Co, Ni, Cu, Zn, Ga, Rb, Sr, Cs, Ba, Pb, Th, U, Sc, Y and fourteen REEs and the other containing W, Mo, Nb, Ta, Zr, and Hf, respectively. G2 and G3 (granites) were used as reference materials. The accuracies of the ICP–MS analyses are estimated to be better than ca.5% (relative) for most elements. Geochemical data are presented in Table 2.

### 4.2. Zircon separation and CL imaging

After sample crushing, zircons were separated by standard heavy liquid and magnetic techniques. Zircon grains from the>25 μm non-magnetic fractions were hand-picked and mounted on adhesive tape, then enclosed in epoxy resin and polished to about half of their thickness. After being photographed under reflected and transmitted light, the samples were prepared for Cath-odoluminescence (CL) imaging, U–Pb dating and Hf isotope analysis.

In order to investigate the origin and structure of zircons and to choose target sites for U–Pb and Hf isotopic analyses, CL imaging was carried out using a JXA-8100 Electron Probe Microanalyzer with a Mono CL3 Cathodoluminescence System for high resolution imaging and spectroscopy at the Guangzhou Institute of Geochemistry, Chinese Academy of Sciences.

### 4.3. U–Pb zircon geochronology

The U–Pb isotopic composition of zircon was analyzed on a VG PQ Excel IC-PMS equipped with New Wave Research UV213 laser ablation system, installed in the Department of Earth Sciences, the University of Hong Kong. The laser system delivers a beam of 213 nm UV light from a frequency-quintupled Nd:YAG laser. Most analyses were carried out with a beam diameter of 40 μm, 10 Hz repetition rate, and energy of 0.6–1.3 mJ per pulse. This gave a $^{238}U$ signal of $3\times10^4$ to $200\times10^4$ counts per second, depending on U contents. Typical ablation time was 30–60 s, resulting in pits 20–40 μm deep. The instrumental settings and detailed analytical procedures were described by Xia et al. (2004). U–Pb ages of zircons were calculated using the U decay constants of $^{238}U=1.55125\times10^{-10}$ year$^{-1}$, $^{235}U=9.8454\times10^{-10}$ year$^{-1}$ and the Isoplot 3 software (Ludwig, 2003). Individual analyses are presented with $1\sigma$ errors in Table 3 and in concordia diagrams, and uncertainties in age results are quoted at the 95% level

Table 2
Geochemical composition of banded gneiss and gneissic granitoid in the Chinese Altai

| Sample | Banded gneiss | | | | | Gneissic granitoid | | | |
|---|---|---|---|---|---|---|---|---|---|
| | BU-4 | BU-5 | BU-13 | BU-14 | BU-19 | BU-1 | BU-2 | BU-3 | BU-12 |
| $SiO_2$ | 64.5 | 63.5 | 75.7 | 71.1 | 77.3 | 72.6 | 81.6 | 73.9 | 69.8 |
| $TiO_2$ | 0.71 | 0.73 | 0.54 | 0.63 | 0.37 | 0.31 | 0.14 | 0.36 | 0.48 |
| $Al_2O_3$ | 15.8 | 16.1 | 10.9 | 13.1 | 9.59 | 13.9 | 10.0 | 13.8 | 14.1 |
| $\sum Fe_2O_3$ | 6.62 | 7.02 | 4.61 | 5.14 | 2.88 | 3.37 | 1.77 | 2.05 | 3.94 |
| MnO | 0.14 | 0.11 | 0.06 | 0.06 | 0.05 | 0.13 | 0.06 | 0.09 | 0.07 |
| MgO | 3.87 | 4.04 | 2.40 | 2.53 | 1.39 | 1.28 | 0.56 | 0.53 | 1.05 |
| CaO | 2.41 | 1.81 | 1.25 | 1.34 | 3.27 | 0.59 | 0.49 | 2.02 | 2.81 |
| $Na_2O$ | 2.16 | 2.43 | 1.92 | 2.15 | 1.46 | 5.15 | 4.08 | 4.40 | 3.26 |
| $K_2O$ | 2.55 | 2.81 | 1.67 | 2.32 | 0.98 | 0.97 | 0.28 | 1.84 | 2.62 |
| $P_2O_5$ | 0.23 | 0.18 | 0.14 | 0.16 | 0.26 | 0.05 | 0.01 | 0.09 | 0.13 |
| LOI | 0.96 | 0.94 | 0.73 | 0.95 | 1.21 | 1.33 | 0.92 | 0.62 | 1.64 |
| TOTAL | 99.9 | 99.7 | 99.9 | 99.5 | 98.7 | 99.7 | 99.9 | 99.7 | 99.9 |
| Sc | 15.1 | 15.6 | 12.2 | 13.1 | 7.81 | 15.7 | 6.92 | 8.63 | 11.7 |
| V | 93.0 | 108 | 71.5 | 79.6 | 51.1 | 10.8 | 7.94 | 11.7 | 40.3 |
| Cr | 136 | 142 | 127 | 150 | 77.6 | 4.87 | 15.4 | 6.39 | 23.4 |
| Co | 17.6 | 18.4 | 13.0 | 13.9 | 7.50 | 3.40 | 1.97 | 2.09 | 6.23 |
| Ni | 89.5 | 94.5 | 62.1 | 74.2 | 33.5 | 9.34 | 12.0 | 7.83 | 18.0 |
| Ga | 17.7 | 18.7 | 12.7 | 15.1 | 11.4 | 12.7 | 6.92 | 15.0 | 16.3 |
| Rb | 104 | 108 | 70.6 | 93.2 | 51.0 | 28.3 | 5.18 | 80.8 | 105 |
| Sr | 209 | 187 | 169 | 193 | 172 | 157 | 107 | 141 | 141 |
| Ba | 447 | 330 | 232 | 306 | 127 | 109 | 15.5 | 506 | 400 |
| Y | 40.7 | 36.9 | 25.2 | 29.8 | 27.2 | 68.7 | 47.4 | 39.1 | 45.7 |
| Nb | 9.67 | 8.32 | 6.92 | 8.91 | 6.69 | 4.17 | 4.23 | 13.8 | 9.56 |
| Ta | 1.12 | 0.74 | 0.56 | 0.89 | 0.57 | 0.29 | 0.33 | 0.60 | 0.71 |
| Zr | 121 | 125 | 150 | 164 | 132 | 156 | 162 | 218 | 227 |
| Hf | 3.93 | 4.15 | 4.62 | 5.11 | 4.08 | 5.46 | 5.67 | 7.09 | 6.52 |
| Pb | 23.1 | 18.2 | 16.9 | 19.6 | 16.1 | 7.44 | 7.60 | 13.5 | 15.9 |
| Th | 8.96 | 9.24 | 9.76 | 11.3 | 10.3 | 4.37 | 3.33 | 12.9 | 14.0 |
| U | 4.47 | 2.54 | 2.49 | 3.45 | 2.93 | 1.37 | 1.30 | 1.08 | 1.24 |
| La | 25.5 | 23.0 | 26.7 | 29.7 | 19.9 | 10.4 | 6.9 | 30.0 | 38.3 |
| Ce | 55.6 | 49.5 | 58.2 | 64.5 | 47.3 | 36.2 | 21.9 | 65.9 | 92.5 |
| Pr | 6.27 | 5.82 | 6.62 | 7.51 | 4.74 | 4.33 | 3.17 | 7.93 | 10.2 |
| Nd | 25.7 | 23.5 | 26.9 | 28.3 | 20.0 | 22.4 | 19.1 | 32.8 | 41.6 |
| Sm | 5.39 | 5.10 | 5.24 | 5.74 | 4.23 | 6.75 | 5.16 | 7.07 | 8.44 |
| Eu | 1.07 | 1.15 | 1.04 | 1.09 | 0.71 | 1.27 | 0.70 | 1.37 | 1.38 |
| Gd | 5.35 | 5.01 | 5.23 | 5.70 | 4.17 | 7.64 | 4.57 | 6.87 | 8.53 |
| Tb | 0.74 | 0.71 | 0.62 | 0.70 | 0.59 | 1.34 | 0.76 | 0.89 | 1.08 |
| Dy | 5.34 | 5.14 | 4.15 | 4.74 | 4.24 | 10.3 | 6.45 | 6.09 | 7.13 |
| Ho | 1.14 | 1.03 | 0.76 | 0.90 | 0.80 | 2.13 | 1.40 | 1.12 | 1.35 |
| Er | 3.61 | 3.34 | 2.40 | 2.84 | 2.49 | 6.46 | 4.66 | 3.25 | 4.00 |
| Tm | 0.76 | 0.68 | 0.44 | 0.55 | 0.50 | 1.33 | 0.99 | 0.57 | 0.75 |
| Yb | 3.91 | 3.33 | 2.27 | 2.71 | 2.43 | 6.70 | 5.39 | 2.78 | 3.67 |
| Lu | 0.59 | 0.51 | 0.33 | 0.39 | 0.37 | 1.04 | 0.80 | 0.42 | 0.53 |
| Mg# | 53.7 | 53.5 | 50.9 | 49.4 | 49.0 | 43.0 | 38.4 | 34.0 | 34.6 |
| A/NK | 2.49 | 2.29 | 2.19 | 2.15 | 2.77 | 1.46 | 1.42 | 1.50 | 1.72 |
| A/CNK | 1.47 | 1.56 | 1.50 | 1.54 | 1.02 | 1.32 | 1.26 | 1.07 | 1.06 |
| DF | −3 | −3 | −5 | −3 | −4 | 1 | −1 | 2 | 1 |
| ∑REE | 140 | 127 | 140 | 155 | 112 | 116 | 80.5 | 166 | 218 |
| (La/Yb)N | 4.40 | 4.67 | 7.95 | 7.41 | 5.52 | 1.05 | 0.87 | 7.27 | 7.05 |
| Eu/Eu* | 0.61 | 0.69 | 0.60 | 0.58 | 0.51 | 0.54 | 0.44 | 0.60 | 0.50 |
| Sr/Y | 5.13 | 5.05 | 6.72 | 6.48 | 6.34 | 2.28 | 2.26 | 3.60 | 3.08 |
| Nb/Zr | 0.08 | 0.07 | 0.05 | 0.05 | 0.05 | 0.03 | 0.03 | 0.06 | 0.04 |
| Th/U | 2.00 | 3.63 | 3.92 | 3.28 | 3.50 | 3.20 | 2.57 | 12.0 | 11.2 |

(continued on next page)

Table 2 (*continued*)

| Sample | Banded gneiss | | | | | Gneissic granitoid | | | |
|---|---|---|---|---|---|---|---|---|---|
| | BU-4 | BU-5 | BU-13 | BU-14 | BU-19 | BU-1 | BU-2 | BU-3 | BU-12 |
| Rb/Sr | 0.50 | 0.58 | 0.42 | 0.48 | 0.30 | 0.18 | 0.05 | 0.57 | 0.75 |
| Zr/Sc | 7.99 | 7.97 | 12.2 | 12.5 | 16.9 | 9.90 | 23.5 | 25.2 | 19.5 |
| Th/Sc | 0.59 | 0.59 | 0.80 | 0.87 | 1.31 | 0.28 | 0.48 | 1.50 | 1.20 |

Note: LOI: weight loss between 120 and 900 °C; A/NK = molar ratio of $Al_2O_3/(Na_2O+K_2O)$; A/CNK = molar ratio of $Al_2O_3/(CaO+Na_2O+K_2O)$; *df* = 0.55 CaO + 1.46$Na_2O$ + 0.54 $K_2O$ − 0.21$SiO_2$ − 0.32∑$Fe_2O_3$ − 0.98 MgO + 10.44.

(2$\sigma$). In this study, $^{207}Pb/^{206}Pb$ ages are used for zircons older than 1000 Ma, but $^{206}Pb/^{238}U$ ages are used for zircons younger than 1000 Ma, because the relative small amount of $^{207}Pb$ accumulated in young zircons does not permit precise $^{207}Pb/^{206}Pb$ dating (Black et al., 2003).

### 4.4. Hf isotope analysis

Hf isotope analyses were carried out using an ArF excimer laser ablation system, attached to a Neptune Plasma multi-collector ICP–MS, at the Institute of Geology and Geophysics, Chinese Academy of Science in Beijing. The analyses for zircons from paragneiss were conducted with a beam diameter of 32 μm, 8 Hz repetition rate, and energy of 15 mJ/cm$^2$, whereas a beam diameter of 63 μm and 6 Hz repetition rate were used for gneissic granitoids. All of the settings yielded a signal intensity of ~10 V at $^{180}Hf$ for the standard zircon 91500. Typical ablation time was 26 s, resulting in pits 20–30 μm deep. Masses 172, 173, 175–180 and 182 were simultaneously measured in static-collection mode. Data were normalized to $^{176}Hf/^{177}Hf = 0.7325$, using exponential correction for mass bias. Due to the extremely low $^{176}Lu/^{177}Hf$ ratio in zircon (normally <0.002), the isobaric interference of $^{176}Lu$ on $^{176}Hf$ is negligible (Iizuka and Hirata, 2005). The mean $\beta_{Yb}$ value was applied for the isobaric interference correction of $^{176}Yb$ on $^{176}Hf$ in the same spot. The ratio of $^{176}Yb/^{172}Yb$ (0.5887) was also applied for the Yb correction. Detailed instrumental settings and analytical procedures were described by Wu et al. (2006). In order to evaluate the reliability of the analytical data, standard zircon 91500 was analyzed during the course of this study and a weighted mean $^{176}Hf/^{177}Hf$ ratio of 0.282306±25 (2$\sigma$) was yielded, which is the same as a weighted mean $^{176}Hf/^{177}Hf$ ratio of 0.282306±10 (2$\sigma$) by solution analysis of Woodhead et al. (2004). More reference zircons were analyzed in the same laboratory by Wu et al. (2006), giving results of 0.282680±31 (2SD) for TEMORA, 0.281729±21 (2SD) for CZ3, 282177±17 (2SD) for CN92-1, 0.282983±17 (2SD) for FM0411 and 0.281234±11 (2SD) for Phalaborwa.

The measured $^{176}Lu/^{177}Hf$ ratios and the $^{176}Lu$ decay constant of $1.865\times10^{-11}$ yr$^{-1}$ reported by Scherer et al. (2001) were used to calculate initial $^{176}Hf/^{177}Hf$ ratios. The chondritic values of $^{176}Hf/^{177}Hf = 0.0332$ and $^{176}Lu/^{177}Hf = 0.282772$ reported by Blichert-Toft and Albarede (1997) were used for the calculation of $\varepsilon$Hf values. The depleted mantle Hf model ages ($T_{DM}$) were calculated using the measured $^{176}Lu/^{177}Hf$ ratios of zircon based on an assumption that the depleted mantle reservoir has a linear isotopic growth from $^{176}Hf/^{177}Hf = 0.279718$ at 4.55 Ga to 0.283250 at present, with $^{176}Lu/^{177}Hf = 0.0384$ (Griffin et al., 2000). However this $T_{DM}$ model age can only give a minimum age for the source material of the magma from which the zircon crystallized because the fractionation between Lu and Hf has taken place when zircons formed. In order to circumvent such a problem, Hf model age $T^C_{DM}$ was calculated, which is derived from projecting the initial $^{176}Hf/^{177}Hf$ of a zircon (after determination of its U/Pb age) back to the depleted mantle model growth line by using a $^{176}Lu/^{177}Hf$ ratio of 0.008, the mean value for upper continental crust (Rudnick and Gao, 2004). The upper continental crust Lu/Hf ratio, other than the average ratio of the whole continent ($^{176}Lu/^{177}Hf = 0.015$; e.g. Griffin et al., 2004) or mafic crust ($^{176}Lu/^{177}Hf = 0.019$), is adopted here because the residence time of mafic crust is usually short and especially since Archean granitoids appear to be derived by partial melting of young subducted oceanic crust (Martin 1986). The discussion in this study is based on $T^C_{DM}$ model ages.

## 5. Geochemical results

The Chemical Index of Alteration [CIA = $Al_2O_3/(Al_2O_3+CaO^*+Na_2O+K_2O)\times100$, molar ratio] and Index of Compositional Variability [ICV = $(Fe_2O_3+K_2O+Na_2O+CaO+MgO+TiO_2)/Al_2O_3$, molar ratio] have been frequently used to study the weathering

Table 3
U–Pb isotopic data for zircons from banded gneiss and gneissic granitoid in the Chinese Altai

| Grain no. | Contents | | Ratios | | | | | | | Ages (Ma) | | | | | | Disc. (%) |
|---|---|---|---|---|---|---|---|---|---|---|---|---|---|---|---|---|
| | Th | U | Th/U | $Pb^{207}/Pb^{206}$ | 1σ | $Pb^{207}/U^{235}$ | 1σ | $Pb^{206}/U^{238}$ | 1σ | $Pb^{207}/Pb^{206}$ | 1σ | $Pb^{207}/U^{235}$ | 1σ | $Pb^{206}/U^{238}$ | 1σ | |
| *Banded gneiss BU-4* | | | | | | | | | | | | | | | | |
| 1 | 56 | 156 | 0.36 | 0.06109 | 0.00156 | 0.64912 | 0.01574 | 0.07707 | 0.00150 | 642 | 54 | 508 | 10 | 479 | 9 | 29 |
| 2 | 218 | 280 | 0.78 | 0.05943 | 0.00154 | 0.63345 | 0.01564 | 0.07731 | 0.00152 | 583 | 55 | 498 | 10 | 480 | 9 | 19 |
| 3 | 149 | 551 | 0.27 | 0.06024 | 0.00152 | 0.64204 | 0.01564 | 0.07734 | 0.00154 | 612 | 54 | 504 | 10 | 480 | 9 | 24 |
| 4 | 72 | 135 | 0.54 | 0.06071 | 0.00210 | 0.66439 | 0.02236 | 0.07942 | 0.00170 | 629 | 73 | 517 | 14 | 493 | 10 | 24 |
| 5 | 145 | 388 | 0.37 | 0.06303 | 0.00172 | 0.68982 | 0.01816 | 0.07942 | 0.00160 | 709 | 57 | 533 | 11 | 493 | 10 | 36 |
| 6 | 98 | 141 | 0.70 | 0.05643 | 0.00148 | 0.61817 | 0.01562 | 0.07948 | 0.00158 | 469 | 57 | 489 | 10 | 493 | 9 | −5 |
| 7 | 86 | 132 | 0.65 | 0.05994 | 0.00214 | 0.65854 | 0.02284 | 0.07973 | 0.00170 | 601 | 75 | 514 | 14 | 495 | 10 | 20 |
| 8 | 65 | 104 | 0.62 | 0.06149 | 0.00160 | 0.67609 | 0.01666 | 0.07973 | 0.00156 | 656 | 55 | 524 | 10 | 495 | 9 | 28 |
| 9 | 20 | 209 | 0.10 | 0.05971 | 0.00246 | 0.65638 | 0.02616 | 0.07975 | 0.00176 | 593 | 87 | 512 | 16 | 495 | 10 | 18 |
| 10 | 59 | 114 | 0.52 | 0.05872 | 0.00162 | 0.65263 | 0.01734 | 0.08064 | 0.00162 | 557 | 59 | 510 | 11 | 500 | 10 | 11 |
| 11 | 13 | 138 | 0.10 | 0.05865 | 0.00166 | 0.65242 | 0.01786 | 0.08072 | 0.00162 | 554 | 61 | 510 | 11 | 500 | 10 | 10 |
| 12 | 48 | 155 | 0.31 | 0.05768 | 0.00190 | 0.64318 | 0.02046 | 0.08091 | 0.00168 | 518 | 71 | 504 | 13 | 502 | 10 | 3 |
| 13 | 22 | 105 | 0.21 | 0.05778 | 0.00210 | 0.64741 | 0.02260 | 0.08126 | 0.00170 | 521 | 78 | 507 | 14 | 504 | 10 | 3 |
| 14 | 56 | 94 | 0.60 | 0.05988 | 0.00184 | 0.67428 | 0.02010 | 0.08172 | 0.00168 | 599 | 65 | 523 | 12 | 506 | 10 | 17 |
| 15 | 105 | 188 | 0.56 | 0.05908 | 0.00164 | 0.66851 | 0.01798 | 0.08211 | 0.00166 | 570 | 59 | 520 | 11 | 509 | 10 | 11 |
| 16 | 241 | 698 | 0.34 | 0.06023 | 0.00140 | 0.69025 | 0.01500 | 0.08309 | 0.00158 | 612 | 49 | 533 | 9 | 515 | 9 | 17 |
| 17 | 57 | 43 | 1.31 | 0.05902 | 0.00182 | 0.67746 | 0.02002 | 0.08327 | 0.00168 | 568 | 66 | 525 | 12 | 516 | 10 | 10 |
| 18 | 60 | 72 | 0.83 | 0.05871 | 0.00186 | 0.67514 | 0.02052 | 0.08340 | 0.00170 | 556 | 68 | 524 | 12 | 516 | 10 | 7 |
| 19 | 5 | 50 | 0.09 | 0.05935 | 0.00200 | 0.68694 | 0.02224 | 0.08395 | 0.00174 | 580 | 72 | 531 | 13 | 520 | 10 | 11 |
| 20 | 137 | 262 | 0.52 | 0.05748 | 0.00140 | 0.66827 | 0.01536 | 0.08434 | 0.00164 | 510 | 53 | 520 | 9 | 522 | 10 | −2 |
| 21 | 37 | 49 | 0.75 | 0.06067 | 0.00190 | 0.70698 | 0.02118 | 0.08454 | 0.00172 | 628 | 66 | 543 | 13 | 523 | 10 | 18 |
| 22 | 85 | 127 | 0.67 | 0.05861 | 0.00184 | 0.68781 | 0.02104 | 0.08516 | 0.00178 | 553 | 67 | 531 | 13 | 527 | 11 | 5 |
| 23 | 275 | 732 | 0.38 | 0.05992 | 0.00162 | 0.70866 | 0.01836 | 0.08580 | 0.00170 | 601 | 57 | 544 | 11 | 531 | 10 | 12 |
| 24 | 491 | 287 | 1.71 | 0.05916 | 0.00152 | 0.70293 | 0.01750 | 0.08621 | 0.00172 | 573 | 55 | 541 | 10 | 533 | 10 | 7 |
| 25 | 47 | 50 | 0.94 | 0.05968 | 0.00184 | 0.75845 | 0.02266 | 0.09222 | 0.00190 | 592 | 65 | 573 | 13 | 569 | 11 | 4 |
| 26 | 213 | 422 | 0.50 | 0.05994 | 0.00150 | 0.76530 | 0.01844 | 0.09265 | 0.00184 | 601 | 53 | 577 | 11 | 571 | 11 | 5 |
| 27 | 91 | 1121 | 0.08 | 0.05870 | 0.00140 | 0.75425 | 0.01714 | 0.09322 | 0.00182 | 556 | 51 | 571 | 10 | 575 | 11 | −3 |
| 28 | 27 | 241 | 0.11 | 0.06276 | 0.00196 | 0.81661 | 0.02436 | 0.09439 | 0.00192 | 700 | 65 | 606 | 14 | 581 | 11 | 19 |
| 29 | 34 | 82 | 0.41 | 0.06244 | 0.00218 | 0.89588 | 0.03004 | 0.10402 | 0.00218 | 689 | 73 | 650 | 16 | 638 | 13 | 8 |
| 30 | 16 | 106 | 0.15 | 0.06601 | 0.00192 | 1.10939 | 0.03122 | 0.12194 | 0.00248 | 807 | 60 | 758 | 15 | 742 | 14 | 8 |
| 31 | 290 | 881 | 0.33 | 0.06898 | 0.00152 | 1.25502 | 0.02590 | 0.13191 | 0.00250 | 898 | 45 | 826 | 12 | 799 | 14 | 12 |
| 32 | 66 | 241 | 0.27 | 0.07112 | 0.00198 | 1.50669 | 0.04082 | 0.15375 | 0.00314 | 961 | 56 | 933 | 16 | 922 | 18 | 4 |
| 33 | 131 | 370 | 0.35 | 0.07616 | 0.00218 | 1.80484 | 0.05022 | 0.17197 | 0.00356 | 1099 | 56 | 1047 | 18 | 1023 | 20 | 7 |
| 34 | 35 | 36 | 0.99 | 0.12254 | 0.00306 | 6.05008 | 0.14552 | 0.35822 | 0.00718 | 1994 | 44 | 1983 | 21 | 1974 | 34 | 1 |
| 35 | 150 | 299 | 0.50 | 0.16583 | 0.00366 | 8.76234 | 0.18154 | 0.38308 | 0.00732 | 2516 | 37 | 2314 | 19 | 2091 | 34 | 18 |
| *Banded gneiss BU-5* | | | | | | | | | | | | | | | | |
| 1 | 49 | 216 | 0.23 | 0.05794 | 0.00158 | 0.61651 | 0.01662 | 0.07722 | 0.00158 | 527 | 59 | 488 | 10 | 480 | 9 | 10 |
| 2 | 206 | 335 | 0.61 | 0.06113 | 0.00152 | 0.67186 | 0.01602 | 0.07980 | 0.00156 | 644 | 53 | 522 | 10 | 495 | 9 | 26 |
| 3 | 31 | 89 | 0.35 | 0.05828 | 0.00176 | 0.64963 | 0.01894 | 0.08091 | 0.00166 | 540 | 65 | 508 | 12 | 502 | 10 | 7 |
| 4 | 119 | 217 | 0.55 | 0.05765 | 0.00172 | 0.65760 | 0.01902 | 0.08281 | 0.00170 | 516 | 64 | 513 | 12 | 513 | 10 | 1 |
| 5 | 104 | 396 | 0.26 | 0.05726 | 0.00168 | 0.65405 | 0.01854 | 0.08293 | 0.00166 | 502 | 63 | 511 | 11 | 514 | 10 | −2 |
| 6 | 155 | 208 | 0.74 | 0.05758 | 0.00160 | 0.65760 | 0.01722 | 0.08294 | 0.00162 | 514 | 60 | 513 | 10 | 514 | 10 | 0 |
| 7 | 89 | 225 | 0.40 | 0.05848 | 0.00158 | 0.66957 | 0.01792 | 0.08310 | 0.00170 | 548 | 58 | 520 | 11 | 515 | 10 | 6 |
| 8 | 121 | 203 | 0.59 | 0.05846 | 0.00162 | 0.67576 | 0.01836 | 0.08390 | 0.00172 | 547 | 59 | 524 | 11 | 519 | 10 | 5 |
| 9 | 318 | 686 | 0.46 | 0.06682 | 0.00180 | 0.77397 | 0.02112 | 0.08404 | 0.00178 | 832 | 55 | 582 | 12 | 520 | 11 | 46 |
| 10 | 6 | 291 | 0.02 | 0.05795 | 0.00142 | 0.67261 | 0.01554 | 0.08428 | 0.00162 | 528 | 53 | 522 | 9 | 522 | 10 | 1 |
| 11 | 102 | 274 | 0.37 | 0.06561 | 0.00242 | 0.76674 | 0.02850 | 0.08477 | 0.00196 | 794 | 76 | 578 | 16 | 525 | 12 | 41 |
| 12 | 269 | 1016 | 0.26 | 0.06496 | 0.00182 | 0.75937 | 0.02158 | 0.08481 | 0.00182 | 773 | 58 | 574 | 12 | 525 | 11 | 38 |
| 13 | 227 | 510 | 0.44 | 0.05917 | 0.00166 | 0.69959 | 0.02008 | 0.08577 | 0.00184 | 573 | 60 | 539 | 12 | 530 | 11 | 8 |
| 14 | 77 | 103 | 0.75 | 0.06327 | 0.00226 | 0.75146 | 0.02574 | 0.08625 | 0.00180 | 717 | 74 | 569 | 15 | 533 | 11 | 29 |
| 15 | 441 | 822 | 0.54 | 0.06237 | 0.00168 | 0.74271 | 0.02042 | 0.08639 | 0.00182 | 687 | 56 | 564 | 12 | 534 | 11 | 25 |
| 16 | 288 | 590 | 0.49 | 0.06099 | 0.00182 | 0.73250 | 0.02328 | 0.08711 | 0.00198 | 639 | 63 | 558 | 14 | 538 | 12 | 17 |
| 17 | 75 | 141 | 0.54 | 0.06187 | 0.00198 | 0.82009 | 0.02722 | 0.09615 | 0.00216 | 670 | 67 | 608 | 15 | 592 | 13 | 12 |

(continued on next page)

Table 3 (*continued*)

| Grain no. | Contents | | Ratios | | | | | | | Ages (Ma) | | | | | | Disc. (%) |
|---|---|---|---|---|---|---|---|---|---|---|---|---|---|---|---|---|
| | Th | U | Th/U | $Pb^{207}/Pb^{206}$ | 1σ | $Pb^{207}/U^{235}$ | 1σ | $Pb^{206}/U^{238}$ | 1σ | $Pb^{207}/Pb^{206}$ | 1σ | $Pb^{207}/U^{235}$ | 1σ | $Pb^{206}/U^{238}$ | 1σ | |
| *Banded gneiss BU-5* | | | | | | | | | | | | | | | | |
| 18 | 94 | 569 | 0.17 | 0.06006 | 0.00206 | 0.82168 | 0.03196 | 0.09921 | 0.00248 | 606 | 73 | 609 | 18 | 610 | 15 | −1 |
| 19 | 363 | 1042 | 0.35 | 0.06047 | 0.00172 | 0.83651 | 0.02482 | 0.10034 | 0.00220 | 620 | 60 | 617 | 14 | 616 | 13 | 1 |
| 20 | 740 | 1259 | 0.59 | 0.06361 | 0.00208 | 0.89018 | 0.03236 | 0.10149 | 0.00246 | 729 | 68 | 646 | 17 | 623 | 14 | 16 |
| 21 | 268 | 1222 | 0.22 | 0.06320 | 0.00198 | 0.93624 | 0.03198 | 0.10743 | 0.00252 | 715 | 65 | 671 | 17 | 658 | 15 | 8 |
| 22 | 40 | 127 | 0.31 | 0.06245 | 0.00212 | 0.93752 | 0.03098 | 0.10897 | 0.00232 | 690 | 71 | 672 | 16 | 667 | 13 | 3 |
| 23 | 107 | 303 | 0.35 | 0.06354 | 0.00198 | 0.95984 | 0.03174 | 0.10955 | 0.00252 | 726 | 65 | 683 | 16 | 670 | 15 | 8 |
| 24 | 53 | 145 | 0.37 | 0.06533 | 0.00208 | 1.00472 | 0.03278 | 0.11156 | 0.00250 | 785 | 65 | 706 | 16 | 682 | 14 | 14 |
| 25 | 90 | 109 | 0.82 | 0.06708 | 0.00212 | 1.09220 | 0.03526 | 0.11812 | 0.00262 | 840 | 64 | 750 | 17 | 720 | 15 | 15 |
| 26 | 47 | 86 | 0.55 | 0.06517 | 0.00180 | 1.08389 | 0.02858 | 0.12077 | 0.00240 | 780 | 57 | 746 | 14 | 735 | 14 | 6 |
| 27 | 134 | 727 | 0.18 | 0.06567 | 0.00204 | 1.11362 | 0.03730 | 0.12298 | 0.00286 | 796 | 64 | 760 | 18 | 748 | 16 | 6 |
| 28 | 12 | 36 | 0.34 | 0.06723 | 0.00222 | 1.20326 | 0.03900 | 0.12990 | 0.00278 | 845 | 67 | 802 | 18 | 787 | 16 | 7 |
| 29 | 35 | 64 | 0.55 | 0.06901 | 0.00220 | 1.38397 | 0.04260 | 0.14559 | 0.00304 | 899 | 64 | 882 | 18 | 876 | 17 | 3 |
| 30 | 257 | 473 | 0.54 | 0.12637 | 0.00426 | 5.85888 | 0.22124 | 0.33621 | 0.00834 | 2048 | 58 | 1955 | 32 | 1868 | 40 | 9 |
| 31 | 112 | 693 | 0.16 | 0.13458 | 0.00426 | 7.74017 | 0.26930 | 0.41709 | 0.00992 | 2159 | 54 | 2201 | 31 | 2247 | 45 | −4 |
| *Banded gneiss BU-13* | | | | | | | | | | | | | | | | |
| 1 | 25 | 69 | 0.37 | 0.05678 | 0.00238 | 0.55697 | 0.02060 | 0.07159 | 0.00138 | 483 | 90 | 450 | 13 | 446 | 8 | 8 |
| 2 | 15 | 149 | 0.10 | 0.05763 | 0.00146 | 0.57589 | 0.01386 | 0.07242 | 0.00140 | 516 | 55 | 462 | 9 | 451 | 8 | 13 |
| 3 | 95 | 194 | 0.49 | 0.05880 | 0.00198 | 0.59471 | 0.01796 | 0.07350 | 0.00138 | 560 | 72 | 474 | 11 | 457 | 8 | 20 |
| 4 | 24 | 46 | 0.52 | 0.05952 | 0.00232 | 0.61228 | 0.02156 | 0.07485 | 0.00146 | 586 | 82 | 485 | 13 | 465 | 9 | 23 |
| 5 | 12 | 52 | 0.23 | 0.05603 | 0.00320 | 0.57785 | 0.03104 | 0.07503 | 0.00168 | 454 | 122 | 463 | 20 | 466 | 10 | −3 |
| 6 | 31 | 99 | 0.32 | 0.05877 | 0.00252 | 0.60695 | 0.02280 | 0.07538 | 0.00146 | 559 | 91 | 482 | 14 | 468 | 9 | 18 |
| 7 | 89 | 177 | 0.50 | 0.06029 | 0.00228 | 0.62553 | 0.02074 | 0.07562 | 0.00142 | 614 | 80 | 493 | 13 | 470 | 9 | 27 |
| 8 | 6 | 21 | 0.31 | 0.06506 | 0.00310 | 0.67928 | 0.02944 | 0.07612 | 0.00158 | 776 | 97 | 526 | 18 | 473 | 9 | 49 |
| 9 | 48 | 109 | 0.44 | 0.05897 | 0.00242 | 0.61782 | 0.02270 | 0.07631 | 0.00148 | 566 | 87 | 488 | 14 | 474 | 9 | 18 |
| 10 | 86 | 245 | 0.35 | 0.05706 | 0.00190 | 0.60119 | 0.01918 | 0.07639 | 0.00156 | 494 | 72 | 478 | 12 | 475 | 9 | 4 |
| 11 | 26 | 49 | 0.54 | 0.05993 | 0.00232 | 0.63274 | 0.02214 | 0.07680 | 0.00148 | 601 | 82 | 498 | 14 | 477 | 9 | 23 |
| 12 | 19 | 43 | 0.44 | 0.06155 | 0.00266 | 0.65633 | 0.02590 | 0.07762 | 0.00156 | 659 | 90 | 512 | 16 | 482 | 9 | 31 |
| 13 | 216 | 293 | 0.74 | 0.05817 | 0.00130 | 0.64539 | 0.01360 | 0.08041 | 0.00154 | 536 | 48 | 506 | 8 | 499 | 9 | 7 |
| 14 | 90 | 202 | 0.45 | 0.05742 | 0.00206 | 0.64178 | 0.02086 | 0.08126 | 0.00154 | 508 | 77 | 503 | 13 | 504 | 9 | 1 |
| 15 | 93 | 85 | 1.10 | 0.06551 | 0.00324 | 0.73973 | 0.03492 | 0.08183 | 0.00186 | 791 | 100 | 562 | 20 | 507 | 11 | 44 |
| 16 | 33 | 49 | 0.68 | 0.06177 | 0.00224 | 0.71072 | 0.02364 | 0.08357 | 0.00162 | 666 | 76 | 545 | 14 | 517 | 10 | 25 |
| 17 | 119 | 331 | 0.36 | 0.05781 | 0.00134 | 0.66648 | 0.01484 | 0.08358 | 0.00162 | 523 | 50 | 519 | 9 | 517 | 10 | 1 |
| 18 | 69 | 93 | 0.74 | 0.06062 | 0.00224 | 0.69937 | 0.02354 | 0.08381 | 0.00162 | 626 | 78 | 538 | 14 | 519 | 10 | 19 |
| 19 | 87 | 500 | 0.17 | 0.05929 | 0.00142 | 0.76069 | 0.01678 | 0.09298 | 0.00174 | 578 | 51 | 574 | 10 | 573 | 10 | 1 |
| 20 | 159 | 931 | 0.17 | 0.06216 | 0.00154 | 0.81507 | 0.01904 | 0.09502 | 0.00182 | 680 | 52 | 605 | 11 | 585 | 11 | 15 |
| 21 | 14 | 20 | 0.70 | 0.06807 | 0.00304 | 1.06487 | 0.04378 | 0.11375 | 0.00236 | 871 | 90 | 736 | 21 | 694 | 14 | 23 |
| 22 | 19 | 40 | 0.48 | 0.06928 | 0.00206 | 1.09874 | 0.03036 | 0.11495 | 0.00222 | 907 | 60 | 753 | 15 | 701 | 13 | 26 |
| 23 | 39 | 54 | 0.72 | 0.06852 | 0.00224 | 1.11410 | 0.03340 | 0.11795 | 0.00228 | 884 | 66 | 760 | 16 | 719 | 13 | 21 |
| 24 | 15 | 63 | 0.24 | 0.06823 | 0.00212 | 1.12092 | 0.03180 | 0.11923 | 0.00226 | 876 | 63 | 763 | 15 | 726 | 13 | 19 |
| 25 | 10 | 58 | 0.17 | 0.07087 | 0.00264 | 1.27541 | 0.04164 | 0.13114 | 0.00248 | 954 | 74 | 835 | 18 | 794 | 14 | 18 |
| 26 | 3 | 22 | 0.11 | 0.06839 | 0.00302 | 1.25462 | 0.05284 | 0.13295 | 0.00298 | 880 | 89 | 825 | 24 | 805 | 17 | 9 |
| 27 | 173 | 255 | 0.68 | 0.07353 | 0.00178 | 1.62196 | 0.03658 | 0.15986 | 0.00300 | 1029 | 48 | 979 | 14 | 956 | 17 | 7 |
| 28 | 25 | 65 | 0.38 | 0.09769 | 0.00290 | 2.92428 | 0.08162 | 0.21691 | 0.00440 | 1580 | 55 | 1388 | 21 | 1266 | 23 | 22 |
| 29 | 31 | 91 | 0.33 | 0.11907 | 0.00366 | 4.00898 | 0.11326 | 0.24417 | 0.00482 | 1942 | 54 | 1636 | 23 | 1408 | 25 | 32 |
| 30 | 13 | 15 | 0.87 | 0.15012 | 0.00644 | 5.63089 | 0.21284 | 0.27353 | 0.00588 | 2347 | 72 | 1921 | 32 | 1559 | 30 | 40 |
| 31 | 5 | 35 | 0.15 | 0.17709 | 0.00494 | 10.78572 | 0.26970 | 0.44199 | 0.00824 | 2626 | 46 | 2505 | 23 | 2360 | 37 | 11 |
| *Banded gneiss BU-14* | | | | | | | | | | | | | | | | |
| 1 | 70 | 460 | 0.15 | 0.05866 | 0.00254 | 0.55200 | 0.02002 | 0.06833 | 0.00138 | 555 | 92 | 446 | 13 | 426 | 8 | 26 |
| 2 | 121 | 790 | 0.15 | 0.05815 | 0.00250 | 0.54911 | 0.01966 | 0.06857 | 0.00138 | 535 | 91 | 444 | 13 | 428 | 8 | 22 |
| 3 | 11 | 625 | 0.02 | 0.06092 | 0.00188 | 0.58596 | 0.01718 | 0.06977 | 0.00140 | 636 | 65 | 468 | 11 | 435 | 8 | 38 |
| 4 | 259 | 1336 | 0.19 | 0.06284 | 0.00234 | 0.60790 | 0.01962 | 0.07022 | 0.00138 | 703 | 77 | 482 | 12 | 437 | 8 | 47 |
| 5 | 128 | 571 | 0.22 | 0.06161 | 0.00228 | 0.59948 | 0.01994 | 0.07062 | 0.00142 | 661 | 77 | 477 | 13 | 440 | 9 | 40 |

Table 3 (*continued*)

| Grain no. | Contents | | Ratios | | | | | | | Ages (Ma) | | | | | | Disc. (%) |
|---|---|---|---|---|---|---|---|---|---|---|---|---|---|---|---|---|
| | Th | U | Th/U | $Pb^{207}/Pb^{206}$ | 1σ | $Pb^{207}/U^{235}$ | 1σ | $Pb^{206}/U^{238}$ | 1σ | $Pb^{207}/Pb^{206}$ | 1σ | $Pb^{207}/U^{235}$ | 1σ | $Pb^{206}/U^{238}$ | 1σ | |
| *Banded gneiss BU-14* | | | | | | | | | | | | | | | | |
| 6 | 139 | 244 | 0.57 | 0.06113 | 0.00246 | 0.60434 | 0.02178 | 0.07176 | 0.00146 | 644 | 84 | 480 | 14 | 447 | 9 | 36 |
| 7 | 341 | 1289 | 0.26 | 0.06572 | 0.00270 | 0.65229 | 0.02254 | 0.07207 | 0.00144 | 797 | 84 | 510 | 14 | 449 | 9 | 56 |
| 8 | 199 | 459 | 0.43 | 0.05754 | 0.00210 | 0.57949 | 0.01970 | 0.07308 | 0.00150 | 512 | 78 | 464 | 13 | 455 | 9 | 12 |
| 9 | 134 | 261 | 0.51 | 0.05984 | 0.00212 | 0.60533 | 0.01928 | 0.07341 | 0.00146 | 598 | 75 | 481 | 12 | 457 | 9 | 27 |
| 10 | 562 | 1049 | 0.54 | 0.05530 | 0.00174 | 0.55968 | 0.01630 | 0.07344 | 0.00144 | 424 | 69 | 451 | 11 | 457 | 9 | −7 |
| 11 | 247 | 1246 | 0.20 | 0.05733 | 0.00216 | 0.58213 | 0.01928 | 0.07370 | 0.00146 | 504 | 81 | 466 | 12 | 458 | 9 | 10 |
| 12 | 210 | 657 | 0.32 | 0.05909 | 0.00216 | 0.60071 | 0.01918 | 0.07379 | 0.00146 | 570 | 78 | 478 | 12 | 459 | 9 | 22 |
| 13 | 98 | 434 | 0.23 | 0.06062 | 0.00266 | 0.61814 | 0.02358 | 0.07403 | 0.00152 | 626 | 92 | 489 | 15 | 460 | 9 | 30 |
| 14 | 71 | 533 | 0.13 | 0.05677 | 0.00210 | 0.58513 | 0.02046 | 0.07478 | 0.00156 | 483 | 80 | 468 | 13 | 465 | 9 | 4 |
| 15 | 518 | 1121 | 0.46 | 0.06446 | 0.00254 | 0.67041 | 0.02256 | 0.07550 | 0.00150 | 757 | 81 | 521 | 14 | 469 | 9 | 47 |
| 16 | 573 | 693 | 0.83 | 0.06621 | 0.00278 | 0.69580 | 0.02492 | 0.07630 | 0.00154 | 813 | 85 | 536 | 15 | 474 | 9 | 53 |
| 17 | 55 | 139 | 0.39 | 0.05947 | 0.00210 | 0.62881 | 0.02072 | 0.07672 | 0.00156 | 584 | 75 | 495 | 13 | 477 | 9 | 20 |
| 18 | 79 | 153 | 0.51 | 0.05807 | 0.00262 | 0.61954 | 0.02468 | 0.07745 | 0.00162 | 532 | 96 | 490 | 15 | 481 | 10 | 10 |
| 19 | 365 | 716 | 0.51 | 0.06006 | 0.00188 | 0.64425 | 0.01878 | 0.07783 | 0.00154 | 606 | 66 | 505 | 12 | 483 | 9 | 23 |
| 20 | 57 | 1206 | 0.05 | 0.05552 | 0.00164 | 0.60684 | 0.01676 | 0.07930 | 0.00156 | 433 | 64 | 482 | 11 | 492 | 9 | −13 |
| 21 | 136 | 295 | 0.46 | 0.05777 | 0.00168 | 0.64373 | 0.01804 | 0.08083 | 0.00164 | 521 | 63 | 505 | 11 | 501 | 10 | 4 |
| 22 | 247 | 481 | 0.51 | 0.05908 | 0.00228 | 0.66835 | 0.02320 | 0.08211 | 0.00166 | 570 | 82 | 520 | 14 | 509 | 10 | 11 |
| 23 | 60 | 200 | 0.30 | 0.06175 | 0.00278 | 0.71535 | 0.02752 | 0.08411 | 0.00174 | 665 | 94 | 548 | 16 | 521 | 10 | 24 |
| 24 | 235 | 654 | 0.36 | 0.05931 | 0.00166 | 0.69202 | 0.01844 | 0.08464 | 0.00168 | 578 | 60 | 534 | 11 | 524 | 10 | 10 |
| 25 | 146 | 292 | 0.50 | 0.06367 | 0.00190 | 0.91607 | 0.02578 | 0.10438 | 0.00210 | 731 | 62 | 660 | 14 | 640 | 12 | 13 |
| 26 | 70 | 191 | 0.36 | 0.06688 | 0.00242 | 1.10698 | 0.03556 | 0.12014 | 0.00238 | 834 | 74 | 757 | 17 | 731 | 14 | 13 |
| 27 | 75 | 167 | 0.45 | 0.06650 | 0.00206 | 1.12207 | 0.03222 | 0.12243 | 0.00244 | 822 | 63 | 764 | 15 | 745 | 14 | 10 |
| 28 | 76 | 340 | 0.22 | 0.07091 | 0.00272 | 1.23325 | 0.04080 | 0.12626 | 0.00250 | 955 | 77 | 816 | 18 | 766 | 14 | 22 |
| 29 | 20 | 57 | 0.34 | 0.06720 | 0.00382 | 1.18013 | 0.06246 | 0.12749 | 0.00316 | 844 | 114 | 791 | 29 | 774 | 18 | 9 |
| 30 | 213 | 535 | 0.40 | 0.07126 | 0.00212 | 1.33412 | 0.03648 | 0.13584 | 0.00266 | 965 | 60 | 861 | 16 | 821 | 15 | 16 |
| 31 | 264 | 1231 | 0.21 | 0.06735 | 0.00202 | 1.33085 | 0.03684 | 0.14338 | 0.00282 | 849 | 61 | 859 | 16 | 864 | 16 | −2 |
| 32 | 140 | 499 | 0.28 | 0.07129 | 0.00194 | 1.48527 | 0.03826 | 0.15113 | 0.00300 | 966 | 55 | 924 | 16 | 907 | 17 | 6 |
| 33 | 42 | 140 | 0.30 | 0.17806 | 0.00710 | 7.81979 | 0.26564 | 0.31884 | 0.00646 | 2635 | 65 | 2210 | 30 | 1784 | 31 | 39 |
| 34 | 701 | 2203 | 0.32 | 0.11563 | 0.00374 | 5.15090 | 0.14834 | 0.32331 | 0.00628 | 1890 | 57 | 1845 | 24 | 1806 | 31 | 5 |
| 35 | 161 | 422 | 0.38 | 0.16154 | 0.00498 | 9.39939 | 0.27598 | 0.42213 | 0.00912 | 2472 | 51 | 2378 | 27 | 2270 | 41 | 9 |
| *Banded gneiss BU-19* | | | | | | | | | | | | | | | | |
| 1 | 125 | 350 | 0.36 | 0.05879 | 0.00172 | 0.62229 | 0.01890 | 0.07685 | 0.00174 | 559 | 63 | 491 | 12 | 477 | 10 | 16 |
| 2 | 569 | 930 | 0.61 | 0.05568 | 0.00126 | 0.59697 | 0.01324 | 0.07776 | 0.00154 | 440 | 50 | 475 | 8 | 483 | 9 | -9 |
| 3 | 149 | 461 | 0.32 | 0.05792 | 0.00134 | 0.64205 | 0.01484 | 0.08041 | 0.00164 | 527 | 50 | 504 | 9 | 499 | 10 | 5 |
| 4 | 191 | 538 | 0.35 | 0.06165 | 0.00146 | 0.68918 | 0.01658 | 0.08111 | 0.00170 | 662 | 50 | 532 | 10 | 503 | 10 | 27 |
| 5 | 375 | 1119 | 0.34 | 0.05930 | 0.00128 | 0.66832 | 0.01398 | 0.08174 | 0.00160 | 578 | 46 | 520 | 8 | 507 | 10 | 13 |
| 6 | 502 | 751 | 0.67 | 0.05992 | 0.00134 | 0.68176 | 0.01526 | 0.08253 | 0.00168 | 601 | 48 | 528 | 9 | 511 | 10 | 16 |
| 7 | 367 | 665 | 0.55 | 0.05923 | 0.00132 | 0.68368 | 0.01510 | 0.08373 | 0.00168 | 576 | 48 | 529 | 9 | 518 | 10 | 10 |
| 8 | 154 | 239 | 0.64 | 0.05897 | 0.00156 | 0.69117 | 0.01884 | 0.08506 | 0.00186 | 566 | 57 | 534 | 11 | 526 | 11 | 7 |
| 9 | 257 | 573 | 0.45 | 0.05850 | 0.00126 | 0.68734 | 0.01450 | 0.08523 | 0.00168 | 549 | 46 | 531 | 9 | 527 | 10 | 4 |
| 10 | 385 | 985 | 0.39 | 0.06247 | 0.00156 | 0.73994 | 0.01978 | 0.08601 | 0.00194 | 690 | 52 | 562 | 11 | 532 | 12 | 26 |
| 11 | 450 | 605 | 0.74 | 0.05786 | 0.00140 | 0.68683 | 0.01748 | 0.08617 | 0.00190 | 524 | 52 | 531 | 10 | 533 | 11 | −2 |
| 12 | 291 | 758 | 0.38 | 0.05639 | 0.00138 | 0.67613 | 0.01788 | 0.08707 | 0.00196 | 468 | 53 | 524 | 11 | 538 | 12 | −14 |
| 13 | 95 | 344 | 0.27 | 0.06131 | 0.00180 | 0.74908 | 0.02182 | 0.08865 | 0.00192 | 650 | 62 | 568 | 13 | 548 | 11 | 17 |
| 14 | 1419 | 791 | 1.79 | 0.05747 | 0.00140 | 0.70554 | 0.01818 | 0.08912 | 0.00196 | 510 | 53 | 542 | 11 | 550 | 12 | −8 |
| 15 | 104 | 161 | 0.64 | 0.06348 | 0.00270 | 0.78473 | 0.03272 | 0.08968 | 0.00212 | 724 | 88 | 588 | 18 | 554 | 13 | 27 |
| 16 | 155 | 295 | 0.52 | 0.06069 | 0.00170 | 0.77411 | 0.02128 | 0.09251 | 0.00192 | 628 | 59 | 582 | 12 | 570 | 11 | 10 |
| 17 | 183 | 541 | 0.34 | 0.05736 | 0.00144 | 0.74427 | 0.02022 | 0.09424 | 0.00216 | 505 | 54 | 565 | 12 | 581 | 13 | −14 |
| 18 | 512 | 1199 | 0.43 | 0.05802 | 0.00138 | 0.76798 | 0.01912 | 0.09608 | 0.00210 | 531 | 51 | 579 | 11 | 591 | 12 | −11 |
| 19 | 685 | 743 | 0.92 | 0.05868 | 0.00144 | 0.78491 | 0.02036 | 0.09711 | 0.00216 | 555 | 53 | 588 | 12 | 597 | 13 | −7 |
| 20 | 93 | 456 | 0.20 | 0.06533 | 0.00148 | 1.07867 | 0.02392 | 0.11976 | 0.00240 | 785 | 47 | 743 | 12 | 729 | 14 | 7 |
| 21 | 323 | 726 | 0.44 | 0.06557 | 0.00144 | 1.14372 | 0.02542 | 0.12654 | 0.00262 | 793 | 45 | 774 | 12 | 768 | 15 | 3 |
| 22 | 188 | 156 | 1.20 | 0.06980 | 0.00168 | 1.21925 | 0.02918 | 0.12671 | 0.00262 | 922 | 49 | 809 | 13 | 769 | 15 | 18 |
| 23 | 1125 | 2468 | 0.46 | 0.06434 | 0.00150 | 1.17424 | 0.02808 | 0.13242 | 0.00280 | 753 | 48 | 789 | 13 | 802 | 16 | −6 |

*(continued on next page)*

Table 3 (*continued*)

| Grain no. | Contents | | Ratios | | | | | | | Ages (Ma) | | | | | | Disc. (%) |
|---|---|---|---|---|---|---|---|---|---|---|---|---|---|---|---|---|
| | Th | U | Th/U | $Pb^{207}/Pb^{206}$ | 1σ | $Pb^{207}/U^{235}$ | 1σ | $Pb^{206}/U^{238}$ | 1σ | $Pb^{207}/Pb^{206}$ | 1σ | $Pb^{207}/U^{235}$ | 1σ | $Pb^{206}/U^{238}$ | 1σ | |
| *Banded gneiss BU-19* | | | | | | | | | | | | | | | | |
| 24 | 235 | 637 | 0.37 | 0.06954 | 0.00150 | 1.47128 | 0.03150 | 0.15347 | 0.00310 | 915 | 44 | 919 | 13 | 920 | 17 | −1 |
| 25 | 231 | 536 | 0.43 | 0.06943 | 0.00180 | 1.49429 | 0.04210 | 0.15631 | 0.00362 | 912 | 52 | 928 | 17 | 936 | 20 | −3 |
| *Gneissic granitoid BU-1* | | | | | | | | | | | | | | | | |
| 1 | 220 | 353 | 0.62 | 0.05929 | 0.00142 | 0.52484 | 0.01252 | 0.06420 | 0.00130 | 578 | 51 | 428 | 8 | 401 | 8 | 36 |
| 2 | 398 | 474 | 0.84 | 0.06250 | 0.00132 | 0.55488 | 0.01436 | 0.06439 | 0.00164 | 691 | 44 | 448 | 9 | 402 | 10 | 53 |
| 3 | 141 | 255 | 0.55 | 0.06033 | 0.00164 | 0.53482 | 0.01734 | 0.06429 | 0.00156 | 616 | 58 | 435 | 11 | 402 | 9 | 42 |
| 4 | 315 | 446 | 0.71 | 0.05769 | 0.00176 | 0.51427 | 0.02706 | 0.06465 | 0.00226 | 518 | 66 | 421 | 18 | 404 | 14 | 25 |
| 5 | 120 | 215 | 0.56 | 0.05815 | 0.00166 | 0.52065 | 0.01464 | 0.06494 | 0.00134 | 535 | 61 | 426 | 10 | 406 | 8 | 28 |
| 6 | 703 | 594 | 1.18 | 0.06261 | 0.00134 | 0.56398 | 0.01222 | 0.06533 | 0.00136 | 695 | 45 | 454 | 8 | 408 | 8 | 52 |
| 7 | 178 | 289 | 0.62 | 0.05595 | 0.00214 | 0.51078 | 0.02702 | 0.06621 | 0.00196 | 450 | 83 | 419 | 18 | 413 | 12 | 9 |
| 8 | 610 | 567 | 1.08 | 0.06281 | 0.00158 | 0.57438 | 0.01420 | 0.06632 | 0.00136 | 702 | 53 | 461 | 9 | 414 | 8 | 52 |
| 9 | 192 | 331 | 0.58 | 0.05752 | 0.00190 | 0.52780 | 0.05008 | 0.06655 | 0.00400 | 512 | 71 | 430 | 33 | 415 | 24 | 21 |
| 10 | 209 | 491 | 0.43 | 0.05622 | 0.00150 | 0.52289 | 0.01322 | 0.06745 | 0.00134 | 461 | 58 | 427 | 9 | 421 | 8 | 9 |
| 11 | 356 | 388 | 0.92 | 0.06129 | 0.00302 | 0.57714 | 0.02638 | 0.06830 | 0.00130 | 649 | 102 | 463 | 17 | 426 | 8 | 42 |
| 12 | 360 | 558 | 0.65 | 0.05672 | 0.00142 | 0.54338 | 0.01926 | 0.06948 | 0.00202 | 481 | 54 | 441 | 13 | 433 | 12 | 10 |
| 13 | 685 | 685 | 1.00 | 0.06009 | 0.00132 | 0.63209 | 0.01786 | 0.07629 | 0.00204 | 607 | 47 | 497 | 11 | 474 | 12 | 25 |
| 14 | 1666 | 1635 | 1.02 | 0.05763 | 0.00122 | 0.61107 | 0.02386 | 0.07690 | 0.00288 | 516 | 46 | 484 | 15 | 478 | 17 | 8 |
| 15 | 616 | 473 | 1.30 | 0.05745 | 0.00224 | 0.63020 | 0.02214 | 0.07956 | 0.00148 | 509 | 84 | 496 | 14 | 493 | 9 | 3 |
| 16 | 140 | 102 | 1.38 | 0.06129 | 0.00248 | 0.70693 | 0.02798 | 0.08366 | 0.00184 | 649 | 85 | 543 | 17 | 518 | 11 | 23 |
| 17 | 232 | 650 | 0.36 | 0.05681 | 0.00174 | 0.66700 | 0.05014 | 0.08515 | 0.00428 | 484 | 66 | 519 | 30 | 527 | 25 | −8 |
| 18 | 75 | 77 | 0.98 | 0.06321 | 0.00160 | 0.76031 | 0.01412 | 0.08724 | 0.00134 | 715 | 53 | 574 | 8 | 539 | 8 | 28 |
| 19 | 1125 | 711 | 1.58 | 0.06576 | 0.00122 | 0.89853 | 0.01704 | 0.09910 | 0.00206 | 799 | 38 | 651 | 9 | 609 | 12 | 27 |
| 20 | 790 | 677 | 1.17 | 0.06311 | 0.00192 | 0.93094 | 0.04692 | 0.10699 | 0.00372 | 712 | 63 | 668 | 24 | 655 | 22 | 8 |
| 21 | 742 | 562 | 1.32 | 0.06848 | 0.00122 | 1.31937 | 0.02064 | 0.13973 | 0.00248 | 883 | 36 | 854 | 9 | 843 | 14 | 5 |
| 22 | 660 | 522 | 1.26 | 0.06529 | 0.00140 | 1.31286 | 0.02814 | 0.14583 | 0.00294 | 784 | 44 | 851 | 12 | 878 | 17 | −11 |
| *Gneissic granitoid BU-2* | | | | | | | | | | | | | | | | |
| 1 | 19 | 35 | 0.55 | 0.05923 | 0.00478 | 0.47791 | 0.03694 | 0.05848 | 0.00166 | 576 | 166 | 397 | 25 | 366 | 10 | 44 |
| 2 | 58 | 102 | 0.57 | 0.06864 | 0.00308 | 0.55818 | 0.02366 | 0.05896 | 0.00128 | 888 | 90 | 450 | 15 | 369 | 8 | 83 |
| 3 | 17 | 32 | 0.53 | 0.05736 | 0.00362 | 0.46925 | 0.02846 | 0.05933 | 0.00146 | 505 | 133 | 391 | 19 | 372 | 9 | 31 |
| 4 | 26 | 42 | 0.61 | 0.06294 | 0.00280 | 0.52066 | 0.02196 | 0.05997 | 0.00130 | 706 | 92 | 426 | 15 | 375 | 8 | 61 |
| 5 | 55 | 77 | 0.72 | 0.05372 | 0.00156 | 0.44604 | 0.01220 | 0.06022 | 0.00116 | 359 | 64 | 375 | 9 | 377 | 7 | −5 |
| 6 | 48 | 56 | 0.86 | 0.05867 | 0.00256 | 0.48767 | 0.02014 | 0.06025 | 0.00128 | 555 | 92 | 403 | 14 | 377 | 8 | 38 |
| 7 | 20 | 30 | 0.68 | 0.05656 | 0.00272 | 0.47059 | 0.02156 | 0.06031 | 0.00130 | 474 | 103 | 392 | 15 | 378 | 8 | 23 |
| 8 | 38 | 57 | 0.68 | 0.05941 | 0.00310 | 0.49503 | 0.02464 | 0.06040 | 0.00138 | 582 | 109 | 408 | 17 | 378 | 8 | 43 |
| 9 | 36 | 67 | 0.53 | 0.05944 | 0.00190 | 0.49618 | 0.01508 | 0.06057 | 0.00120 | 583 | 68 | 409 | 10 | 379 | 7 | 42 |
| 10 | 26 | 48 | 0.55 | 0.05475 | 0.00200 | 0.45770 | 0.01576 | 0.06063 | 0.00122 | 402 | 80 | 383 | 11 | 379 | 7 | 6 |
| 11 | 26 | 38 | 0.70 | 0.05582 | 0.00226 | 0.46723 | 0.01814 | 0.06071 | 0.00124 | 445 | 88 | 389 | 12 | 380 | 8 | 16 |
| 12 | 25 | 44 | 0.58 | 0.05925 | 0.00408 | 0.49959 | 0.03290 | 0.06113 | 0.00158 | 576 | 143 | 411 | 22 | 382 | 10 | 40 |
| 13 | 24 | 44 | 0.55 | 0.05528 | 0.00380 | 0.46703 | 0.03092 | 0.06128 | 0.00158 | 424 | 146 | 389 | 21 | 383 | 10 | 10 |
| 14 | 29 | 43 | 0.68 | 0.05985 | 0.00572 | 0.50576 | 0.04646 | 0.06129 | 0.00196 | 598 | 195 | 416 | 31 | 383 | 12 | 44 |
| 15 | 37 | 58 | 0.63 | 0.06123 | 0.00302 | 0.52011 | 0.02458 | 0.06162 | 0.00138 | 647 | 103 | 425 | 16 | 385 | 8 | 51 |
| 16 | 30 | 44 | 0.69 | 0.06579 | 0.00282 | 0.56061 | 0.02274 | 0.06180 | 0.00132 | 800 | 87 | 452 | 15 | 387 | 8 | 70 |
| 17 | 28 | 39 | 0.73 | 0.06158 | 0.00256 | 0.52728 | 0.02068 | 0.06206 | 0.00130 | 660 | 87 | 430 | 14 | 388 | 8 | 52 |
| 18 | 30 | 37 | 0.81 | 0.05547 | 0.00240 | 0.47482 | 0.01966 | 0.06210 | 0.00132 | 431 | 94 | 395 | 13 | 388 | 8 | 10 |
| 19 | 45 | 62 | 0.73 | 0.05657 | 0.00228 | 0.48962 | 0.01872 | 0.06278 | 0.00130 | 475 | 87 | 405 | 13 | 393 | 8 | 19 |
| 20 | 24 | 29 | 0.82 | 0.06238 | 0.00332 | 0.54032 | 0.02736 | 0.06280 | 0.00144 | 687 | 110 | 439 | 18 | 393 | 9 | 55 |
| 21 | 32 | 34 | 0.94 | 0.05920 | 0.00294 | 0.52135 | 0.02460 | 0.06383 | 0.00142 | 574 | 104 | 426 | 16 | 399 | 9 | 36 |
| 22 | 28 | 36 | 0.77 | 0.05368 | 0.00212 | 0.49194 | 0.01864 | 0.06649 | 0.00134 | 358 | 87 | 406 | 13 | 415 | 8 | −15 |
| 23 | 45 | 49 | 0.92 | 0.06428 | 0.00292 | 0.59933 | 0.02610 | 0.06764 | 0.00148 | 751 | 93 | 477 | 16 | 422 | 9 | 56 |
| 24 | 61 | 84 | 0.73 | 0.06283 | 0.00252 | 0.58674 | 0.02226 | 0.06771 | 0.00140 | 702 | 83 | 469 | 14 | 422 | 8 | 50 |
| 25 | 21 | 23 | 0.90 | 0.06445 | 0.00306 | 0.60525 | 0.02718 | 0.06806 | 0.00150 | 756 | 97 | 481 | 17 | 424 | 9 | 56 |
| 26 | 30 | 36 | 0.84 | 0.05874 | 0.00498 | 0.55125 | 0.04504 | 0.06807 | 0.00196 | 557 | 175 | 446 | 29 | 425 | 12 | 27 |

Table 3 (*continued*)

| Grain no. | Contents | | Ratios | | | | | | | Ages (Ma) | | | | | | Disc. (%) |
|---|---|---|---|---|---|---|---|---|---|---|---|---|---|---|---|---|
| | Th | U | Th/U | $Pb^{207}/Pb^{206}$ | 1σ | $Pb^{207}/U^{235}$ | 1σ | $Pb^{206}/U^{238}$ | 1σ | $Pb^{207}/Pb^{206}$ | 1σ | $Pb^{207}/U^{235}$ | 1σ | $Pb^{206}/U^{238}$ | 1σ | |
| *Gneissic granitoid BU-2* | | | | | | | | | | | | | | | | |
| 27 | 20 | 23 | 0.87 | 0.06620 | 0.00792 | 0.62478 | 0.07176 | 0.06846 | 0.00268 | 813 | 232 | 493 | 44 | 427 | 16 | 62 |
| 28 | 19 | 19 | 1.00 | 0.06452 | 0.00464 | 0.60892 | 0.04198 | 0.06848 | 0.00186 | 759 | 145 | 483 | 26 | 427 | 11 | 56 |
| 29 | 49 | 60 | 0.82 | 0.06014 | 0.00392 | 0.57014 | 0.03576 | 0.06878 | 0.00176 | 609 | 135 | 458 | 23 | 429 | 11 | 35 |
| 30 | 41 | 47 | 0.88 | 0.06811 | 0.00270 | 0.64786 | 0.02416 | 0.06896 | 0.00144 | 872 | 80 | 507 | 15 | 430 | 9 | 68 |
| 31 | 14 | 16 | 0.88 | 0.06140 | 0.00366 | 0.64813 | 0.03696 | 0.07654 | 0.00184 | 653 | 123 | 507 | 23 | 475 | 11 | 32 |
| 32 | 49 | 37 | 1.30 | 0.05945 | 0.00660 | 0.64396 | 0.06884 | 0.07856 | 0.00282 | 584 | 224 | 505 | 42 | 488 | 17 | 18 |
| 33 | 33 | 35 | 0.94 | 0.05941 | 0.00446 | 0.64747 | 0.04686 | 0.07906 | 0.00216 | 582 | 155 | 507 | 28 | 491 | 13 | 17 |
| *Gneissic granitoid BU-3* | | | | | | | | | | | | | | | | |
| 1 | 166 | 298 | 0.56 | 0.05574 | 0.00194 | 0.43111 | 0.01490 | 0.05612 | 0.00126 | 442 | 76 | 364 | 11 | 352 | 8 | 23 |
| 2 | 313 | 503 | 0.62 | 0.05388 | 0.00116 | 0.41937 | 0.00920 | 0.05645 | 0.00118 | 366 | 48 | 356 | 7 | 354 | 7 | 3 |
| 3 | 20 | 86 | 0.23 | 0.05608 | 0.00148 | 0.44570 | 0.01176 | 0.05768 | 0.00124 | 456 | 58 | 374 | 8 | 362 | 8 | 23 |
| 4 | 87 | 174 | 0.50 | 0.05412 | 0.00126 | 0.43906 | 0.01026 | 0.05885 | 0.00124 | 376 | 52 | 370 | 7 | 369 | 8 | 2 |
| 5 | 47 | 84 | 0.56 | 0.05818 | 0.00156 | 0.50210 | 0.01338 | 0.06258 | 0.00132 | 537 | 58 | 413 | 9 | 391 | 8 | 31 |
| 6 | 553 | 453 | 1.22 | 0.05791 | 0.00138 | 0.50982 | 0.01232 | 0.06390 | 0.00136 | 526 | 51 | 418 | 8 | 399 | 8 | 27 |
| 7 | 91 | 149 | 0.61 | 0.05909 | 0.00154 | 0.52043 | 0.01356 | 0.06393 | 0.00136 | 570 | 56 | 425 | 9 | 399 | 8 | 35 |
| 8 | 60 | 141 | 0.43 | 0.05510 | 0.00130 | 0.48881 | 0.01170 | 0.06436 | 0.00136 | 416 | 52 | 404 | 8 | 402 | 8 | 3 |
| 9 | 54 | 151 | 0.36 | 0.05636 | 0.00144 | 0.51120 | 0.01304 | 0.06577 | 0.00138 | 467 | 56 | 419 | 9 | 411 | 8 | 13 |
| 10 | 96 | 197 | 0.48 | 0.05811 | 0.00138 | 0.53344 | 0.01280 | 0.06658 | 0.00140 | 534 | 51 | 434 | 8 | 416 | 8 | 25 |
| 11 | 91 | 111 | 0.82 | 0.05631 | 0.00132 | 0.51820 | 0.01232 | 0.06675 | 0.00140 | 465 | 51 | 424 | 8 | 417 | 8 | 11 |
| 12 | 69 | 54 | 1.27 | 0.05781 | 0.00170 | 0.53614 | 0.01578 | 0.06730 | 0.00146 | 523 | 63 | 436 | 10 | 420 | 9 | 22 |
| 13 | 118 | 226 | 0.52 | 0.05720 | 0.00128 | 0.53732 | 0.01224 | 0.06812 | 0.00142 | 499 | 49 | 437 | 8 | 425 | 9 | 16 |
| 14 | 112 | 156 | 0.72 | 0.05514 | 0.00126 | 0.51854 | 0.01204 | 0.06820 | 0.00142 | 418 | 50 | 424 | 8 | 425 | 9 | −2 |
| 15 | 32 | 32 | 1.00 | 0.06008 | 0.00218 | 0.56758 | 0.02034 | 0.06857 | 0.00156 | 606 | 77 | 456 | 13 | 428 | 9 | 35 |
| 16 | 70 | 69 | 1.02 | 0.05889 | 0.00146 | 0.55852 | 0.01384 | 0.06880 | 0.00146 | 563 | 53 | 451 | 9 | 429 | 9 | 27 |
| 17 | 32 | 52 | 0.62 | 0.05512 | 0.00156 | 0.52883 | 0.01496 | 0.06964 | 0.00150 | 417 | 62 | 431 | 10 | 434 | 9 | −4 |
| 18 | 92 | 193 | 0.48 | 0.05737 | 0.00136 | 0.55741 | 0.01330 | 0.07050 | 0.00148 | 506 | 51 | 450 | 9 | 439 | 9 | 14 |
| 19 | 368 | 332 | 1.11 | 0.05573 | 0.00120 | 0.54233 | 0.01176 | 0.07056 | 0.00146 | 442 | 47 | 440 | 8 | 440 | 9 | 0 |
| 20 | 141 | 211 | 0.67 | 0.05651 | 0.00142 | 0.54969 | 0.01388 | 0.07060 | 0.00150 | 472 | 55 | 445 | 9 | 440 | 9 | 7 |
| 21 | 49 | 64 | 0.77 | 0.05781 | 0.00176 | 0.56287 | 0.01710 | 0.07068 | 0.00156 | 523 | 65 | 453 | 11 | 440 | 9 | 17 |
| 22 | 56 | 65 | 0.85 | 0.05837 | 0.00156 | 0.56941 | 0.01514 | 0.07077 | 0.00150 | 544 | 57 | 458 | 10 | 441 | 9 | 21 |
| 23 | 85 | 135 | 0.63 | 0.05665 | 0.00138 | 0.55392 | 0.01362 | 0.07091 | 0.00150 | 478 | 53 | 448 | 9 | 442 | 9 | 8 |
| 24 | 129 | 148 | 0.87 | 0.05749 | 0.00162 | 0.56296 | 0.01576 | 0.07101 | 0.00152 | 510 | 61 | 453 | 10 | 442 | 9 | 14 |
| 25 | 74 | 84 | 0.89 | 0.05655 | 0.00148 | 0.55454 | 0.01458 | 0.07118 | 0.00152 | 474 | 57 | 448 | 9 | 443 | 9 | 7 |
| 26 | 69 | 171 | 0.41 | 0.05865 | 0.00146 | 0.57851 | 0.01440 | 0.07151 | 0.00150 | 554 | 53 | 464 | 9 | 445 | 9 | 22 |
| 27 | 16 | 23 | 0.71 | 0.05648 | 0.00198 | 0.55946 | 0.01952 | 0.07191 | 0.00162 | 471 | 76 | 451 | 13 | 448 | 10 | 5 |
| *Gneissic granitoid BU-12* | | | | | | | | | | | | | | | | |
| 1 | 42 | 56 | 0.75 | 0.05503 | 0.00138 | 0.52436 | 0.01266 | 0.06911 | 0.00136 | 413 | 55 | 428 | 8 | 431 | 8 | −4 |
| 2 | 56 | 82 | 0.68 | 0.05633 | 0.00130 | 0.54005 | 0.01200 | 0.06954 | 0.00136 | 465 | 50 | 438 | 8 | 433 | 8 | 7 |
| 3 | 29 | 55 | 0.53 | 0.06282 | 0.00224 | 0.60264 | 0.02068 | 0.06958 | 0.00148 | 702 | 74 | 479 | 13 | 434 | 9 | 47 |
| 4 | 33 | 66 | 0.50 | 0.05907 | 0.00138 | 0.57181 | 0.01288 | 0.07022 | 0.00138 | 570 | 50 | 459 | 8 | 437 | 8 | 26 |
| 5 | 45 | 106 | 0.42 | 0.05419 | 0.00140 | 0.52488 | 0.01308 | 0.07025 | 0.00140 | 379 | 57 | 428 | 9 | 438 | 8 | −14 |
| 6 | 42 | 114 | 0.37 | 0.06292 | 0.00190 | 0.60984 | 0.01784 | 0.07030 | 0.00144 | 706 | 63 | 483 | 11 | 438 | 9 | 47 |
| 7 | 21 | 61 | 0.34 | 0.05732 | 0.00134 | 0.55596 | 0.01252 | 0.07035 | 0.00138 | 504 | 51 | 449 | 8 | 438 | 8 | 14 |
| 8 | 132 | 135 | 0.97 | 0.05627 | 0.00132 | 0.54710 | 0.01244 | 0.07052 | 0.00138 | 463 | 51 | 443 | 8 | 439 | 8 | 5 |
| 9 | 26 | 97 | 0.26 | 0.05652 | 0.00126 | 0.54994 | 0.01170 | 0.07057 | 0.00138 | 473 | 49 | 445 | 8 | 440 | 8 | 7 |
| 10 | 31 | 190 | 0.16 | 0.05850 | 0.00174 | 0.57227 | 0.01646 | 0.07096 | 0.00144 | 549 | 64 | 459 | 11 | 442 | 9 | 22 |
| 11 | 18 | 67 | 0.28 | 0.05714 | 0.00132 | 0.55926 | 0.01238 | 0.07099 | 0.00138 | 497 | 50 | 451 | 8 | 442 | 8 | 12 |
| 12 | 22 | 29 | 0.74 | 0.06016 | 0.00160 | 0.59496 | 0.01536 | 0.07174 | 0.00144 | 609 | 56 | 474 | 10 | 447 | 9 | 31 |
| 13 | 24 | 55 | 0.43 | 0.05710 | 0.00136 | 0.56472 | 0.01304 | 0.07174 | 0.00140 | 495 | 52 | 455 | 8 | 447 | 8 | 10 |
| 14 | 51 | 116 | 0.44 | 0.05649 | 0.00138 | 0.56122 | 0.01314 | 0.07206 | 0.00142 | 472 | 53 | 452 | 9 | 449 | 9 | 5 |
| 15 | 71 | 162 | 0.44 | 0.05877 | 0.00124 | 0.58716 | 0.01192 | 0.07247 | 0.00140 | 559 | 45 | 469 | 8 | 451 | 8 | 21 |
| 16 | 28 | 45 | 0.62 | 0.06041 | 0.00190 | 0.60482 | 0.01836 | 0.07262 | 0.00150 | 618 | 66 | 480 | 12 | 452 | 9 | 31 |
| 17 | 46 | 104 | 0.45 | 0.06575 | 0.00148 | 0.65932 | 0.01434 | 0.07273 | 0.00142 | 798 | 46 | 514 | 9 | 453 | 9 | 55 |

*(continued on next page)*

Table 3 (*continued*)

| Grain no. | Contents | | Ratios | | | | | | | Ages (Ma) | | | | | | Disc. (%) |
|---|---|---|---|---|---|---|---|---|---|---|---|---|---|---|---|---|
| | Th | U | Th/U | $Pb^{207}/Pb^{206}$ | 1σ | $Pb^{207}/U^{235}$ | 1σ | $Pb^{206}/U^{238}$ | 1σ | $Pb^{207}/Pb^{206}$ | 1σ | $Pb^{207}/U^{235}$ | 1σ | $Pb^{206}/U^{238}$ | 1σ | |
| *Gneissic granitoid BU-12* | | | | | | | | | | | | | | | | |
| 18 | 95 | 186 | 0.51 | 0.05642 | 0.00122 | 0.56582 | 0.01176 | 0.07274 | 0.00142 | 469 | 47 | 455 | 8 | 453 | 9 | 4 |
| 19 | 20 | 51 | 0.40 | 0.05478 | 0.00136 | 0.55307 | 0.01330 | 0.07324 | 0.00144 | 403 | 55 | 447 | 9 | 456 | 9 | −12 |
| 20 | 52 | 109 | 0.47 | 0.05852 | 0.00148 | 0.59103 | 0.01446 | 0.07325 | 0.00146 | 549 | 54 | 472 | 9 | 456 | 9 | 19 |
| 21 | 11 | 20 | 0.53 | 0.06439 | 0.00390 | 0.65061 | 0.03816 | 0.07329 | 0.00192 | 754 | 123 | 509 | 23 | 456 | 12 | 49 |
| 22 | 36 | 47 | 0.77 | 0.06128 | 0.00162 | 0.62031 | 0.01582 | 0.07343 | 0.00146 | 649 | 56 | 490 | 10 | 457 | 9 | 35 |
| 23 | 51 | 115 | 0.45 | 0.05683 | 0.00126 | 0.57561 | 0.01218 | 0.07347 | 0.00142 | 485 | 48 | 462 | 8 | 457 | 9 | 6 |
| 24 | 30 | 79 | 0.38 | 0.06030 | 0.00168 | 0.61321 | 0.01640 | 0.07376 | 0.00148 | 614 | 59 | 486 | 10 | 459 | 9 | 29 |
| 25 | 142 | 350 | 0.41 | 0.06539 | 0.00158 | 0.66529 | 0.01536 | 0.07379 | 0.00146 | 787 | 50 | 518 | 9 | 459 | 9 | 53 |
| 26 | 186 | 345 | 0.54 | 0.05575 | 0.00114 | 0.57023 | 0.01126 | 0.07418 | 0.00142 | 442 | 45 | 458 | 7 | 461 | 9 | −4 |
| 27 | 18 | 43 | 0.42 | 0.05847 | 0.00164 | 0.60097 | 0.01620 | 0.07456 | 0.00150 | 547 | 60 | 478 | 10 | 464 | 9 | 17 |
| 28 | 33 | 38 | 0.87 | 0.05618 | 0.00156 | 0.57766 | 0.01544 | 0.07459 | 0.00150 | 459 | 60 | 463 | 10 | 464 | 9 | −1 |
| 29 | 95 | 180 | 0.53 | 0.06409 | 0.00174 | 0.65982 | 0.01728 | 0.07468 | 0.00150 | 745 | 56 | 515 | 11 | 464 | 9 | 46 |
| 30 | 80 | 157 | 0.51 | 0.05584 | 0.00118 | 0.57975 | 0.01184 | 0.07530 | 0.00146 | 446 | 46 | 464 | 8 | 468 | 9 | −5 |
| 31 | 38 | 87 | 0.44 | 0.06324 | 0.00168 | 0.66075 | 0.01700 | 0.07579 | 0.00152 | 716 | 55 | 515 | 10 | 471 | 9 | 41 |
| 32 | 43 | 250 | 0.17 | 0.05982 | 0.00128 | 0.62697 | 0.01298 | 0.07602 | 0.00148 | 597 | 46 | 494 | 8 | 472 | 9 | 23 |
| 33 | 72 | 188 | 0.38 | 0.06053 | 0.00126 | 0.63583 | 0.01276 | 0.07619 | 0.00148 | 623 | 44 | 500 | 8 | 473 | 9 | 27 |
| 34 | 24 | 46 | 0.53 | 0.05467 | 0.00136 | 0.58278 | 0.01390 | 0.07732 | 0.00152 | 399 | 55 | 466 | 9 | 480 | 9 | −19 |
| 35 | 41 | 106 | 0.38 | 0.05508 | 0.00124 | 0.58924 | 0.01274 | 0.07760 | 0.00152 | 415 | 50 | 470 | 8 | 482 | 9 | −15 |
| 36 | 103 | 297 | 0.35 | 0.05869 | 0.00122 | 0.62889 | 0.01258 | 0.07772 | 0.00150 | 556 | 45 | 495 | 8 | 482 | 9 | 14 |

intensity of the sedimentary source and the nature of the sedimentary provenance (Nesbitt and Young, 1982; Cox et al., 1995; Fedo et al., 1995). If elements were mobile during the metamorphism for the banded gneiss, CIA would increase and ICV would decrease because $Na_2O$ and $K_2O$ would be more easily removed than other elements from the system. However, the banded gneisses in this study all have low CIA and high ICV values (Fig. 3), indicating that metamorphism took place in a closed system and their chemical compositions, including CIA and ICV values, can be used to study the nature of their protoliths.

The banded gneisses have $SiO_2$, $Al_2O_3$, and CaO compositions similar to the associated gneissic granitoids (Table 2). However, the banded gneisses have higher A/NK [molar ratio of $Al_2O_3/(Na_2O+K_2O)$, 2.15–2.77] and A/CNK values [molar ratio of $Al_2O_3/(CaO+Na_2O+K_2O)$, mostly ~1.5]. These rocks are moderately enriched in light rare earth elements (LREE) ($La_N/Yb_N$=4.4–8.0), have negative Eu anomalies (Eu/Eu*=0.5–0.7) and show Nb, Ta, and Sr troughs on a continental crust-normalized diagram (Fig. 4a and b). The occurrence of Al-rich minerals such as sillimanite and garnet is consistent with the chemical composition of the gneissic rocks. However, these rocks have relatively high contents of MgO, Ni, Cr, and U (Table 2), not favoring a pelitic source. The banded gneisses have Th/U ratios (2.0–3.9), lower than, or close to, the average value of the upper crust (3.8, McLennan and Taylor, 1980). These rocks also have relatively low Zr/Sc ratios (8–16.9, Table 2), lower than, or close to, those for the associated gneissic granitoids (9.9–25.3, Table 2).

The gneissic granitoids are chemically metaluminous to weakly peraluminous (A/CNK=1.06–1.32, Table 2), and biotite is the major mafic mineral. These rocks show an I-type granite trend in the $SiO_2$–$P_2O_5$ diagram of Chappell and White (1992) (not shown). They have negative Eu anomalies (Eu/Eu*=0.4–0.6) and show two types of REE patterns, one with moderately LREE enrichment ($La_N/Yb_N$ ~7) and the other without LREE enrichment but with some tetrad effect ($La_N/Yb_N$ ~1) (Fig. 4c), possibly due to extensive differentiation with strong hydrothermal interaction (e.g. Basu, 1996; Irber, 1999; Jahn et al., 2001; Monecke et al., 2002; Wu et al., 2004). These granitoids are depleted in Nb, Ta, and Sr on a continental crust-normalized diagram, a pattern broadly similar to that of the banded gneisses (Fig. 4d), are characterized by low Sr/Y ratios (2.3–3.6, Table 2) and fall in the volcanic arc field in discrimination diagrams [such as the Rb–(Y+Nb) and Nb–Y diagrams of Pearce et al. (1984) and the Rb/10–Hf–Ta*3 diagram of Harris et al. (1986), not shown].

## 6. Zircon U–Pb ages and Hf isotopic systematics

Zircon U–Pb and Hf isotopic results are presented in Tables 3 and 4 respectively. Hf isotopic analyses were performed on selected large zircon grains. Zircon

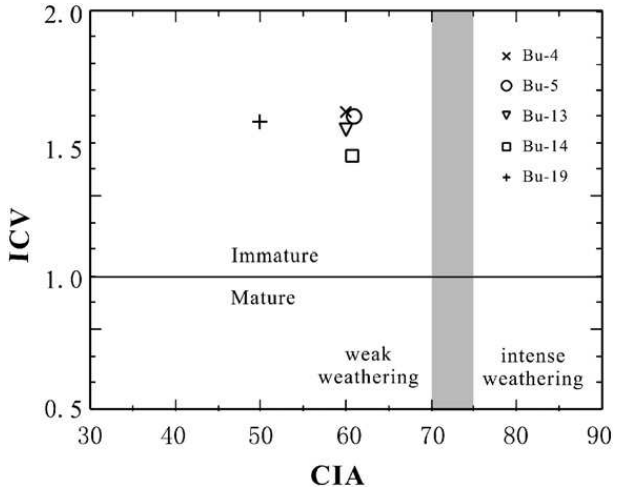


Fig. 3. CIA–ICV diagram for the banded paragneisses.

U and Th contents, Th/U ratios, morphological features, U–Pb ages and Hf isotopic compositions for each population of the analyzed samples are summarized in Table 5.

### 6.1. Banded gneisses

Three types of zircons are recognized from samples of banded paragneiss. Type-I zircons occur as euhedral, stubby, prismatic crystals (length/width ratio < 2.5), with concentric oscillatory zoning (Fig. 5a–f), and lack inherited cores. Their Th/U ratios are dominantly in the range of 0.1 to 1.0, implying an igneous origin (Hanchar and Rudnick, 1995) (Table 3). We interpret these zircons as possibly having been derived from nearby igneous rocks, with a very short sedimentary

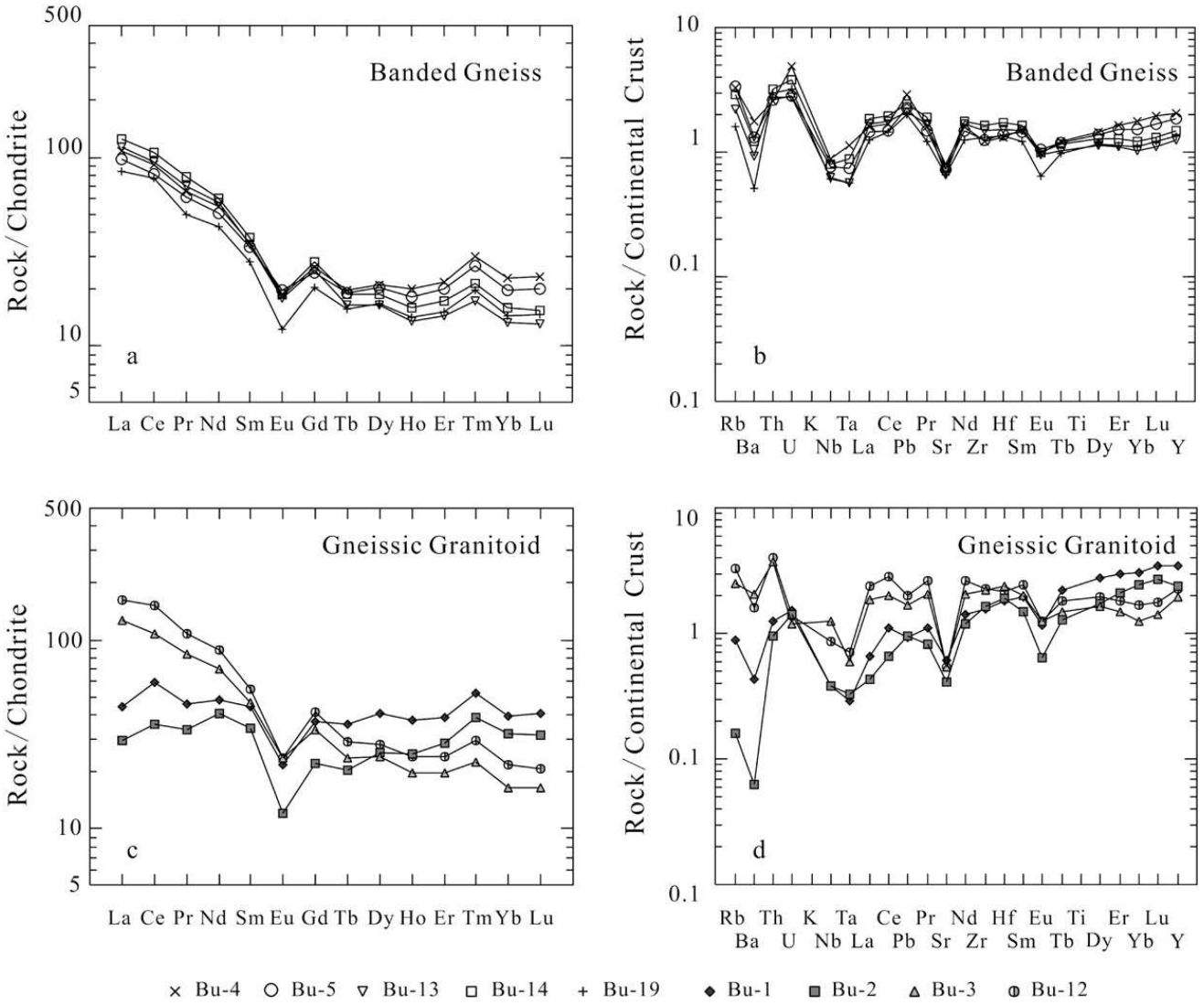


Fig. 4. Chondrite-normalized REE patterns and trace element spider variation diagrams for the banded paragneiss (a and b, respectively) and gneissic granitoids (c and d, respectively). Normalized values are from Sun and McDonough (1989).

transport. Type-II zircons are generally granular, with large, rounded cores surrounded by structureless, low-luminescence rims (Fig. 5g-j). Some cores show oscillatory zoning. One zircon grain in this group displays three stages of growth (Fig. 5h). The rounded zircon cores suggest derivation from a more distant source. Type-III zircons are also granular, but their cores appear to be broken fragments of an earlier generation, surrounded by low-luminescence, structureless rims (Fig. 5k-o). We suggest that the broken zircon cores may have been derived from pyroclastic rocks. Zircons from all analyzed samples of banded gneiss show large variations in U and Th contents, irrespective of their age (Table 3).

#### 6.1.1. Sample Bu-4

The majority of zircons from this sample give a weighted mean $^{206}Pb/^{238}U$ age of 505±7 Ma (Table 5 and Fig. 6a). These zircons have Type-I morphological features (Fig. 5) and yield $\varepsilon_{Hf}(t)$ values from −7.0 to+7.6 and $T^{C}_{DM}$ model ages from 0.90 to 1.59 Ga (Table 4 and Fig. 7a).

In addition, four zircon grains give a weighted mean $^{206}Pb/^{238}U$ age of 574±11 Ma. Five zircons yield Neoproterozoic or late Mesoproterozoic ages ($^{206}Pb/^{238}U$ ages from 638 to 1023 Ma, Tables 3 and 5 and Fig. 6a). These zircons have Type-I or Type-III characteristics and the Proterozoic zircons have been analysed for Hf isotopic compositions, giving $\varepsilon_{Hf}(t)$ values from −1.8 to +2.6 and $T^{C}_{DM}$ model ages from 1.45 to 1.81 Ga (Table 4 and Fig. 7a).

Two rounded cores of Type-II zircons were analysed and give one concordant and one highly discordant data, i.e. $^{207}Pb/^{206}Pb$ age of 1994±44 Ma and 2516±37 Ma, respectively (Table 3 and Fig. 6a). The 1994 Ma zircon has an $\varepsilon_{Hf}(t)$ value of −11.2 and a $T^{C}_{DM}$ model age of 3.04 Ga (Table 4 and Fig. 7a).

#### 6.1.2. Sample Bu-5

The majority of zircon populations of this sample give a weighted mean $^{206}Pb/^{238}U$ age of 517±8 Ma (Fig. 6b and Table 5). These zircons have Type-I or Type III morphological features, and yield $\varepsilon_{Hf}(t)$ values from −17.5 to +12.6, and $T^{C}_{DM}$ model ages from 0.64 to 2.12 Ga (Table 4 and Fig. 7b).

Additional 13 zircon grains yield Neoproterozoic $^{206}Pb/^{238}U$ ages between 592 and 876 Ma, $\varepsilon_{Hf}(t)$ values from −5.5 to +10.7 and $T^{C}_{DM}$ model ages from 0.83 to 1.71 Ga. One largely discordant analysis yielded a $^{207}Pb/^{206}Pb$ age of 2048±58 Ma, with an $\varepsilon_{Hf}(t)$ value of +2.2 and a $T^{C}_{DM}$ model age of 2.43 Ga (Table 4 and Fig. 7b), and one slightly reversed point gave a $^{207}Pb/^{206}Pb$ age of 2159±54 Ma (Fig. 6b, Table 3).

#### 6.1.3. Sample Bu-13

The major population of zircons from this sample give a weighted mean $^{206}Pb/^{238}U$ age of 481±11 Ma (Fig. 6c and Table 5). These zircons have Type-I features and give $\varepsilon_{Hf}(t)$ values from −6.4 to +14.7 and $T^{C}_{DM}$ model ages from 0.54 to 1.55 Ga (Table 4 and Fig. 7c).

One concordant and one discordant analysis gave $^{206}Pb/^{238}U$ ages of 573±10 Ma and 585±11 Ma, respectively. Seven zircons with Type-I or Type-III features give Neoproterozoic $^{206}Pb/^{238}U$ ages between 694 and 956 Ma, $\varepsilon_{Hf}(t)$ values from −15.8 to +7.19 and $T^{C}_{DM}$ model ages from 1.07 to 2.21 Ga (Table 4 and Fig. 7c). One Type-I and one Type-III zircon give discordant Meso- and Paleo-proterozoic $^{207}Pb/^{206}Pb$ ages of 1580±55 and 1942±54 Ma, respectively (Fig. 6c and Table 3). Two Type-II zircons yield discordant $^{207}Pb/^{206}Pb$ ages of 2347±72, and 2626±46 Ma, respectively (Fig. 6c and Table 3), and the 2347 Ma zircon yields an $\varepsilon_{Hf}(t)$ value of −4.7 and a $T^{C}_{DM}$ model age of 3.01 Ga (Table 4 and Fig. 7c).

#### 6.1.4. Sample Bu-14

The majority of zircons from this sample give a weighted mean $^{206}Pb/^{238}U$ age of 466±11 Ma (Fig. 6d and Table 5). These zircons have Type-I structural features, and yield $\varepsilon_{Hf}(t)$ values from −17.4 to +3.8 and $T^{C}_{DM}$ model ages from 1.03 to 2.07 Ga (Table 4 and Fig. 7d).

Other Type-I zircons are mostly Neoproterozoic ($^{206}Pb/^{238}U$ ages between 640 and 907 Ma), with $\varepsilon_{Hf}(t)$ values from −12 to +10 and $T^{C}_{DM}$ model ages from 0.99 to 1.96 Ga (Table 4 and Fig. 7d). Two Type-II zircons yield Paleoproterozoic or Archean $^{207}Pb/^{206}Pb$ ages (1890±57, 2472±51 and 2634±65 Ma, respectively, Fig. 6d and Table 3), and the 2472 Ma zircon gives an $\varepsilon_{Hf}(t)$ value of-0.9 and a $T^{C}_{DM}$ model age of 2.93 Ga (Table 4 and Fig. 7d).

#### 6.1.5. Sample Bu-19

The major population give a weighted mean $^{206}Pb/^{238}U$ age of 528±16 Ma (Fig. 6e and Table 5). These zircons have Type-I morphological features, and thier $\varepsilon_{Hf}(t)$ values vary from −16.7 to +11.8, and their $T^{C}_{DM}$ model ages range from 0.72 to 2.09 Ga (Table 4 and Fig. 7e).

Five zircons with Type-I and one with Type-II features give Neoproterozoic $^{206}Pb/^{238}U$ ages (729–936 Ma, Fig. 6e and Table 3), $\varepsilon_{Hf}(t)$ values from −4.2 to +9.5 and $T^{C}_{DM}$ model ages from 1.0 to 1.8 Ga (Table 4 and Fig. 7e).

### 6.2. Gneissic granitoids

Zircons from the gneissic granitoids are long, euhedral prisms (length/width ratio up to 4.5) (Fig. 8), similar to the Type-I morphology of zircons from the banded

Table 4
Lu–Hf isotopic data for zircons from banded gneiss and gneissic granitoid in the Chinese Altai

| Grain no. | U–Pb age* | 1σ | $^{176}Yb/^{177}Hf$ | 2σ | $^{176}Lu/^{177}Hf$ | 2σ | $^{176}Hf/^{177}Hf$ | 2σ | $(^{176}Hf/^{177}Hf)i$ | εHf | $T_{DM}$ (Ga) | 2σ | $T^{C}_{DM}$ (Ga) | 2σ |
|---|---|---|---|---|---|---|---|---|---|---|---|---|---|---|
| *Banded gneiss BU-4* | | | | | | | | | | | | | | |
| 3 | 480 | 9 | 0.047227 | 0.000567 | 0.001559 | 0.000010 | 0.282404 | 0.000023 | 0.282390 | −2.93 | 1.22 | 0.03 | 1.38 | 0.02 |
| 4 | 493 | 10 | 0.060872 | 0.001073 | 0.001430 | 0.000025 | 0.282461 | 0.000041 | 0.282447 | −0.64 | 1.13 | 0.06 | 1.28 | 0.02 |
| 5 | 493 | 10 | 0.030111 | 0.000132 | 0.000827 | 0.000005 | 0.282277 | 0.000019 | 0.282269 | −6.95 | 1.37 | 0.03 | 1.59 | 0.02 |
| 8 | 495 | 9 | 0.022433 | 0.000135 | 0.000678 | 0.000005 | 0.282434 | 0.000026 | 0.282428 | −1.29 | 1.15 | 0.04 | 1.31 | 0.02 |
| 10 | 500 | 10 | 0.035897 | 0.000406 | 0.001113 | 0.000027 | 0.282569 | 0.000022 | 0.282558 | 3.45 | 0.97 | 0.03 | 1.08 | 0.02 |
| 13 | 504 | 10 | 0.059931 | 0.000468 | 0.002002 | 0.000032 | 0.282290 | 0.000022 | 0.282271 | −6.65 | 1.40 | 0.03 | 1.58 | 0.02 |
| 14 | 506 | 10 | 0.023860 | 0.000240 | 0.000717 | 0.000011 | 0.282456 | 0.000023 | 0.282449 | −0.28 | 1.12 | 0.03 | 1.27 | 0.02 |
| 18 | 516 | 10 | 0.030841 | 0.000128 | 0.001001 | 0.000015 | 0.282302 | 0.000018 | 0.282292 | −5.62 | 1.34 | 0.02 | 1.54 | 0.02 |
| 19 | 520 | 10 | 0.061513 | 0.000216 | 0.001945 | 0.000011 | 0.282681 | 0.000021 | 0.282662 | 7.57 | 0.83 | 0.03 | 0.90 | 0.02 |
| 29 | 638 | 13 | 0.042875 | 0.000521 | 0.001569 | 0.000027 | 0.282344 | 0.000029 | 0.282325 | −1.76 | 1.30 | 0.04 | 1.45 | 0.02 |
| 32 | 922 | 18 | 0.040659 | 0.000507 | 0.001086 | 0.000022 | 0.282289 | 0.000043 | 0.282270 | 2.61 | 1.36 | 0.06 | 1.48 | 0.02 |
| 33 | 1099 | 20 | 0.036440 | 0.001345 | 0.001135 | 0.000063 | 0.282073 | 0.000066 | 0.280490 | −1.24 | 1.67 | 0.09 | 1.81 | 0.02 |
| 34 | 1994 | 34 | 0.011828 | 0.000138 | 0.000314 | 0.000004 | 0.281211 | 0.000020 | 0.281199 | −11.20 | 2.80 | 0.03 | 3.04 | 0.02 |
| *Banded gneiss BU-5* | | | | | | | | | | | | | | |
| 3 | 502 | 10 | 0.026313 | 0.001689 | 0.000922 | 0.000061 | 0.282416 | 0.000036 | 0.282407 | −1.88 | 1.18 | 0.05 | 1.35 | 0.05 |
| 4 | 513 | 10 | 0.044306 | 0.000967 | 0.001594 | 0.000025 | 0.282499 | 0.000048 | 0.282484 | 1.11 | 1.08 | 0.07 | 1.21 | 0.07 |
| 5 | 514 | 10 | 0.024182 | 0.002315 | 0.000910 | 0.000091 | 0.281966 | 0.000075 | 0.281958 | −17.52 | 1.81 | 0.10 | 2.12 | 0.10 |
| 7 | 515 | 10 | 0.067432 | 0.003282 | 0.002561 | 0.000118 | 0.282833 | 0.000209 | 0.282808 | 12.62 | 0.62 | 0.31 | 0.64 | 0.31 |
| 8 | 519 | 10 | 0.062453 | 0.001430 | 0.001913 | 0.000028 | 0.282714 | 0.000043 | 0.282695 | 8.73 | 0.78 | 0.06 | 0.84 | 0.06 |
| 10 | 522 | 10 | 0.018257 | 0.001843 | 0.000652 | 0.000071 | 0.282181 | 0.000051 | 0.282175 | −9.64 | 1.50 | 0.07 | 1.74 | 0.07 |
| 12 | 525 | 11 | 0.042776 | 0.001479 | 0.001405 | 0.000049 | 0.282788 | 0.000091 | 0.282774 | 11.63 | 0.67 | 0.13 | 0.70 | 0.13 |
| 13 | 530 | 11 | 0.024129 | 0.001438 | 0.000816 | 0.000050 | 0.282535 | 0.000038 | 0.282527 | 3.01 | 1.01 | 0.05 | 1.13 | 0.05 |
| 14 | 533 | 11 | 0.047413 | 0.003850 | 0.001721 | 0.000131 | 0.282325 | 0.000035 | 0.282307 | −4.70 | 1.34 | 0.05 | 1.51 | 0.05 |
| 16 | 538 | 12 | 0.041964 | 0.000858 | 0.001321 | 0.000021 | 0.282589 | 0.000035 | 0.282575 | 4.89 | 0.95 | 0.05 | 1.04 | 0.05 |
| 17 | 592 | 13 | 0.038650 | 0.001450 | 0.001214 | 0.000054 | 0.282590 | 0.000038 | 0.282576 | 6.11 | 0.94 | 0.05 | 1.03 | 0.05 |
| 18 | 610 | 15 | 0.046207 | 0.001041 | 0.001452 | 0.000023 | 0.282386 | 0.000048 | 0.282369 | −0.83 | 1.24 | 0.07 | 1.39 | 0.07 |
| 20 | 623 | 14 | 0.024491 | 0.000126 | 0.000787 | 0.000011 | 0.282695 | 0.000023 | 0.282686 | 10.69 | 0.79 | 0.03 | 0.83 | 0.03 |
| 22 | 667 | 13 | 0.020278 | 0.001605 | 0.000760 | 0.000059 | 0.282230 | 0.000054 | 0.282220 | −4.82 | 1.43 | 0.08 | 1.63 | 0.08 |
| 25 | 720 | 15 | 0.029156 | 0.000547 | 0.000913 | 0.000018 | 0.282181 | 0.000028 | 0.282168 | −5.50 | 1.51 | 0.04 | 1.71 | 0.04 |
| 26 | 735 | 14 | 0.034249 | 0.000732 | 0.001146 | 0.000024 | 0.282344 | 0.000033 | 0.282328 | 0.50 | 1.29 | 0.05 | 1.42 | 0.05 |
| 28 | 787 | 16 | 0.019504 | 0.000528 | 0.000686 | 0.000018 | 0.282545 | 0.000034 | 0.282535 | 8.99 | 0.99 | 0.05 | 1.05 | 0.05 |
| 29 | 876 | 17 | 0.021296 | 0.000334 | 0.000759 | 0.000021 | 0.282531 | 0.000045 | 0.282518 | 10.39 | 1.01 | 0.06 | 1.05 | 0.06 |
| 30 | 2048 | 40 | 0.026698 | 0.000243 | 0.000947 | 0.000010 | 0.281577 | 0.000026 | 0.281540 | 2.17 | 2.34 | 0.04 | 2.43 | 0.04 |
| *Banded gneiss BU-13* | | | | | | | | | | | | | | |
| 1 | 446 | 8 | 0.038181 | 0.000781 | 0.001232 | 0.000020 | 0.282469 | 0.000045 | 0.282458 | −1.29 | 1.12 | 0.06 | 1.27 | 0.06 |
| 2 | 451 | 8 | 0.041609 | 0.000484 | 0.001480 | 0.000025 | 0.282801 | 0.000035 | 0.282788 | 10.50 | 0.65 | 0.05 | 0.69 | 0.05 |
| 3 | 457 | 8 | 0.025574 | 0.000279 | 0.001012 | 0.000010 | 0.282545 | 0.000027 | 0.282536 | 1.71 | 1.00 | 0.04 | 1.13 | 0.04 |
| 4 | 465 | 9 | 0.044046 | 0.001008 | 0.001598 | 0.000050 | 0.282663 | 0.000043 | 0.282649 | 5.91 | 0.85 | 0.06 | 0.93 | 0.06 |
| 5 | 466 | 10 | 0.026232 | 0.001916 | 0.000941 | 0.000070 | 0.282486 | 0.000033 | 0.282478 | −0.15 | 1.08 | 0.05 | 1.23 | 0.05 |
| 6 | 468 | 9 | 0.032288 | 0.000556 | 0.001166 | 0.000023 | 0.282555 | 0.000040 | 0.282545 | 2.26 | 0.99 | 0.06 | 1.12 | 0.06 |
| 11 | 477 | 9 | 0.025591 | 0.001076 | 0.000949 | 0.000044 | 0.282304 | 0.000038 | 0.282296 | −6.35 | 1.34 | 0.05 | 1.55 | 0.05 |
| 14 | 504 | 9 | 0.013696 | 0.000650 | 0.000640 | 0.000030 | 0.282753 | 0.000076 | 0.282747 | 10.22 | 0.70 | 0.11 | 0.75 | 0.11 |
| 15 | 507 | 11 | 0.029167 | 0.001320 | 0.001023 | 0.000059 | 0.282548 | 0.000038 | 0.282538 | 2.88 | 1.00 | 0.05 | 1.12 | 0.05 |
| 16 | 517 | 10 | 0.026767 | 0.001594 | 0.000890 | 0.000047 | 0.282340 | 0.000039 | 0.282331 | −4.22 | 1.29 | 0.05 | 1.47 | 0.05 |
| 17 | 517 | 10 | 0.031689 | 0.000702 | 0.001011 | 0.000022 | 0.282874 | 0.000036 | 0.282864 | 14.67 | 0.54 | 0.05 | 0.54 | 0.05 |
| 19 | 573 | 10 | 0.036148 | 0.001281 | 0.001141 | 0.000042 | 0.282216 | 0.000053 | 0.282203 | −7.50 | 1.47 | 0.07 | 1.68 | 0.07 |
| 22 | 701 | 13 | 0.013533 | 0.000734 | 0.000544 | 0.000032 | 0.282545 | 0.000037 | 0.282538 | 7.19 | 0.99 | 0.05 | 1.07 | 0.05 |
| 23 | 719 | 13 | 0.020339 | 0.000622 | 0.000703 | 0.000017 | 0.281887 | 0.000043 | 0.281878 | −15.80 | 1.90 | 0.06 | 2.21 | 0.06 |
| 24 | 726 | 13 | 0.055304 | 0.001645 | 0.001704 | 0.000047 | 0.282542 | 0.000085 | 0.282518 | 7.05 | 1.03 | 0.12 | 1.09 | 0.12 |
| 25 | 794 | 14 | 0.034504 | 0.001869 | 0.001101 | 0.000058 | 0.282218 | 0.000041 | 0.282202 | −2.64 | 1.46 | 0.06 | 1.63 | 0.06 |
| 27 | 956 | 17 | 0.057136 | 0.003901 | 0.001605 | 0.000087 | 0.282315 | 0.000043 | 0.282286 | 3.95 | 1.35 | 0.06 | 1.44 | 0.06 |
| 30 | 2347 | 30 | 0.006214 | 0.000983 | 0.000218 | 0.000039 | 0.281163 | 0.000063 | 0.281154 | −4.72 | 2.85 | 0.08 | 3.01 | 0.08 |

*(continued on next page)*

Table 4 (*continued*)

| Grain no. | U–Pb age* | 1σ | $^{176}Yb/^{177}Hf$ | 2σ | $^{176}Lu/^{177}Hf$ | 2σ | $^{176}Hf/^{177}Hf$ | 2σ | $(^{176}Hf/^{177}Hf)i$ | εHf | $T_{DM}$ (Ga) | 2σ | $T^{C}_{DM}$ (Ga) | 2σ |
|---|---|---|---|---|---|---|---|---|---|---|---|---|---|---|
| *Banded gneiss BU-14* | | | | | | | | | | | | | | |
| 3 | 435 | 8 | 0.059109 | 0.001909 | 0.002104 | 0.000079 | 0.282584 | 0.000034 | 0.282567 | 2.32 | 0.97 | 0.05 | 1.09 | 0.05 |
| 5 | 440 | 9 | 0.061922 | 0.001128 | 0.002123 | 0.000021 | 0.282549 | 0.000035 | 0.282532 | 1.17 | 1.03 | 0.05 | 1.15 | 0.05 |
| 6 | 447 | 9 | 0.037358 | 0.001736 | 0.001256 | 0.000057 | 0.282091 | 0.000037 | 0.282081 | −14.64 | 1.65 | 0.05 | 1.92 | 0.05 |
| 7 | 449 | 9 | 0.028654 | 0.000748 | 0.000974 | 0.000031 | 0.282314 | 0.000029 | 0.282305 | −6.65 | 1.33 | 0.04 | 1.54 | 0.04 |
| 8 | 455 | 9 | 0.032742 | 0.000996 | 0.001222 | 0.000035 | 0.282608 | 0.000030 | 0.282597 | 3.83 | 0.92 | 0.04 | 1.03 | 0.04 |
| 9 | 457 | 9 | 0.044209 | 0.001932 | 0.001661 | 0.000081 | 0.282325 | 0.000069 | 0.282311 | −6.27 | 1.33 | 0.10 | 1.52 | 0.10 |
| 10 | 457 | 9 | 0.030293 | 0.000323 | 0.000980 | 0.000013 | 0.282418 | 0.000033 | 0.282410 | −2.77 | 1.18 | 0.05 | 1.35 | 0.05 |
| 13 | 460 | 9 | 0.020041 | 0.001032 | 0.000722 | 0.000041 | 0.282001 | 0.000033 | 0.281995 | −17.37 | 1.75 | 0.04 | 2.07 | 0.04 |
| 15 | 469 | 9 | 0.029765 | 0.000331 | 0.001086 | 0.000009 | 0.282436 | 0.000028 | 0.282427 | −1.90 | 1.16 | 0.04 | 1.32 | 0.04 |
| 16 | 474 | 9 | 0.078844 | 0.003733 | 0.002888 | 0.000139 | 0.282601 | 0.000035 | 0.282575 | 3.48 | 0.97 | 0.05 | 1.06 | 0.05 |
| 19 | 483 | 9 | 0.036941 | 0.000702 | 0.001194 | 0.000010 | 0.282311 | 0.000056 | 0.282300 | −6.06 | 1.34 | 0.08 | 1.54 | 0.08 |
| 23 | 521 | 10 | 0.051747 | 0.000904 | 0.001683 | 0.000028 | 0.282206 | 0.000032 | 0.282189 | −9.16 | 1.50 | 0.05 | 1.72 | 0.05 |
| 24 | 524 | 10 | 0.023180 | 0.000274 | 0.000857 | 0.000011 | 0.282301 | 0.000033 | 0.282293 | −5.42 | 1.34 | 0.05 | 1.54 | 0.05 |
| 25 | 640 | 12 | 0.113708 | 0.002535 | 0.003733 | 0.000093 | 0.282076 | 0.000036 | 0.282031 | −12.13 | 1.79 | 0.05 | 1.96 | 0.05 |
| 27 | 745 | 14 | 0.033239 | 0.000385 | 0.001289 | 0.000019 | 0.282183 | 0.000036 | 0.282165 | −5.05 | 1.52 | 0.05 | 1.70 | 0.05 |
| 28 | 766 | 14 | 0.017388 | 0.000301 | 0.000554 | 0.000009 | 0.282215 | 0.000031 | 0.282207 | −3.09 | 1.45 | 0.04 | 1.63 | 0.04 |
| 29 | 774 | 18 | 0.017559 | 0.000392 | 0.000651 | 0.000011 | 0.282580 | 0.000028 | 0.282571 | 9.96 | 0.94 | 0.04 | 0.99 | 0.04 |
| 30 | 821 | 15 | 0.066782 | 0.001307 | 0.002251 | 0.000061 | 0.282467 | 0.000062 | 0.282432 | 6.12 | 1.15 | 0.09 | 1.22 | 0.09 |
| 32 | 907 | 17 | 0.040129 | 0.003047 | 0.001241 | 0.000068 | 0.282442 | 0.000037 | 0.282421 | 7.63 | 1.15 | 0.05 | 1.21 | 0.05 |
| 35 | 2472 | 41 | 0.036894 | 0.000421 | 0.001215 | 0.000014 | 0.281238 | 0.000033 | 0.281180 | −0.90 | 2.83 | 0.05 | 2.93 | 0.05 |
| *Banded gneiss BU-19* | | | | | | | | | | | | | | |
| 1 | 477 | 10 | 0.109696 | 0.008804 | 0.002806 | 0.000222 | 0.282655 | 0.000055 | 0.282630 | 5.48 | 0.89 | 0.08 | 0.96 | 0.02 |
| 2 | 483 | 9 | 0.038299 | 0.002504 | 0.000962 | 0.000049 | 0.282559 | 0.000021 | 0.282550 | 2.78 | 0.98 | 0.03 | 1.10 | 0.02 |
| 3 | 499 | 10 | 0.035754 | 0.000554 | 0.001095 | 0.000029 | 0.282432 | 0.000022 | 0.282422 | −1.42 | 1.16 | 0.03 | 1.32 | 0.02 |
| 4 | 503 | 10 | 0.052423 | 0.001505 | 0.001698 | 0.000053 | 0.282399 | 0.000051 | 0.282383 | −2.69 | 1.23 | 0.07 | 1.39 | 0.02 |
| 9 | 527 | 10 | 0.042901 | 0.000780 | 0.001012 | 0.000019 | 0.281983 | 0.000024 | 0.281973 | −16.68 | 1.79 | 0.03 | 2.09 | 0.02 |
| 12 | 538 | 12 | 0.063694 | 0.003244 | 0.001964 | 0.000092 | 0.282712 | 0.000024 | 0.282692 | 9.04 | 0.79 | 0.03 | 0.84 | 0.02 |
| 15 | 554 | 13 | 0.033317 | 0.001441 | 0.001183 | 0.000054 | 0.282772 | 0.000125 | 0.282759 | 11.76 | 0.68 | 0.18 | 0.72 | 0.02 |
| 16 | 570 | 11 | 0.106679 | 0.000957 | 0.002378 | 0.000033 | 0.282485 | 0.000059 | 0.282459 | 1.50 | 1.13 | 0.09 | 1.24 | 0.02 |
| 17 | 581 | 13 | 0.023812 | 0.000173 | 0.000837 | 0.000010 | 0.282469 | 0.000018 | 0.282459 | 1.73 | 1.10 | 0.03 | 1.24 | 0.02 |
| 18 | 591 | 12 | 0.029093 | 0.000190 | 0.000862 | 0.000008 | 0.282299 | 0.000024 | 0.282290 | −4.04 | 1.34 | 0.03 | 1.53 | 0.02 |
| 21 | 768 | 15 | 0.030391 | 0.001248 | 0.001020 | 0.000046 | 0.282574 | 0.000049 | 0.282560 | 9.45 | 0.96 | 0.07 | 1.01 | 0.02 |
| 24 | 920 | 17 | 0.048214 | 0.000503 | 0.001521 | 0.000021 | 0.282105 | 0.000029 | 0.282079 | −4.20 | 1.64 | 0.04 | 1.81 | 0.02 |
| *Gneissic granitoid BU-1* | | | | | | | | | | | | | | |
| 3 | 402 | 9 | 0.158440 | 0.002550 | 0.005005 | 0.000114 | 0.282639 | 0.000026 | 0.282601 | 2.79 | 0.97 | 0.04 | 1.03 | 0.04 |
| 4 | 404 | 14 | 0.081314 | 0.001776 | 0.002263 | 0.000050 | 0.282645 | 0.000026 | 0.282628 | 3.78 | 0.89 | 0.04 | 0.99 | 0.04 |
| 5 | 406 | 8 | 0.048478 | 0.000580 | 0.001521 | 0.000026 | 0.282693 | 0.000025 | 0.282681 | 5.72 | 0.80 | 0.04 | 0.89 | 0.04 |
| 7 | 413 | 12 | 0.108331 | 0.001434 | 0.003771 | 0.000043 | 0.282628 | 0.000035 | 0.282598 | 2.95 | 0.96 | 0.05 | 1.04 | 0.05 |
| 8 | 414 | 8 | 0.088701 | 0.002463 | 0.003066 | 0.000069 | 0.282784 | 0.000052 | 0.282760 | 8.69 | 0.70 | 0.08 | 0.75 | 0.08 |
| 9 | 415 | 24 | 0.091991 | 0.001105 | 0.002979 | 0.000034 | 0.282667 | 0.000024 | 0.282643 | 4.59 | 0.88 | 0.04 | 0.96 | 0.04 |
| 10 | 421 | 8 | 0.065373 | 0.001157 | 0.002116 | 0.000034 | 0.282632 | 0.000024 | 0.282616 | 3.73 | 0.90 | 0.03 | 1.00 | 0.03 |
| 11 | 426 | 8 | 0.083904 | 0.002672 | 0.002854 | 0.000101 | 0.282734 | 0.000034 | 0.282711 | 7.21 | 0.77 | 0.05 | 0.84 | 0.05 |
| 12 | 433 | 12 | 0.102582 | 0.001228 | 0.002928 | 0.000029 | 0.282682 | 0.000022 | 0.282658 | 5.50 | 0.85 | 0.03 | 0.93 | 0.03 |
| 13 | 474 | 12 | 0.138062 | 0.006301 | 0.004463 | 0.000223 | 0.282711 | 0.000032 | 0.282671 | 6.86 | 0.85 | 0.05 | 0.89 | 0.05 |
| 14 | 478 | 17 | 0.119203 | 0.000882 | 0.003863 | 0.000036 | 0.282649 | 0.000025 | 0.282614 | 4.92 | 0.93 | 0.04 | 0.99 | 0.04 |
| 15 | 493 | 9 | 0.062764 | 0.000316 | 0.001840 | 0.000005 | 0.282668 | 0.000024 | 0.282651 | 6.58 | 0.85 | 0.03 | 0.92 | 0.03 |
| 17 | 527 | 25 | 0.077826 | 0.000669 | 0.002324 | 0.000011 | 0.282637 | 0.000022 | 0.282614 | 6.01 | 0.90 | 0.03 | 0.98 | 0.03 |
| 18 | 539 | 8 | 0.072571 | 0.001591 | 0.002425 | 0.000062 | 0.282707 | 0.000050 | 0.282682 | 8.70 | 0.80 | 0.07 | 0.86 | 0.07 |
| 19 | 609 | 12 | 0.136141 | 0.004302 | 0.004441 | 0.000115 | 0.282681 | 0.000151 | 0.282630 | 8.40 | 0.89 | 0.23 | 0.93 | 0.23 |
| 21 | 843 | 14 | 0.083924 | 0.001583 | 0.002388 | 0.000029 | 0.282721 | 0.000027 | 0.282683 | 15.50 | 0.78 | 0.04 | 0.77 | 0.04 |
| *Gneissic granitoid BU-2* | | | | | | | | | | | | | | |
| 1 | 366 | 10 | 0.104634 | 0.000825 | 0.002822 | 0.000023 | 0.282877 | 0.000035 | 0.282858 | 11.09 | 0.56 | 0.05 | 0.60 | 0.05 |
| 3 | 372 | 9 | 0.109093 | 0.001252 | 0.003048 | 0.000057 | 0.282980 | 0.000036 | 0.282959 | 14.79 | 0.41 | 0.05 | 0.42 | 0.05 |
| 4 | 375 | 8 | 0.129068 | 0.001300 | 0.003282 | 0.000061 | 0.282981 | 0.000043 | 0.282957 | 14.82 | 0.41 | 0.07 | 0.42 | 0.07 |

Table 4 (*continued*)

| Grain no. | U–Pb age* | 1σ | $^{176}Yb/^{177}Hf$ | 2σ | $^{176}Lu/^{177}Hf$ | 2σ | $^{176}Hf/^{177}Hf$ | 2σ | $(^{176}Hf/^{177}Hf)i$ | εHf | $T_{DM}$ (Ga) | 2σ | $T^{C}_{DM}$ (Ga) | 2σ |
|---|---|---|---|---|---|---|---|---|---|---|---|---|---|---|
| *Gneissic granitoid BU-2* | | | | | | | | | | | | | | |
| 5 | 377 | 7 | 0.116985 | 0.001125 | 0.003337 | 0.000054 | 0.283043 | 0.000043 | 0.283019 | 17.03 | 0.32 | 0.07 | 0.31 | 0.07 |
| 8 | 378 | 8 | 0.093337 | 0.000882 | 0.002584 | 0.000040 | 0.282907 | 0.000043 | 0.282888 | 12.44 | 0.51 | 0.06 | 0.54 | 0.06 |
| 15 | 385 | 8 | 0.164779 | 0.005204 | 0.004820 | 0.000257 | 0.283028 | 0.000084 | 0.282993 | 16.31 | 0.35 | 0.13 | 0.35 | 0.13 |
| 16 | 387 | 8 | 0.183991 | 0.008856 | 0.004851 | 0.000195 | 0.282933 | 0.000035 | 0.282898 | 12.95 | 0.50 | 0.05 | 0.52 | 0.05 |
| 25 | 424 | 9 | 0.167217 | 0.004162 | 0.004586 | 0.000096 | 0.283007 | 0.000043 | 0.282970 | 16.35 | 0.38 | 0.07 | 0.38 | 0.07 |
| *Gneissic granitoid BU-3* | | | | | | | | | | | | | | |
| 2 | 354 | 7 | 0.123238 | 0.003613 | 0.003195 | 0.000070 | 0.282666 | 0.000027 | 0.282645 | 3.28 | 0.88 | 0.04 | 0.97 | 0.04 |
| 3 | 362 | 8 | 0.085645 | 0.005231 | 0.002858 | 0.000159 | 0.282720 | 0.000052 | 0.282701 | 5.43 | 0.79 | 0.08 | 0.87 | 0.08 |
| 4 | 369 | 8 | 0.094213 | 0.002815 | 0.002550 | 0.000129 | 0.282787 | 0.000035 | 0.282769 | 8.01 | 0.69 | 0.05 | 0.75 | 0.05 |
| 5 | 391 | 8 | 0.073664 | 0.002381 | 0.002019 | 0.000075 | 0.282672 | 0.000026 | 0.282657 | 4.53 | 0.85 | 0.04 | 0.94 | 0.04 |
| 7 | 399 | 8 | 0.064554 | 0.001622 | 0.001998 | 0.000060 | 0.282707 | 0.000024 | 0.282692 | 5.96 | 0.79 | 0.03 | 0.88 | 0.03 |
| 12 | 420 | 9 | 0.054435 | 0.000717 | 0.001503 | 0.000017 | 0.282654 | 0.000026 | 0.282642 | 4.65 | 0.86 | 0.04 | 0.96 | 0.04 |
| 14 | 425 | 9 | 0.062717 | 0.001987 | 0.001714 | 0.000093 | 0.282828 | 0.000061 | 0.282814 | 10.86 | 0.61 | 0.09 | 0.66 | 0.09 |
| 15 | 428 | 9 | 0.121308 | 0.001984 | 0.004100 | 0.000067 | 0.282629 | 0.000035 | 0.282596 | 3.18 | 0.96 | 0.05 | 1.04 | 0.05 |
| 16 | 429 | 9 | 0.111849 | 0.002614 | 0.003505 | 0.000073 | 0.282732 | 0.000034 | 0.282704 | 7.02 | 0.79 | 0.05 | 0.85 | 0.05 |
| 18 | 439 | 9 | 0.051958 | 0.001413 | 0.001426 | 0.000034 | 0.282703 | 0.000024 | 0.282691 | 6.80 | 0.79 | 0.03 | 0.87 | 0.03 |
| 19 | 440 | 9 | 0.100275 | 0.003193 | 0.002756 | 0.000084 | 0.282653 | 0.000024 | 0.282631 | 4.67 | 0.89 | 0.04 | 0.97 | 0.04 |
| 21 | 440 | 9 | 0.066258 | 0.000660 | 0.001910 | 0.000016 | 0.282682 | 0.000029 | 0.282666 | 5.94 | 0.83 | 0.04 | 0.91 | 0.04 |
| 22 | 441 | 9 | 0.060804 | 0.000439 | 0.001637 | 0.000007 | 0.282727 | 0.000024 | 0.282714 | 7.64 | 0.76 | 0.03 | 0.83 | 0.03 |
| 23 | 442 | 9 | 0.062626 | 0.002447 | 0.002188 | 0.000072 | 0.282625 | 0.000050 | 0.282607 | 3.89 | 0.92 | 0.07 | 1.01 | 0.07 |
| 25 | 443 | 9 | 0.047914 | 0.002322 | 0.001261 | 0.000043 | 0.282678 | 0.000021 | 0.282667 | 6.04 | 0.82 | 0.03 | 0.91 | 0.03 |
| 27 | 448 | 10 | 0.068735 | 0.000500 | 0.002313 | 0.000038 | 0.282707 | 0.000026 | 0.282688 | 6.88 | 0.80 | 0.04 | 0.87 | 0.04 |
| *Gneissic granitoid BU-12* | | | | | | | | | | | | | | |
| 2 | 433 | 8 | 0.081821 | 0.001577 | 0.002328 | 0.000048 | 0.282733 | 0.000031 | 0.282714 | 7.49 | 0.76 | 0.05 | 0.83 | 0.05 |
| 3 | 434 | 9 | 0.067204 | 0.002345 | 0.002181 | 0.000103 | 0.282707 | 0.000048 | 0.282689 | 6.62 | 0.80 | 0.07 | 0.87 | 0.07 |
| 4 | 437 | 8 | 0.067539 | 0.001758 | 0.001944 | 0.000051 | 0.282580 | 0.000039 | 0.282564 | 2.25 | 0.98 | 0.06 | 1.09 | 0.06 |
| 6 | 438 | 9 | 0.025383 | 0.001661 | 0.000820 | 0.000053 | 0.282791 | 0.000039 | 0.282784 | 10.08 | 0.65 | 0.05 | 0.70 | 0.05 |
| 7 | 438 | 8 | 0.064264 | 0.002857 | 0.001950 | 0.000086 | 0.282642 | 0.000031 | 0.282626 | 4.48 | 0.89 | 0.04 | 0.98 | 0.04 |
| 8 | 439 | 8 | 0.272317 | 0.008354 | 0.007947 | 0.000240 | 0.282694 | 0.000037 | 0.282628 | 4.58 | 0.97 | 0.06 | 0.98 | 0.06 |
| 10 | 442 | 9 | 0.063565 | 0.003692 | 0.001707 | 0.000093 | 0.282608 | 0.000027 | 0.282593 | 3.41 | 0.93 | 0.04 | 1.04 | 0.04 |
| 11 | 442 | 8 | 0.041940 | 0.000826 | 0.001395 | 0.000041 | 0.282865 | 0.000047 | 0.282854 | 12.62 | 0.55 | 0.07 | 0.58 | 0.07 |
| 12 | 447 | 9 | 0.069840 | 0.003146 | 0.002131 | 0.000088 | 0.282585 | 0.000028 | 0.282568 | 2.60 | 0.97 | 0.04 | 1.08 | 0.04 |
| 16 | 452 | 9 | 0.049197 | 0.002016 | 0.001484 | 0.000074 | 0.282605 | 0.000034 | 0.282592 | 3.59 | 0.93 | 0.05 | 1.04 | 0.05 |
| 17 | 453 | 9 | 0.061585 | 0.003372 | 0.001811 | 0.000111 | 0.282722 | 0.000029 | 0.282706 | 7.64 | 0.77 | 0.04 | 0.84 | 0.04 |
| 18 | 453 | 9 | 0.046743 | 0.001724 | 0.001436 | 0.000064 | 0.282782 | 0.000030 | 0.282770 | 9.88 | 0.67 | 0.04 | 0.73 | 0.04 |
| 20 | 456 | 9 | 0.067361 | 0.001834 | 0.001956 | 0.000056 | 0.282674 | 0.000033 | 0.282657 | 5.97 | 0.84 | 0.05 | 0.92 | 0.05 |
| 21 | 456 | 12 | 0.069153 | 0.002504 | 0.002089 | 0.000078 | 0.282599 | 0.000027 | 0.282581 | 3.28 | 0.95 | 0.04 | 1.06 | 0.04 |
| 22 | 457 | 9 | 0.066344 | 0.003577 | 0.001977 | 0.000095 | 0.282641 | 0.000033 | 0.282624 | 4.81 | 0.89 | 0.05 | 0.98 | 0.05 |
| 24 | 459 | 9 | 0.050849 | 0.001130 | 0.001427 | 0.000031 | 0.282690 | 0.000025 | 0.282678 | 6.76 | 0.81 | 0.04 | 0.89 | 0.04 |
| 25 | 459 | 9 | 0.050475 | 0.000664 | 0.001454 | 0.000024 | 0.282706 | 0.000036 | 0.282694 | 7.34 | 0.78 | 0.05 | 0.86 | 0.05 |
| 27 | 464 | 9 | 0.066283 | 0.001576 | 0.002000 | 0.000044 | 0.282652 | 0.000034 | 0.282635 | 5.36 | 0.87 | 0.05 | 0.96 | 0.05 |
| 28 | 464 | 9 | 0.069818 | 0.003294 | 0.002088 | 0.000090 | 0.282657 | 0.000030 | 0.282639 | 5.50 | 0.87 | 0.04 | 0.95 | 0.04 |
| 29 | 464 | 9 | 0.047566 | 0.000412 | 0.001413 | 0.000014 | 0.282620 | 0.000056 | 0.282608 | 4.41 | 0.91 | 0.08 | 1.01 | 0.08 |
| 30 | 468 | 9 | 0.075254 | 0.000492 | 0.002114 | 0.000012 | 0.282705 | 0.000026 | 0.282686 | 7.27 | 0.80 | 0.04 | 0.87 | 0.04 |
| 31 | 471 | 9 | 0.109054 | 0.002125 | 0.003696 | 0.000073 | 0.282704 | 0.000067 | 0.282671 | 6.80 | 0.84 | 0.10 | 0.89 | 0.10 |
| 32 | 472 | 9 | 0.049612 | 0.003276 | 0.001603 | 0.000089 | 0.282757 | 0.000026 | 0.282743 | 9.37 | 0.71 | 0.04 | 0.77 | 0.04 |
| 36 | 482 | 9 | 0.052730 | 0.001255 | 0.001573 | 0.000047 | 0.282667 | 0.000030 | 0.282653 | 6.40 | 0.84 | 0.04 | 0.92 | 0.04 |

paragneisses. They show concentric, oscillatory zoning, and have Th/U ratios from 0.2 to 1.6 (Tables 3 and 5). Compared to zircons from the banded gneisses, those from the granitoids lack inherited cores and overgrowth rims, and have lower U and Th contents (Table 3).

#### 6.2.1. Sample BU-1

Most zircons cluster together and give a weighted mean $^{206}Pb/^{238}U$ age of 412±5 Ma (Fig. 9a and Table 5), interpreted to be the crystallization age of the granitoid. Their $\varepsilon_{Hf}(t)$ values vary from +2.8 to +8.7,

Table 5
Summary of zircon U–Pb and Hf isotopic results for the banded gneiss and gneissic granitoid in the Chinese Altai

| | No. of analysis | $^{206}Pb/^{238}U$ age (Ma) | Weighted mean (Ma) | Zircon type | U ppm | Th ppm | Th/U | $\varepsilon_{Hf}(t)$ | $T^{C}_{DM}$ (Ga) |
|---|---|---|---|---|---|---|---|---|---|
| *Banded gneiss* | | | | | | | | | |
| BU-4 | 24 | 479–533 | 505±7 | I | 5–491 | 49–732 | 0.09–1.71 | −7.0 to +7.6 | 0.90–1.59 |
| | 4 | 569–581 | 574±11 | I or III | 27–213 | 50–1121 | 0.08–0.94 | | |
| | 5 | 638–1023 | | I or III | 16–290 | 82–881 | 0.15–0.41 | −1.8 to +2.6 | 1.45–1.81 |
| | 2 | 1994±44[a] | | II | 35–150 | 36–299 | 0.5–0.99 | −11.2 | 3.04 |
| | | 2516±37[a] | | | | | | | |
| BU-5 | 16 | 480–538 | 517±8 | I or III | 6–441 | 89–1016 | 0.02–0.75 | −17.5 to +12.6 | 0.64–2.12 |
| | 13 | 592–876 | | I or III | 12–740 | 36–1259 | 0.17–0.82 | −5.5 to +10.7 | 0.83–1.71 |
| | 2 | 2048±58[a] | | II | 112–257 | 473–693 | 0.54–0.16 | +2.2 | 2.43 |
| | | 2159±54[a] | | | | | | | |
| BU-13 | 18 | 446–519 | 481±11 | I | 6–216 | 21–331 | 0.1–1.1 | −6.4 to +14.7 | 0.54–1.55 |
| | 2 | 573–585 | | I | 87–159 | 500–931 | 0.17 | | |
| | 7 | 694–956 | | I or III | 3–173 | 20–255 | 0.11–0.72 | −15.8 to +7.2 | 1.07–2.21 |
| | 2 | 1580±55[a] | | I or III | 25–31 | 65–91 | 0.33–0.38 | | |
| | | 1942±54[a] | | | | | | | |
| | 2 | 2347±72[a] | | II | 5–13 | 15–35 | 0.15–0.87 | −4.7 | 3.01 |
| | | 2626±46[a] | | | | | | | |
| Bu-14 | 24 | 426–524 | 466±11 | I | 11–573 | 139–1336 | 0.02–0.83 | −17.4 to +3.8 | 1.03–2.07 |
| | 8 | 640–907 | | I | 20–264 | 57–1231 | 0.21–0.50 | −12.1 to +10.0 | 0.99–1.96 |
| | 3 | 1890±57[a] | | II or I | 42–701 | 140–2203 | 0.30–0.38 | −0.9 | 2.93 |
| | | 2472±51[a] | | | | | | | |
| | | 2634±65[a] | | | | | | | |
| BU-19 | 19 | 477–597 | 528±16 | I | 95–1419 | 161–1199 | 0.27–1.79 | −16.7 to +11.8 | 0.72–2.09 |
| | 5 | 729–936 | | I | 93–1125 | 156–2468 | 0.2–1.2 | −4.2 to +9.5 | 1.0–1.8 |
| *Gneissic granitoid* | | | | | | | | | |
| BU-1 | 12 | 401–433 | 412±5 | | 120–703 | 215–594 | 0.43–1.18 | +2.8 to +8.7 | 0.75–1.04 |
| | 6 | 474–539 | 505±23 | | 75–1666 | 77–1635 | 0.36–1.38 | +4.9 to +8.7 | 0.86–0.99 |
| | 4 | 609–878 | | | 660–1125 | 522–711 | 1.17–1.58 | +8.4 to +15.5 | 0.77–0.93 |
| Bu-2 | 21 | 366–399 | 381±4 | | 17–58 | 29–102 | 0.53–0.94 | +11 to +17 | 0.31–0.60 |
| | 9 | 415–430 | 424±3 | | 19–61 | 19–84 | 0.73–1.0 | +16 | 0.38 |
| | 3 | 475–494 | 482±15 | | 14–49 | 16–37 | 0.88–1.3 | | |
| BU-3 | 23 | 391–448 | 425±8 | | 16–553 | 23–453 | 0.36–1.27 | +3.2 to +10.9 | 0.66–1.04 |
| | 4 | 352–369 | 359±7 | | 20–313 | 86–503 | 0.23–0.62 | +3.3 to +8.0 | 0.75–0.97 |
| BU-12 | 36 | 431–482 | 453±5 | | 11–186 | 20–350 | 0.16–0.97 | +2.3 to +12.6 | 0.58–1.09 |

[a] $^{207}Pb/^{206}Pb$ age.

and their $T^{C}_{DM}$ model ages range from 0.75 to 1.04 Ga (Table 4 and Fig. 10a).

Six zircons form a minor population with a weighted mean $^{206}Pb/^{238}U$ age of 505±23 Ma (Fig. 9a, Table 3), and give $\varepsilon_{Hf}(t)$ values from +4.9 to +8.7 and $T^{C}_{DM}$ model ages from 0.86 to 0.99 Ga. Four additional grains give Neoproterozoic $^{206}Pb/^{238}U$ ages (609-878 Ma) (Fig. 9a, Table 3), $\varepsilon_{Hf}(t)$ values from +8.4 to +15.5 and $T^{C}_{DM}$ model ages from 0.77 to 0.93 Ga (Table 4 and Fig. 10a). We note that zircon $\varepsilon_{Hf}(t)$ values of this sample decrease linearly with zircon age (Fig. 10a).

### 6.2.2. Sample BU-2

The majority of zircons give a weighted mean $^{206}Pb/^{238}U$ age of 381±4 Ma (Fig. 9b, Table 3), considered to represent the crystallization age of the granitoid. The $\varepsilon_{Hf}(t)$ values of these zircons vary from +11.1 to +17.0, and their $T^{C}_{DM}$ model ages are from 0.31 to 0.60 Ga (Table 4 and Fig. 10b).

A minor population is defined by nine analyses which give a weighted mean $^{206}Pb/^{238}U$ age of 424±3 Ma. One zircon from this group was analysed for Hf isotopic composition, giving a $\varepsilon_{Hf}(t)$ value of +16 and a $T^{C}_{DM}$ model age of 0.38 Ga (Table 4 and Fig. 10b). Three additional zircons yielded a weighted mean $^{206}Pb/^{238}U$ age of 482±15 Ma. (Fig. 9b, Table 3).

### 6.2.3. Sample Bu-3

Most zircons from this sample form a dense population and give a weighted mean $^{206}Pb/^{238}U$ age of 425±8 Ma (Fig. 9c and Table 3), $\varepsilon_{Hf}(t)$ values from +3.2 to +10.9, and $T^{C}_{DM}$ model ages from 0.66 to 1.04 Ga (Table 4 and Fig. 10c). This $^{206}Pb/^{238}U$ age is considered to represent the crystallization age of this granitoid. The remaining

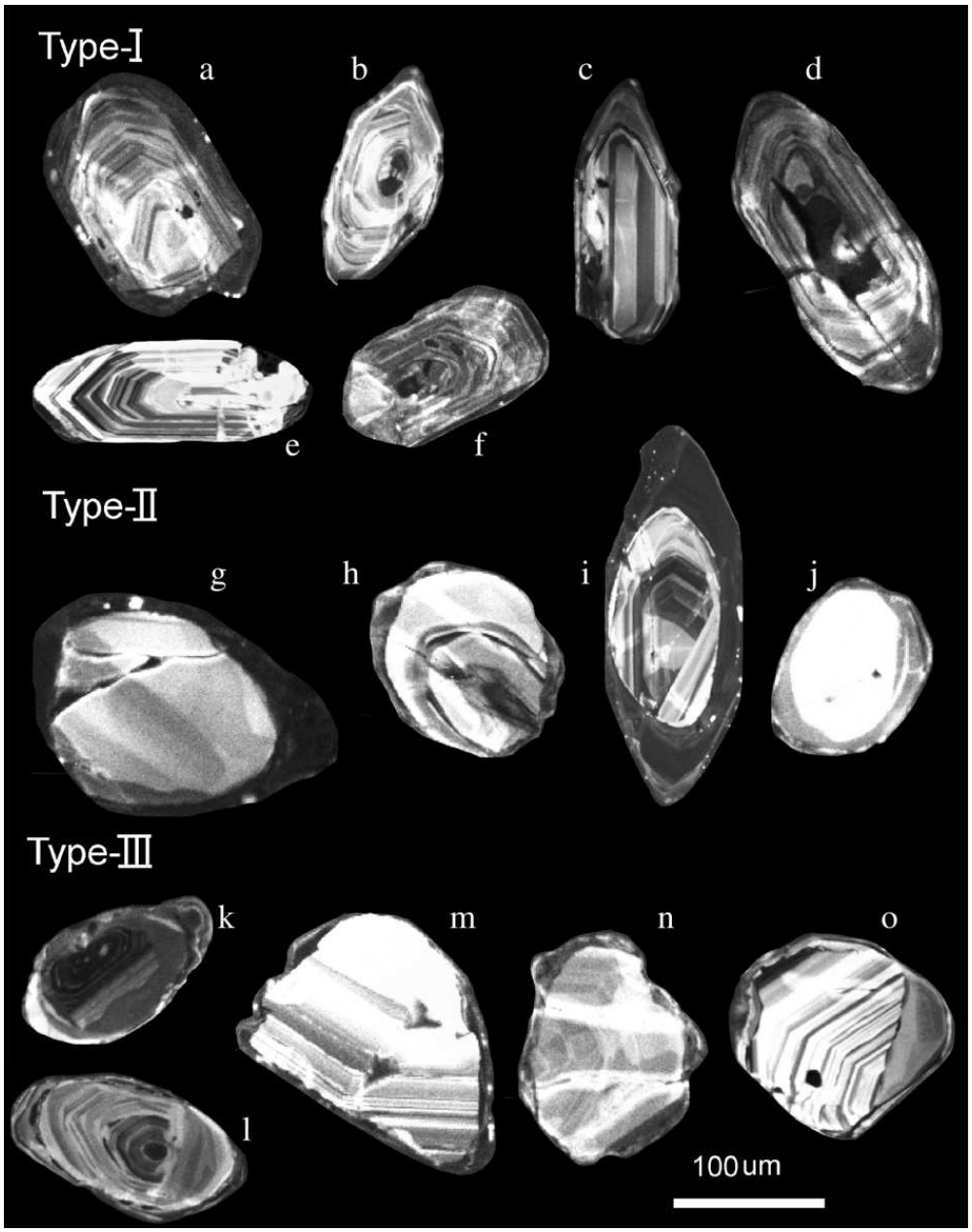


Fig. 5. Representative cathodoluminescence images for detrital zircons from the banded paragneisses. Three types of structural features are recognized: Type-I zircons are euhedral prismatic crystals without obvious cores, Type-II zircons are characterized by rounded cores and Type-III zircons have fragmented cores with overgrowth rims. The zircon grains with alphabetic order are BU-4(14), BU-5(1), BU-5(4), BU-13(15), BU-14 (26), BU-14(12), BU-4(34), BU-13(31), BU-13(30), BU-5(30), BU5(22), BU-14(29), BU-13(29), BU-5(29). Numbers in bracket refer to grain numbers in Table 3.

four grains give a weighted mean $^{206}Pb/^{238}U$ age of 359±7 Ma (Fig. 9c and Table 3), interpreted to be a result of a later thermal disturbance. Their $\varepsilon_{Hf}(t)$ values range from +3.3 to +8.0 and their $T^{C}_{DM}$ model ages range from 0.75 to 0.97 Ga (Table 4 and Fig. 10c).

*6.2.4. Sample Bu-12*

All the thirty six analysed zircons cluster together and yield a weighted mean $^{206}Pb/^{238}U$ age of 453±5 Ma (Fig. 9d and Table 3), $\varepsilon_{Hf}(t)$ values from +2.3 to +12.6 and $T^{C}_{DM}$ model ages from 0.58 to 1.09 Ga (Table 4 and Fig. 10d).

## 7. Discussion

### *7.1. Protoliths of the banded gneisses*

This study shows that the banded gneisses of the Central Altai and Qiongkuer Domains are indistinguishable in geochemistry, zircon U–Pb age and Hf isotopic

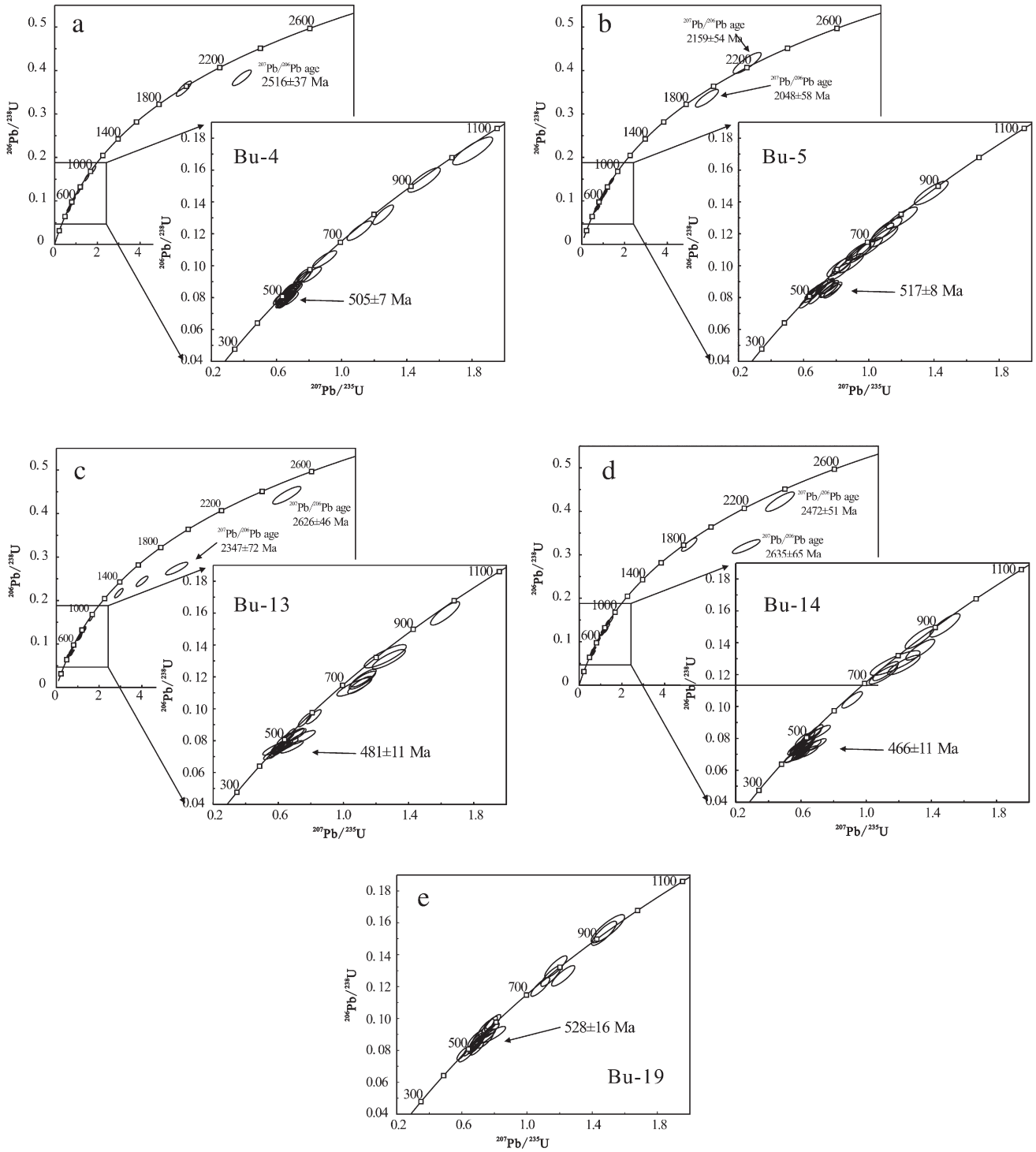


Fig. 6. U–Pb concordia diagrams for detrital zircons from the banded paragneisses.

composition. They have felsic compositions similar to the associated gneissic granitoids in terms of $SiO_2$, $Al_2O_3$, CaO, Sr, Nb, Y, and Zr (Table 2). However, the banded gneisses can be distinguished from the gneissic granitoids by their banded structure, occurrence of sillimanite, relatively high A/NK and A/CNK values, negative DF values of Shaw (1972), and higher MgO contents (Table 2). Their protoliths cannot be mature sediments, because they have relatively high MgO, Ni, Cr, and U contents (Table 2). Removal of labile cations such as $K^+$, $Na^+$ and $Ca^{2+}$relative to stable residual constituents ($Al^{3+}$, $Ti^{4+}$) will result in high CIA values. For example, Phanerozoic shales generally have CIA values from 70 to 75 (Nesbitt and Young, 1982; 1984). On the other hand, because of

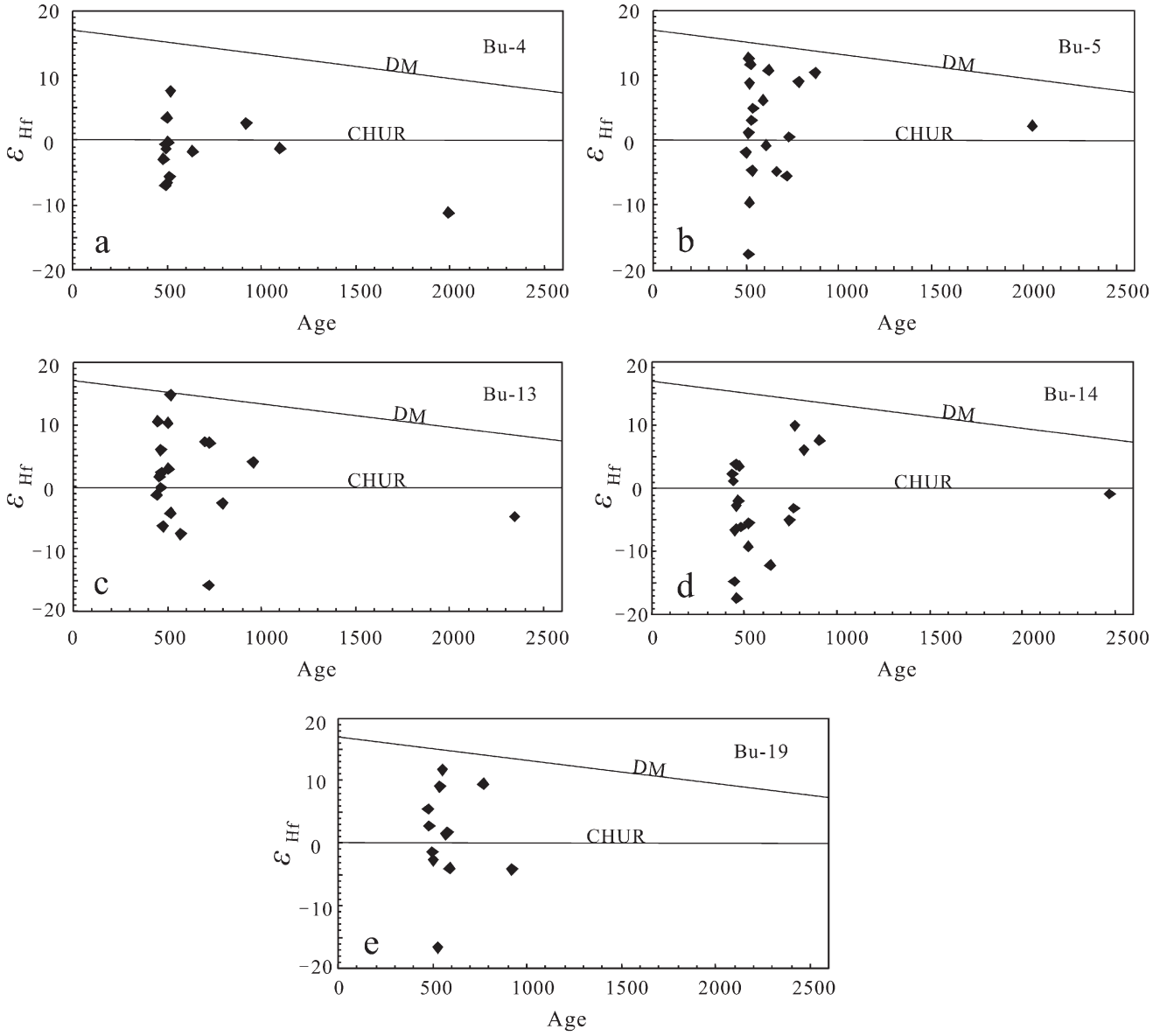


Fig. 7. Diagram of εHf values vs. U–Pb ages for zircons from the banded paragneisses. $^{206}Pb/^{238}U$ ages are used for gains < 1000 Ma, and $^{207}Pb/^{206}Pb$ ages are used for gains > 1000 Ma.

the high contents of $Al_2O_3$ in clay minerals, mature sediments such as passive continental margin deposits have low ICV values (Cox et al., 1995). The banded gneisses in this study all have low CIA and high ICV values (Fig. 4), indicating the immature nature of their protoliths. Their low Zr/Sc and Th/U ratios also suggest the immature nature of these rocks, because these ratios will increase significantly in sediment recycling due to zircon enrichment and formation and removal of highly soluble $U^{+6}$-bearing species, respectively (McLennan and Taylor, 1980). In summary, our geochemical data suggest that the protoliths of these banded gneisses were immature clastic sediments, possibly containing significant amounts of volcanic material.

These paragneisses contain three different types of zircons (Fig. 5). Type-I zircons are interpreted to have had very short sedimentary transport and possibly derived from nearby igneous rocks, based on their euhedral prismatic shape, concentric oscillatory zoning, high Th/U ratios and the lack of inherited cores. Type-II zircons possibly underwent longer transport as shown by their large, rounded cores. The fragmental cores of Type-III zircons are considered to be a result of volcanic eruption and therefore we interpret this type of zircons originally came from a pyroclastic source. We did not study the thin structureless, low-luminescence rims on Type-II and Type-III zircons, which are possibly metamorphic in origin. These variations in zircon

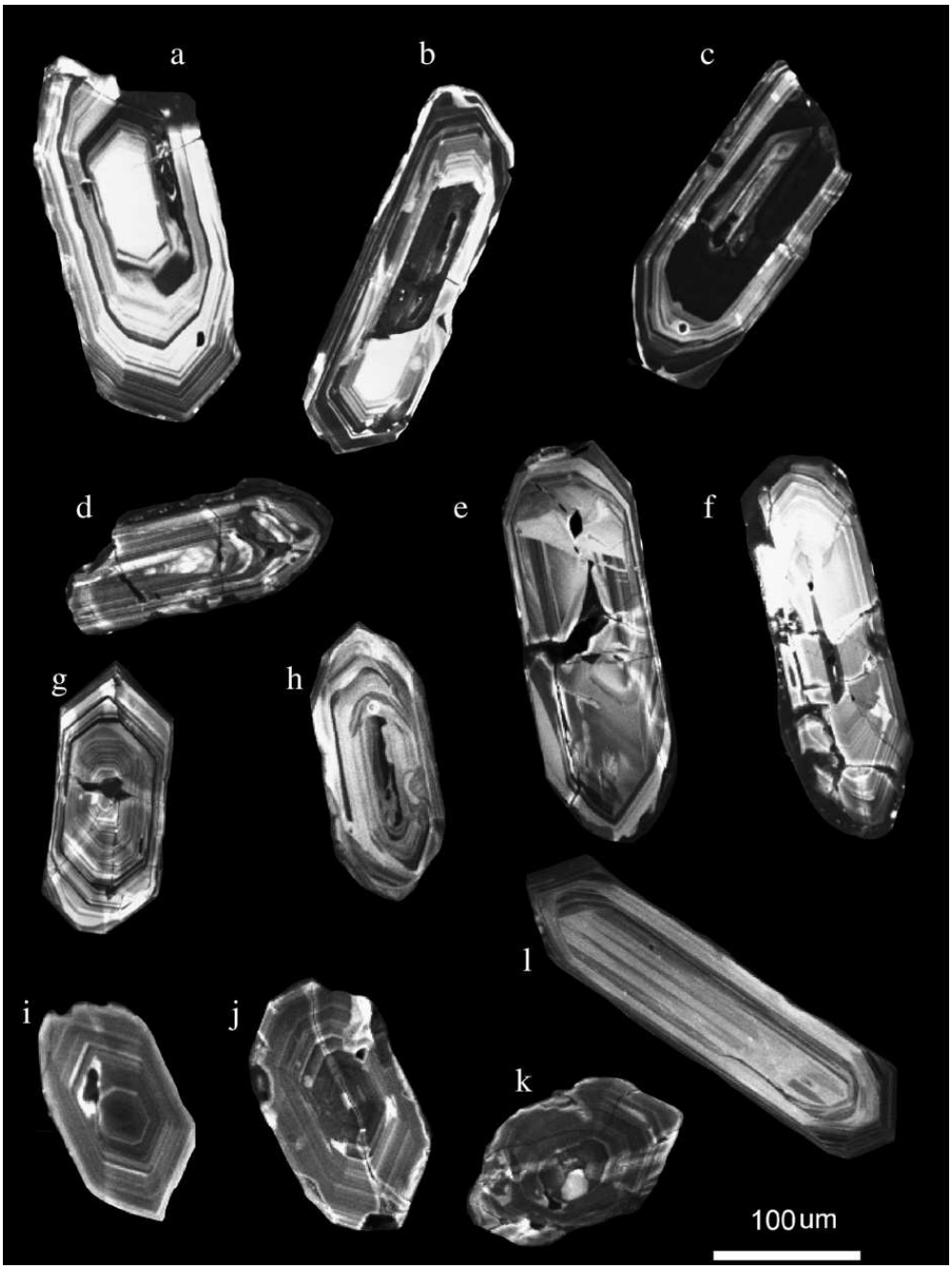


Fig. 8. Representative cathodoluminescence images for magmatic zircons from the gneissic granitoids. All zircons are euhedral prismatic. The zircon grains with alphabetic order are BU-1(18), BU-1(17), BU-1(22), BU-3(21), BU-3(5), BU-3(16), BU-12(36), BU-12(25), BU-2(9), BU-2(4), BU-2 (3), BU-12(22). The numbers in bracket refer to the grain numbers in Table 3.

structure suggest a variety of sources for the banded gneisses, possibly including local magmatic rocks, input of contemporaneous volcanic material, and contributions from remote sedimentary sequences. Compared with the gneissic granitoids, which have zircons with relatively low and narrow ranges of U contents and Th/U ratios, the banded gneisses have zircons with large variations in both Th and U (Table 3, Fig. 11). This feature may also imply diverse sources for their protoliths. Hence, we suggest that the protoliths were immature clastic sediments with significant input from nearby magmatic rocks and minor contributions from distant sedimentary sequences.

### *7.2. Age of banded paragneisses and significance of early Paleozoic zircons*

The high-grade metamorphic rocks in the region were previously considered to be the high-grade metamorphic

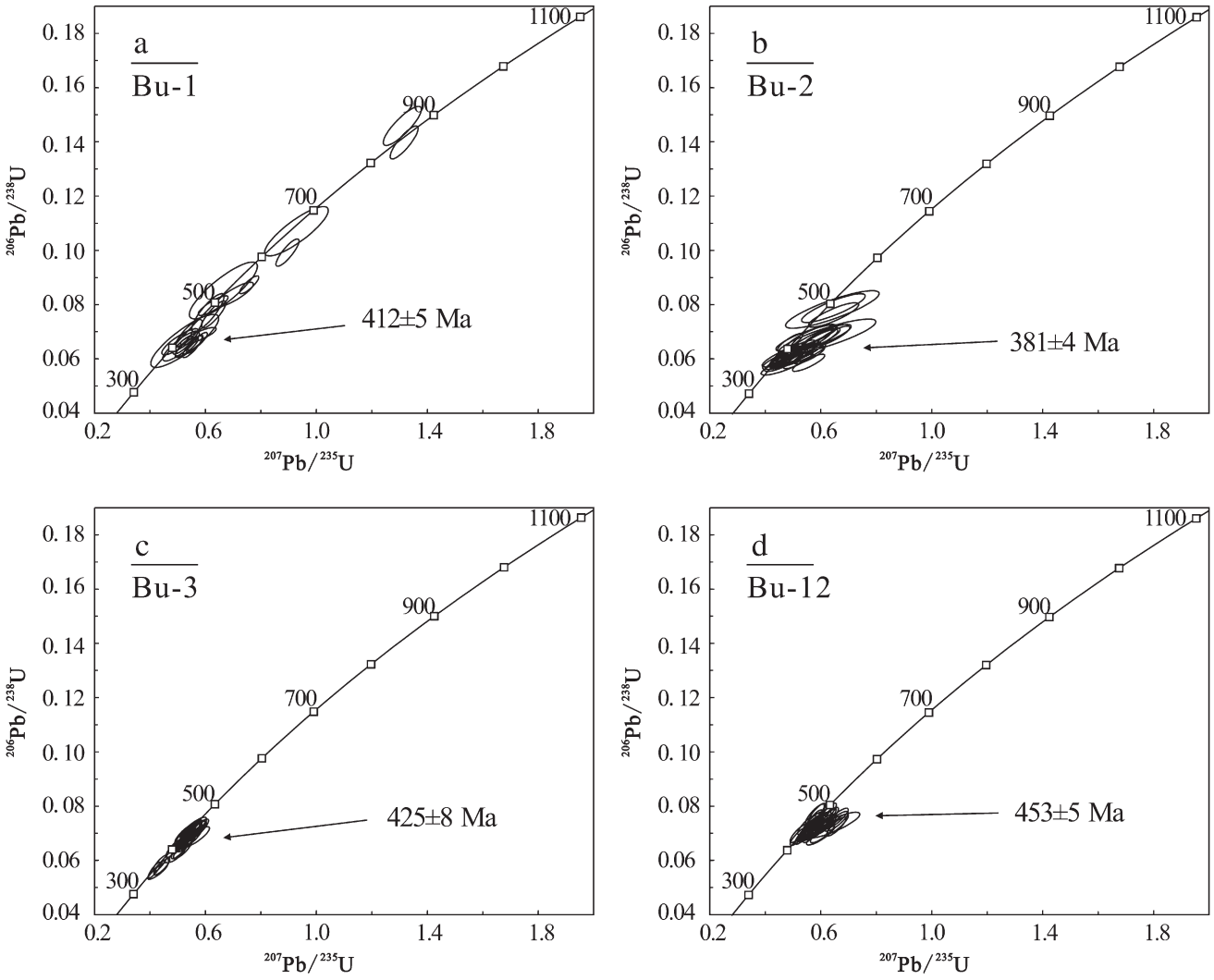


Fig. 9. U–Pb concordia diagrams for zircons from the gneissic granitoids.

equivalents of the Habahe Group, but more recently have been assigned Proterozoic ages (e.g. Li et al., 1996, 2006). Consequently, they were considered to represent a Precambrian basement (e.g. Windley et al., 2002; Li et al., 2003) or a microcontinent that may extend southwards and also underlie the Junggar Basin (Li et al., 2006). Our data indicate that the sedimentary protoliths of the banded gneisses cannot be older than 466 Ma, the youngest zircon population age of these rocks, and cannot be younger than 453 Ma, the oldest intrusive gneissic granitoid dated in this study. Therefore, the banded gneisses cannot represent a Precambrian basement, but, instead, were probably deposited in the Ordovician.

The youngest zircons from each sample of the banded gneisses always form a dominant $^{206}Pb/^{238}U$ age population (Table 3 and Fig. 6), i.e. 466, 481, 505, 517, and 528 Ma, respectively for the analyzed samples. Because these zircons mostly have Type-I, with minor Type-III, morphological features (Table 5 and Fig. 5), we suggest that Early Paleozoic igneous rocks could have been the major source for the banded gneiss protoliths. Indeed, volcanic rocks of this age exist in the Central Altai, such as the 505±2 Ma rhyolite (Pb–Pb zircon evaporation age) dated by Windley et al. (2002) and the 475±5 Ma dacite (zircon U–Pb age) dated by Shan et al. (2005).

The Early Paleozoic zircons from the banded gneisses have a large variation in Hf isotopic compositions, i.e. their $\varepsilon Hf(t)$ values ranging continuously from −17 to +15 (Table 5). Such a large isotopic variation indicates both juvenile and old materials were involved in the generation of magmas in which these zircons crystallized. The continuous $\varepsilon Hf(t)$ variation and the large number of zircons with positive $\varepsilon Hf(t)$ values suggest a possible magma mixing process with juvenile magma as the major component. A subduction

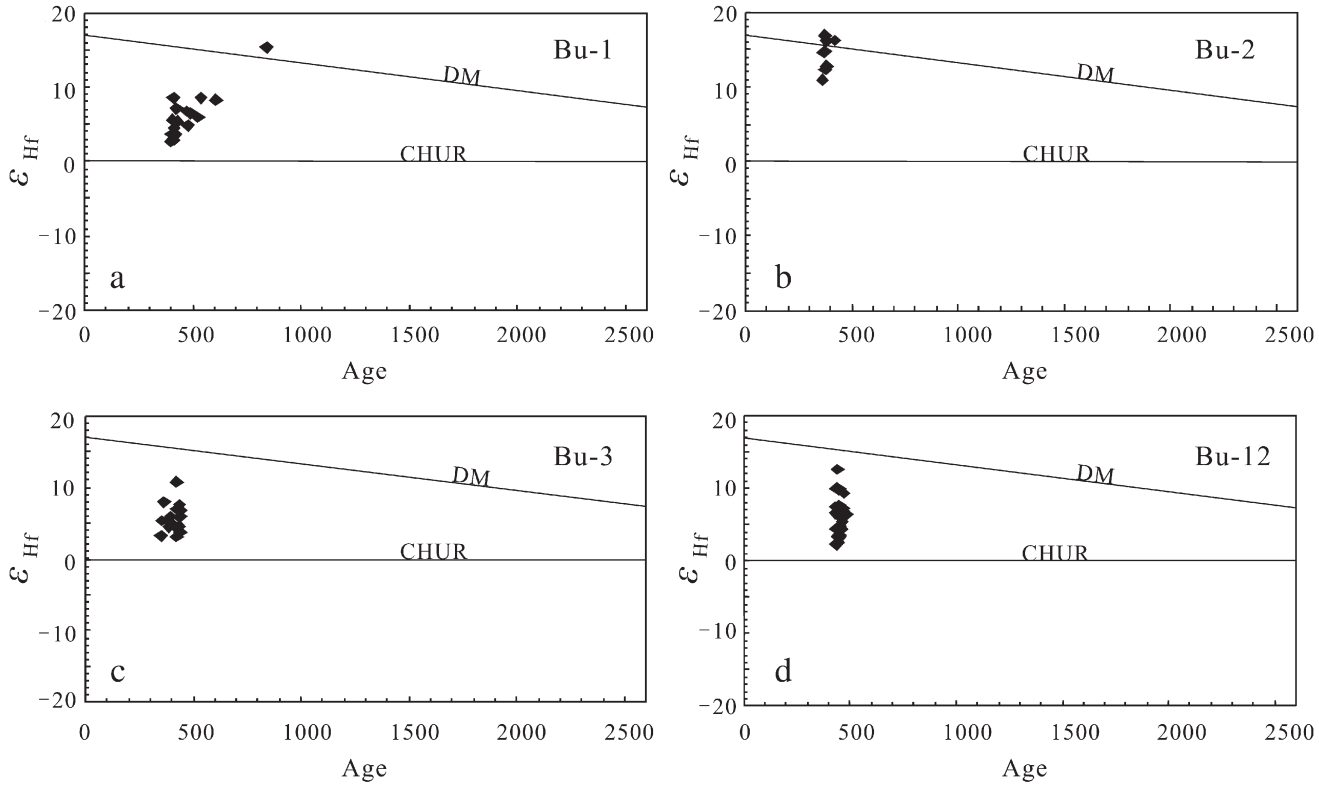


Fig. 10. Diagram of εHf values vs. $^{206}Pb/^{238}U$ ages for zircons from the gneissic granitoids.

environment would be ideal for such a magmatic activity, therefore, our data may imply an important crustal accretionary process in the Early Paleozoic. The calkaline geochemical compositions of the above mentioned Early Paleozoic felsic volcanic rocks in the Chinese Altai support this interpretation (Windley et al., 2002; Shan et al., 2005).

Our recent geochemical and geochronological studies demonstrate that the Habahe Group metasediments contain detrital zircons with ages dominantly in the range of 460 to 570 Ma and may have been deposited in a continental arc or an active continental margin setting (Long et al., 2006, 2007, in press). Results of this study suggest some genetic link between the banded gneisses and the Habahe Group metasedimentary rocks: the banded gneisses are possibly high-grade metamorphic equivalent of the Habahe Group, they both deposited in a continental arc or active continental margin environment. Our data do not support a simple basement-cover relationship in the Chinese Altai.

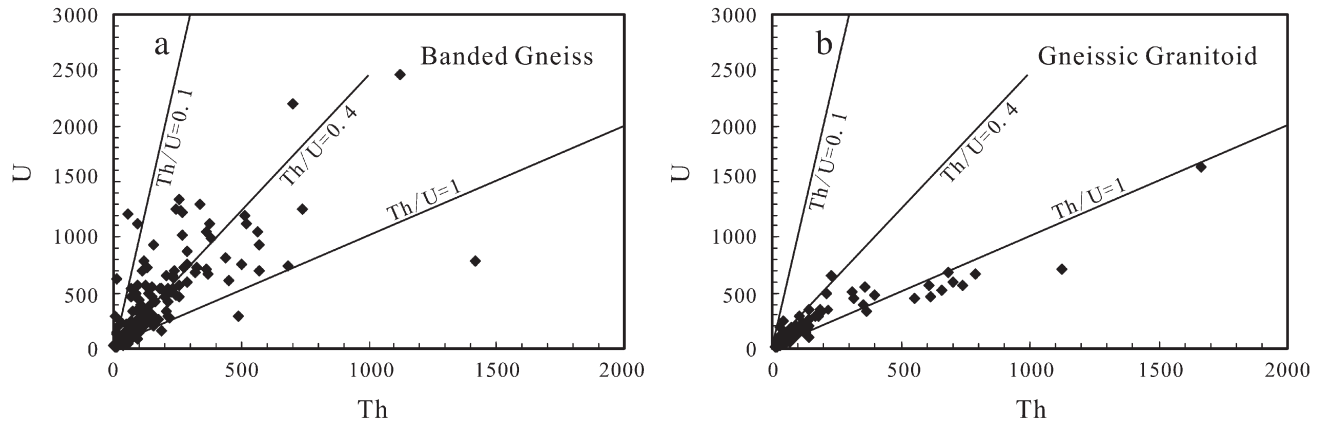


Fig. 11. U–Th diagram for zircons from the banded paragneisses and gneissic granitoids.

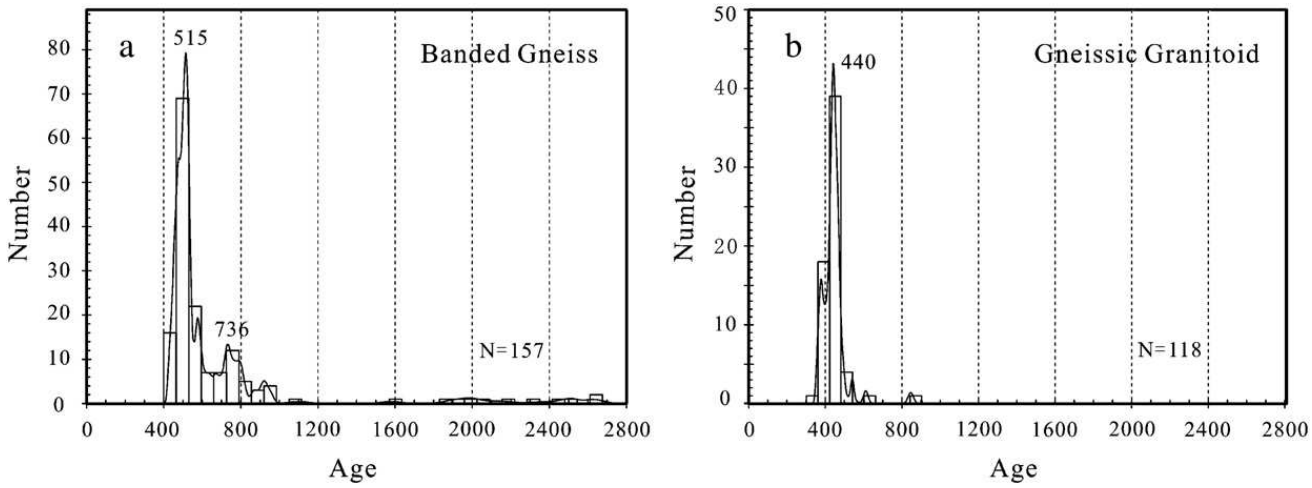


Fig. 12. Zircon age histogram for the banded paragneisses and gneissic granitoids.

### 7.3. Origin and significance of the gneissic granitoids

The gneissic granitoids are metaluminous, show characteristics of I-type granites, and plot in arc field in tectonic discrimination diagrams. Our zircon Hf data clearly indicate contribution of juvenile materials in their petrogenesis. Therefore we suggest that these granitoids were emplaced in a subduction-related environment. Our data indicate that the gneissic granitoids were emplaced between 453 and 381 Ma (Fig. 9 and Table 3). This age range is systematically, but only slightly, younger than the dominant early Paleozoic zircon populations of the banded paragneisses (528 to 466 Ma, Fig. 12 and Table 3). However, zircons from the gneissic granitoids are geochemically different from the Paleozoic zircons of the banded gneisses: (1) they generally have low U contents (mostly <700 ppm) and high Th/U ratios (mostly >0.4), whereas those from the banded gneisses have more variable U contents and Th/U ratios (Fig. 11); and (2) they all have positive $\varepsilon$Hf ($t$) values and the highest ones plot on the depleted mantle evolution line, whereas those from the banded gneisses have more variable $\varepsilon$Hf($t$) values (−17.5 to +14.7) (Figs. 7 and 10). These features may imply a significant increase in the contribution of juvenile material to the magma source in the middle Paleozoic (453–380 Ma). This is also reflected in the Hf model ages ($T_{DM}^{C}$ ); those for the gneissic granitoids are generally younger than 1.0 Ga, whereas those for the early Paleozoic zircons are mostly older than 1.0 Ga (Table 4, Fig. 13).

The gneissic granitoids represent an important episode of magmatic activity in the region, because other large gneissic plutons were also emplaced in the

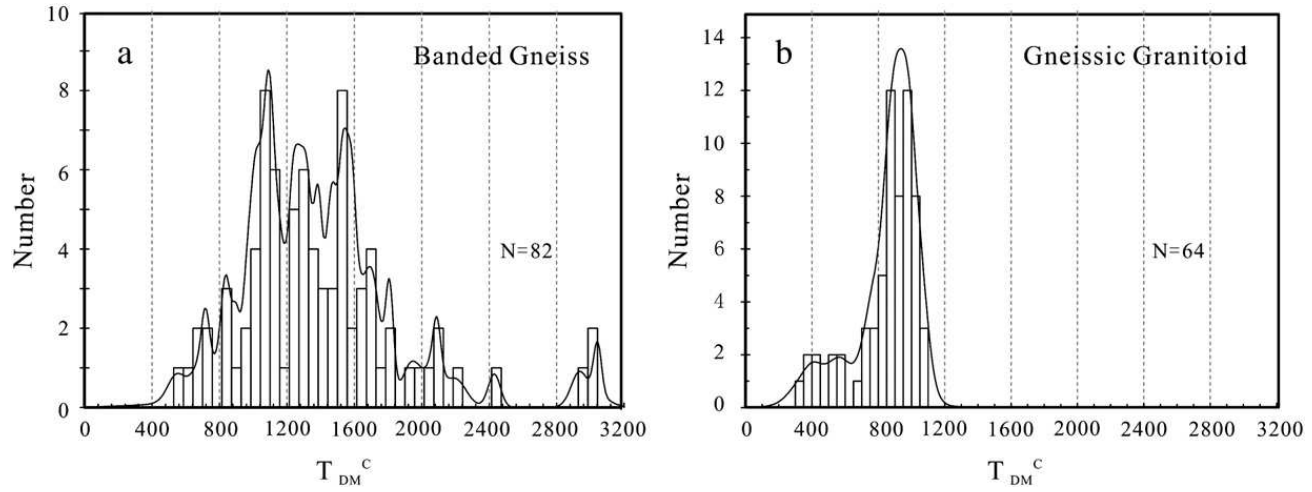


Fig. 13. Hf isotope model age ($T_{DM}^{C}$) histogram for zircons from the banded paragneisses and gneissic granitoids.

Chinese Altai during the same time period, e.g. 402–386 Ma (Wang et al., 1998), 380±1 Ma (Windley et al., 2002), 409±5 Ma (Tong et al., 2005) and 460-375 Ma (Wang et al., 2006).

### 7.4. Prolonged magmatic activity in the Chinese Altai and its tectonic significance

Our study demonstrates a prolonged period of magmatic activity, from the Neoproterozoic to early–middle Palaeozoic, throughout the Central Altai and Qiongkuer Domains. Neoproterozoic detrital zircons are relatively common in the banded paragneisses (Table 3 and Fig. 6), but their sources have not yet been identified although their Type-II and Type-I morphological features imply relatively short sedimentary transport and a nearby origin (Fig. 5). Early and middle Paleozoic magmatic activity is manifested by the dominant zircon populations of the banded paragneisses (466–528 Ma) (Fig. 6 and Table 3) and the associated gneissic granitoids (381–453 Ma) (Fig. 9 and Table 3).

Wang et al. (2006) recently dated six gneissic granite plutons in the Central Altai and Qiongkuer Domains and defined three phases of plutonic activity at ca. 460, 408, and 375 Ma. They concluded that the Altai orogen mainly developed in the early to middle Paleozoic and not in the late Paleozoic as previously proposed (e.g. He et al., 1990, 1994). Our data support this interpretation. Based on the apparent age gap between 460 and 408 Ma, Wang et al. (2006) proposed a model involving the opening and closure of a back-arc basin along the southern margin of the Central Altai Domain. If this model is correct, the Silurian-early Devonian volcanic and pyroclastic rocks of the Kangbutiebo Formation in the Qiongkuer Domain (Fig. 1) should have been formed in this back-arc basin. However, geochemical data suggest an arc setting for the Kangbutiebo Formation (e.g. Windley et al., 2002; Xiao et al., 2004). The four samples of gneissic granitoid dated in this study provided mean $^{206}Pb/^{238}U$ zircon ages of 453, 426, 412, and 381 Ma respectively. These data are in the same range as those reported by Wang et al. (2006) but disprove the assumed age gap in magmatic activity and instead show quasi continuous magmatic activity from the early to middle Palaeozoic in the Central Altai and Qiongkuer Domains. The Kangbutiebao volcanic rocks apparently represent just one eruptive member of the magmatic sequence in the middle Palaeozoic.

We propose the following tectonic scenario for the development of the Chinese Altai. In the early Palaeozoic (528–466 Ma), a magmatic arc was built on a Neoproterozoic continental margin which, in turn, may represent a Neoproterozoic arc system on a still older continental margin. Some zircons from the banded paragneiss have negative $\varepsilon Hf(t)$ values, implying the involvement of some older lower crust in the magma source (Fig. 7), but the dominant Mesoproterozoic zircon Hf model ages from the banded gneiss do not support an Archaean basement (Fig. 13). We emphasize that even if an old basement exists in the Chinese Altai, it is not represented by the banded gneisses studied here. These gneisses represent supracrustal material deposited in an early Palaeozoic active margin setting, and their protoliths may represent contemporaneous volcanic material mixed with components derived from pre-existing Neoproterozoic rocks.

The protoliths of the banded paragneiss were carried to depths of possibly 20 km or more (Wei et al., 2007), probably by subduction along the southern margin of the Qiongkuer Domain, and were intruded by the gneissic granitoids at 453–380 Ma during an on-going tectono-metamorphic process. This plutonic activity is characterized by magma derived predominantly from juvenile (i.e., mantle-derived) sources, as demonstrated by the positive $\varepsilon Hf(t)$ values and mean crustal residence ages younger than 1.0 Ga (Figs. 10 and 13).

### 7.5. Constraints on the tectonic evolution of the Chinese Altai

The evolutionary history of the Chinese Altai is controversial and currently debated. Its early tectonic setting has been envisaged as an island arc (Şengör and Natal'in, 1996), passive continental margin (He et al., 1990), or a Precambrian microcontinent (Li et al., 2006). The traditional opening-closure model proposed for the Altai inferred the existence of a Precambrian microcontinent in the Junggar or Junggar-Altai region (e.g. He et al., 1990, 1994; Huang et al., 1990; Xiao et al., 1990,1992; Yuan, 1995; Li et al., 1996; Liu et al., 1998; Li and Poliyangsiji, 2001). However, recent studies do not support the microcontinent model (e.g. Zhou, 1994; Han et al., 1997; Chen and Jahn, 2002; Wang et al., 2002; Hu and Wei, 2003; Yuan et al., 2006; Zheng et al., 2007; Long et al., 2007). Our date suggest that the banded paragneisses from the Central Altai and Qiongkuer Domains were formed on an active continental margin in the early Paleozoic, and thus do not represent an old continental fragment. Recent Pb isotopic data for magmatic and sedimentary rocks and ore deposits from this region also show predominantly juvenile characteristics (Chiaradia et al., 2006).

Although Neoproterozoic and sparse Paleoproterozoic–Archean detrital zircons are present in the banded

paragneisses, Precambrian rocks have not been identified in the Chinese Altai. The Neoproterozoic zircons mostly have Type-III or Type-I morphological features (Table 3 and Fig. 5), possibly suggesting a nearby source. These data suggest that nearby Neoproterozoic felsic pyroclastic or intrusive rocks were also a source for the protolith of the banded gneisses. We identified some zircons with discordant Paleoproterozoic to Archean $^{207}Pb/^{206}Pb$ ages (1890 to 2634 Ma, Table 3). Most of these have Type-II structural features (e.g., rounded cores), indicating long transport from a remote source. These old zircons may have been derived from a nearby continent or a continental sliver. In the Central Asian Orogenic Belt, Precambrian slivers are interpreted to have been rifted off the Siberia Craton (Berzin and Dobretsov, 1994; Şengör and Natal'in, 1996), or off Eastern Gondwana and drifted across the Paleo-Asian ocean (Zonenshain et al., 1990; Mossakovsky et al., 1993; Kheraskova et al., 2003). There are three major Precambrian cratons in the vicinity of the Chinese Altai, i.e. the Siberia Craton to the north, the North China Craton to the southeast, and the Tarim Craton to the south. Abundant U–Pb age data have been published for zircons from these three cratons. The main magmatic events at 2.9–2.7, 2.6–2.45 and 2.35–1.95 Ga and important metamorphic events have been identified at 2.6–2.4 Ga and 1.9–1.8 Ga for the North China Craton (e.g. Zhang et al., 1996; Zhao et al., 2000; Guan et al., 2002; Zhai and Liu, 2003; Kröner et al., 2005; Wilde and Zhao, 2005; Wan et al., 2006). This craton was tectonically stable from 1.65 to 0.16 Ga (Zhai and Liu, 2003). The Tarim Craton has a basement with ages of 2.6–2.3 Ga intruded by 1.94-Ga granitoids. Neoproterozoic volcanic rocks (700–800 Ma) on its margin have been interpreted to record rifting from Rodinia (e.g. Guo et al., 2003; Xu et al., 2005; Zhang et al., 2006; Hu and Wei, 2006; Lu et al., in press). Early magmatic events on the Siberian Craton are confined to two periods at ~3.4–2.6 Ga and 2.2–1.7 Ga (e.g. Bibikova et al., 1981; Kuzmin et al., 1995; Bruguier, 1996; Frost et al., 1998; Jahn et al., 1998; Ross and Villeneuve, 1998; Khudoley et al., 2001). Zircon ages indicate that the Siberian Craton was bordered, along its present southern margin, by a ~1.0 Ga ophiolite belt (Khain et al., 1997; 2002; Ritsk et al., 1999), and several island arcs, seamounts, accretionary wedges were formed and accreted to the margin of the Siberia Craton between *c*. 900 and 544 Ma (Gladkochub et al., 2006; Windley et al., 2007). The available data show age peaks at 880–860, ~800, 760–720, 700–630 and 536–464 Ma (Gladkochub et al., 2006 and references therein). The zircon age spectra of the banded paragneisses of this study are compatible with a model in which the Precambrian zircons were derived from (a sliver of?) the southern margin of the Siberian Craton. The occurrence of Ordovician ophiolites in the southern, but not northern margin, of the Chinese Altai may also favor this interpretation (Khain et al., 2003; Wang et al., 2003; Xiao et al., 2006). The Tuva–Mongolian block in Mongolia is a nearby microcontinent with a Paleoproterozoic–Archean basement (e.g. Bardarch and Tomurtogoo, 2001; Kuzmichev et al., 2001; Badarch et al., 2002). Paleomagnetic data suggest that this block was still adjacent to Siberia in the Vendian and early Cambrian (Kravchinsky et al., 2001). Early Paleozoic granitoids were emplaced on this block at 536–465 Ma (Salnikova et al., 2001), about the same time as the deposition of the protoliths of the paragneisses from the Chinese Altai (528–466 Ma, this study), possibly implying some genetic link.

## 8. Conclusions

Banded paragneisses from the Chinese Altai contain zircons with diverse chemical and Hf isotopic compositions [$\varepsilon Hf(t)$ from −17 to +15]. These zircons dominantly crystallized in the early Palaeozoic (466–528 Ma), some were formed in the Neoproterozoic, and Paleoproterozoic to Archean zircons are rare. The gneissic granitoids intruded the paragneisses at 380-450 Ma, and their zircons show a juvenile magma source ($\varepsilon Hf(t)$ from +2.3 to +17). Our data suggest that the Chinese Altai does not contain a Precambrian microcontinent, but the gneissic rocks constitute an early to middle Palaeozoic magmatic arc built on a Neoproterozoic continental margin. In the long accretionary history of this region, both juvenile/mantle material and old crust were involved in the early Palaeozoic magmatism, whereas juvenile/mantle material was the dominant ultimate source for the middle Palaeozoic magmatism.

## Acknowledgements

This study was supported by research grants from National Basic Research Program of China (2007CB411308), Hong Kong Research Grants Council (HKU7040/04P), NSFC (40421303, 40572043) German/Hong Kong Joint Research Scheme sponsored by RGC of Hong Kong and GAES of Germany (G-HK030/07), CAS/SAFEA International Partnership Program for Creative research Teams. We thank Liewen Xie, Yueheng Yang, Jean Wong, Yanhong He and Hongyan Geng for laboratory assistance.

## References


Badarch, G., Tomurtogoo, O., 2001. Tectonostratigraphic terranes of Mongolia. Gondwana Research 4, 143–144.

Badarch, G., Cunningham, W.D., Windley, B.F., 2002. A new terrane subdivision for Mongolia: implications for the Phanerozoic crustal growth of Central Asia. Journal of Asian Earth Science 21, 87–110.

Basu, M., 1996. Controls on the fractionation of isovalent trace elements in magmatic and aqueous systems: evidence from Y/Ho, Zr/Hf, and Lanthanide tetrad effect. Contribution to Mineralogy and Petrology 123, 323–333.

Berzin, N.A., Dobretsov, N.L., 1994. Geodynamic evolution of Southern Siberia in Late Precambrian–early Paleozoic time. In: Coleman, R.G. (Ed.), Reconstruction of the Paleo-Aian Ocean. Proceedings of the 29th International Geological Congress, Part B. VSP Utrecht, pp. 53–70.

BGMRX (Bureau of Geology and Mineral Resources of Xinjiang Uygur Autonomous Region), 1993. Regional Geology of Xinjiang Uygur Autonomous Region. People's Republic of China, Ministry of Geology and Mineral Resources. Geological Memoirs, Series 1, No. 32. Geological Publishing House, Beijing. 206 pp., (in Chinese).

Bibikova, E.V., Grachova, T.V., Makarov, V.A., Seslavinsky, K.B., 1981. The oldest metamorphic rocks of the north–east of the USSR (U–Pb method of dating). In: Krats, K.O., Kulish, E.A. (Eds.), Geology and Metallogeny of Precambrian of Far East. Nauka Press, Leningrad, pp. 46–55.

Black, L.P., Kamo, S.L., Williams, I.S., Mundil, R., Davis, D.W., Korsch, R.J., Foudoulis, C., 2003. The application of SHRIMP to Phanerozoic geochronology; a critical appraisal of four zircon standards. Chemical Geology 200, 171–188.

Blichert-Toft, J., Albarede, F., 1997. The Lu–Hf geochemistry of the chondrites and the evolution of the mantle–crust system. Earth and Planetary Science Letters 148, 243–258.

Bruguier, O., 1996. U–Pb ages on single detrital zircon grains from the Tasmiyele Group: implications for the evolution of the Olekma Block (Aldan Shield, Siberia). Precambrian Research 78, 197–210.

Chappell, B.W., White, A.J.R., 1992. I- and S-type granites in the Lachlan Fold Belt. Transaction of Royal Society of Edinburgh Earth Science 83, 1–26.

Chen, B., Jahn, B.M., 2002. Geochemical and isotopic studies of the sedimentary and granitic rocks of the Altai orogen of NW China and their tectonic implications. Geological Magazine 139, 1–13.

Chen, Y.C., Ye, Q.T., Wang, J.B., Rui, X.J., 2003. Geology of ore deposits, metallogenic regularity and technoenocomic evaluation on the Altay metallogenic belt, Xinjiang area, China. Geological Publishing House, Beijing, pp. 1–43 (in Chinese).

Chen, H.L., Yang, S.F., Li, Z.L., Yu, X., Xiao, W.J., Yuan, C., Lin, X.B., Li, J.L., 2006. Zircon SHRIMP U–Pb chronology of Fuyun basic granulite and its tectonic significance in Altaid orogenic belt. Acta Petrologica Sinica 22, 1351–1358.

Chiaradia, M., Konopelko, D., Seltmann, R., Cliff, R.A., 2006. Lead isotope variations across terrane boundaries of the Tien Shan and Chinese Altay. Mineralium Deposita 41, 411–428.

Cox, R., Lowe, D.R., Cullers, R.L., 1995. The influence of sediment recycling and basement composition on evolution of mudrock chemistry in the southwestern United States. Geochimica et Cosmochimica Acta 59, 2919–2940.

Didenko, A.N., Mossakovsky, A.A., Pechersky, D.M., Ruzhentsev, S.V., Samygin, S.G., Kheraskova, T.N., 1994. Geodynamics of the Paleozoic oceans of the Central Asia. Russian Geology and Geophysics 7–8, 59–76.

Fedo, C.M., Nesbitt, H.W., Young, G.M., 1995. Unraveling the eVects of potassium metasomatism in sedimentary rocks and paleosoils, with implications for paleoweathering conditions and provenance. Geology 23, 921–924.

Frost, B.R., Avchenko, O.V., Chamberlain, K.R., Frost, C.D., 1998. Evidence for extensive Proterozoic remobilization of the Aldan shield and implications for Proterozoic plate tectonic reconstructions of Siberia and Laurentia. Precambrian Research 89, 1–23.

Gladkochub, D.P., Wingate, M.T.D., Pisarevsky, S.A., Donskaya, T.V., Mazukabzov, A.M., Ponomarchuk, V.A., Stanevich, A.M., 2006. Mafic intrusions in southwestern Siberia and implications for a Neoproterozoic connection with Laurentia. Precambrian Research 147, 260–278.

Griffin, W.L., Pearson, N.J., Belousova, E., Jackson, S.E., O'Reilly, S.Y., van Achterberg, E., Shee, S.R., 2000. The Hf-isotope composition of cratonic mantle: LAM–MC–ICPMS analysis of zircon megacrysts in kimberlites. Geochimica et Cosmochimica Acta 64, 133–147.

Griffin, W.L., Belousova, E.A., Shee, S.R., Pearson, N.J., O'Reilly, S.Y., 2004. Archaean crustal evolution in the northern Yilgarn Craton: U–Pb and Hf isotope evidence from detrital zircons. Precambrian Research 131, 231–282.

Guan, H., Sun, M., Wilde, S.A., Zhou, X.H., Zhai, M.G., 2002. SHRIMP U–Pb zircon geochronology of the Fuping Complex: implications for formation and assembly of the North China craton. Precambrian Research 113, 1–18.

Guo, S.J., Zhang, Z.C., Liu, S.W., Li, H.M., 2003. U–Pb geochronological evidence for the early Precambrian complex of the Tarim Craton. NW China. Acta Petrologica Sinica 19, 537–542.

Han, B.F., Wang, S.G., Jahn, B.M., Hong, D.W., Kagami, H., Sun, Y.L., 1997. Depleted-mantle source for the Ulungur River A-type granites from North Xinjiang, China: geochemistry and Nd–Sr isotopic evidence, and implications for Phanerozoic crustal growth. Chemical Geology 138, 135–159.

Hanchar, J.M., Rundnick, R.L., 1995. Revealing hidden structures: the application of cathodoluminescene and back-scattered electron imaging to dating zircons from lower crustal xenoliths. Lithos 36, 289–303.

Harris, N.B.W., Pearce, J.A., Tindle, A.G., 1986. Geochemical characteristics of collision-zone magmatism. In: Coward, M.P., Reis, A.C. (Eds.), Collision tectonics. Geological Society Special Publication, 19, pp. 67–81.

He, G.Q., Han, B.F., Yue, Y.J., Wang, J.H., 1990. Tectonic division and crustal evolution of Altay orogenic belt in China. Xinjiang Geology 2, 9–20 (in Chinese).

He, G.Q., Li, M.S., Liu, D.Q., Zhou, N.H., 1994. Palaeozoic crust evolution and mieralization in Xinjiang of China. Xinjiang People's Publishing House, Urumqi. 437 pp., (in Chinese).

Hu, A.Q., Wei, G.J., 2003. A review of ages of basement rocks from Junggar basin in Xinjiang, China — based on studies of geochronology. Xinjiang Geology 21 (4), 389–406.

Hu, A.Q., Wei, G.J., 2006. On the age of the Neo-Archean Qingir gray gneisses from the northern Tarim basin, Xinjiang, China. Acta Geologica Sinica 80, 126–134.

Hu, A.Q., Jahn, B.M., Zhang, G., Chen, Y., Zhang, Q., 2000. Crustal evolution and Phanerozoic crustal growth in northern Xinjiang: Nd isotope evidence. 1. Isotopic characterization of basement rocks. Tectonophysica 328, 15–51.

Hu, A.Q., Zhang, G.X., Chen, Y.B., Zhang, Q.F., 2001. A model of division of the continental crust basement and the time scales of the major geological events in the Xinjiang: based on studies on of

isotopic geochronology and geochemistry. Xinjiang Geology 19, 12–19 (in Chinese).

Hu, A.Q., Zhang, G.X., Zhang, Q.F., Li, T.D., Zhang, J.B., 2002. A review on ages of Precambrian metamorphic rocks from Altai orogen in Xinjiang, NW China. Chinese Journal of Geology 37, 129–142 (in Chinese).

Hu, A.Q., Wei, G.J., Deng, W.F., Chen, L.L., 2006. SHRIMP zircon U–Pb dating and its significance for gneisses from the southwest area to Qinghe County in the Altai, China. Acta Petrologica Sinica 22, 1–10.

Huang, J.Q., Jiang, C.F., Wang, Z.X., 1990. On the opening–closing tectonics and accordion movement of plate in Xiangjiang and adjacent regions. Xinjiang Geology 1, 3–16 (in Chinese).

Iizuka, T., Hirata, T., 2005. Improvements of precision and accuracy in in-situ Hf isotope microanalysis of zircon using the laser ablation-MC–ICPMS technique. Chemical Geology 220, 121–137.

Irber, W., 1999. The lanthanide tetrad effect and its correlation with K/Rb, Eu/Eu*, Sr/Eu, Y/Ho, and Zr Hf of evolving peraluminous granite suites. Geochimica et Cosmochimica Acta 63 (3–4), 489–508.

Jahn, B.M., 2004. The Central Asian Orogenic Belt and growth of the continental crust in the Phanerozoic. In: Malpas, J., Fletcher, C.J.N., Ali, J.R., Aitchison, J.C. (Eds.), Aspects of the Tectonic Evolution of China. Geological Society Special Publications, vol. 226, pp. 73–100. London.

Jahn, B.M., Gruau, G., Capdevila, R., Cornichet, J., Nemchin, A., Pidgeon, R., Rudnik, V.A., 1998. Archean crustal evolution of the Aldan Shield, Siberia: geochemical and isotopic constraints. Precambrian Research 91, 333–363.

Jahn, B.M., Wu, F.Y., Chen, B., 2000a. Massive granitoid generation in Central Asia: Nd isotope evidence and implication for continental growth in the Phanerozoic. Episodes 23, 82–92.

Jahn, B.M., Wu, F., Chen, B., 2000b. Granitoids of the Central Asian orogenic belt and continental growth in the Phanerozoic. Transaction of Royal Society of Edinburgh Earth Science 91, 181–193.

Jahn, B.M., Wu, F.Y., Capdevila, R., Martineau, F., Zhao, Z.H., Wang, Y.X., 2001. Highly evolved juvenile granites with tetrad REE patterns: the Woduhe and Baerzhe granites from the Great Xing'an Mountains in NE China. Lithos 59, 171–198.

Khain, V.E., Gusev, G.S., Khain, E.V., Vernikovsky, V.A., Volobuyev, M.L., 1997. Circum-Siberian Neoproterozoic ophioloite belt. Ofioliti 22, 195–200.

Khain, E.V., Bibokova, E.V., Kroner, A., Zhuravlev, D.Z., Sklyarov, E.V., Fedotova, A.A., Kravchenko-Berezhnoy, I.R., 2002. The most ancient ophiolites of the Central Asian fold belt: U–Pb and Pb–Pb zircon ages for the Dunzhugur complex, Eastern Sayan, Siberia, and geodynamic implications. Earth and Planetary Science Letters 199, 311–325.

Khain, E.V., Bibikova, E.V., Salnikova, E.B., Kröner, A., Gibsher, A.S., Didenko, A.N., Degtyarev, K.E., Fedotova, A.A., 2003. The Palaeo-Asian ocean in the Neoproterozoic and early Palaeozoic: new geochronologic data and palaeotectonic reconstructions. Precambrian Research 122, 329–358.

Kheraskova, T.N., Didenko, A.N., Bush, V.A., Volozh, Y.A., 2003. The Vendian–Early Paleozoic history of the continental margin of eastern Paleogondwana, Paleoasian ocean, and Central Asian foldbelt. Russian Journal of Earth Sciences 5, 165–184.

Khudoley, A.K., Rainbird, R.H., Stern, R.A., Kropachev, A.P., Heaman, L.M., Zanin, A.M., Podkovyrov, V.N., Belova, V.N., Sukhorukov, V.I., 2001. Sedimentary evolution of the Riphean–Vendian basin of southeastern Siberia. Precambrian Research 111, 129–163.

Kravchinsky, V.A., Konstantinov, K.M., Cogne, J.P., 2001. Palaeomagneitc study of Vendian and Early Cambrian rocks of South Sibria and Central Mogolia: was the Siberian platform assembled at this time? Precambrian Research 110, 61–92.

Kröner, A., Wilde, S.A., Li, J.H., Wang, K.Y., 2005. Age and evolution of a late Archean to Paleoproterozoic upper to lower crustal section in the Wutaishan–Hengshan–Fuping terrain of northern China. Journal of Asian Earth Science 24, 577–595.

Kröner, A., Windley, B.F., Badach, G., in press. Accretionary growth and crust-formation in the Central Asian Orogenic Belt and comparison with the Arabian-Nubian shield. Geological Society of America, Memoirs. in press.

Kuzmichev, A.B., Bibikova, E.V., Zhuravlev, D.Z., 2001. Neoproterozoic (800 Ma) orogeny in the Tuva–Mongolian Massif (Siberia): island arc-continent collision at the northeast Rodinia margin. Precambrian Research 110, 109–126.

Kuzmin, V.V., Chukhonin, A.P., Shulezhko, I.K., 1995. Stages of metamorphic evolution of rocks of crystalline basement of the Kukhtui Uplift (Okhotsk Massif). Doklady Russian Academy of Science 142, 789–791.

Li, T.D., Poliyangsiji, B.H., 2001. Tectonics and crustal evolution of Altai in China and Kazakhstan. Xinjiang Geology 19, 27–32 (in Chinese).

Li, T.D., Qi, Z.M., Xiao, S.L., Wu, B.Q., 1996. New improvement of comparative study of geology and mineralization of Altai between China and Kazakhstan. Chinese Geological Society. Thesis Volume of the Symposium of the 8th Five Yea Plan of Geoscience for Contribution to 30th IGC. Metallurgical Industrial Publishing House, Beijing, pp. 256–259 (in Chinese).

Li, J., Xiao, W., Wang, K., Sun, G., Gao, L., 2003. Tectonic and metallogenic evolution of the Altay Shan, Northern Xinjiang Uygur Autonomous Region, Northwestern China. Tectonic evolution and metallogeny of the Chinese Altay and Tianshan, (Mao et al. ed.). CERCAMS, Beijing, pp. 31–74.

Li, H.J., He, G.Q., Wu, T.R., Wu, B., 2006. Confirmation of Altai-Mongolia microcontinent and its implications. Acta Petrologica Sinica 22, 1369–1379.

Liu, D.Q., Tang, Y.L., Zhou, R.H., 1998. On basic continental crust of the pre-Sinian of Xinjiang. Xinjiang Geology 16, 195–202 in Chinese with English abstract.

Long, X.P., Sun, M., Yuan, C., Xiao, W.J., Wu, F.Y., Xia, X.P., Cai, K.D., 2006. The Early Paleozoic Sedimentary environment and tectonic evolution in the Chinese Altai: evidence from U–Pb ages and Hf isotopic composition of detrital zircons. 2006 National Petrology and Geodynamics Meeting. Abstract, pp. 232–233 (in Chinese).

Long, X.P., Sun, M., Yuan, C., Xiao, W.J., Lin, S.F., Wu, F.Y., Xia, X.P., Cai, K.D., 2007. U–Pb and Hf isotopic study of zircons from metasedimentary rocks in the Chinese Altai: implications for Early Paleozoic tectonic evolution. Tectonics 26, TC5015. doi:10.1029/2007TC002128.

Long, X.P., Sun, M., Yuan, C., Xiao,W.J., Cai, K.D., Zhao, Y.J., in press. Early Paleozoic sedimentary record of the Chinese Altai: implications for the tectonic evolution of the Altai orogen. Sedimentary Geology in revision.

Lu, S., Li, H., Zhang, C., Niu, G., in press. Geological and geochronology evidence for Precambrian evolution in the Tarim Platform and surroundings. Precambrian Research, in press.

Ludwig, K.R., 2003. User's Manual for Isoplot 3.00. A Geochronological Toolkit for Microsoft Excel. Berkeley Geochronology Center, Berkeley, CA. Special Publication No. 4a.

Martin, H., 1986. Effect of steeper Archean geothermal gradient on geochemistry of subduction-zone magmas. Geology 14, 753–756.

McLennan, S.M., Taylor, S.R., 1980. Th and U in sedimentary rocks: crustal evolution and sedimentary recycling. Nature 285, 621–624.

Monecke, T., Kempf, U., Monecke, J., Sala, M., Wolf, D., 2002. Tetrad effect in rare earth element distribution patterns: a method of quantification with application to rock and mineral samples from granite-related rare metal deposits. Geochimica et Cosmochimica Acta 66, 1185–1196.

Mossakovsky, A.A., Ruzhentsev, S.V., Samygin, S.G., Kheraskova, T.N., 1993. Central Asian fold belt: geodynamic evolution and history of formation. Geotektonika 6, 3–33 (in Russia).

Nesbitt, H.W., Young, G.M., 1982. Early Proterozoic climates and plate motions inferred from major element chemistry of lutites. Nature 199, 715–717.

Nesbitt, H.W., Young, G.M., 1984. Prediction of some weathering trends of plutonic and volcanic rocks based on thermodynamics and kinetic considerations. Geochimica et Cosmochimica Acta 48, 1523–1534.

Norrish, K., Hutton, J.T., 1969. An accurate X-ray spectrographic method for the analysis of a wide range of geological samples. Geochim. Cosmochim. Acta, 33, 431–453.

Pearce, J.A., Harris, N.B.W., Tindle, A.G., 1984. Trace element discrimination diagrams for the tectonic interpretation of granitic rocks. Journal of Petrology 25, 956–983.

Qi, L., Gregoire, D.C., 2000. Determination of trace elements in 26 Chinese Geochemistry Reference Materials by inductively coupled plasma-mass spectrometry. Geostandard Newsletters 24, 51–63.

Ritsk, E.Y., Amelin, Y.V., Krymski, R.S., Shalaev, V.S., Rizvanova, N.G., 1999. On the age of the Nyurundyukan sequence (Kichera zone, Baikal–Muya fold belt): new U–Pb and Sm–Nd isotopic data. In: Kozakov, I.K. (Ed.), Geologic evolution of Proterozoic marginal Palaeo-oceanic structures of Northern Euraia. Tema, St. Petersburg, pp. 130–132 (in Russia).

Ross, G.M., Villeneuve, M.E., 1998. Provenance of the Belt Purcell Supergroup, southern British Columbia: a SHRIMP study of detrital zircons. In: Cook, F.A., Erdmer, P. (Eds.), Slave-Northern Cordillera lithoprobe evolution (SNORCLE) and Cordilleran Tectonics Workshop Meeting Lithoprobe Report 64, pp. 186–191.

Rudnick, R.L., Gao, S., 2004. Composition of the continental crust. In: The crust (Rudnick, R.L. ed.) Vol. 3 Treatise on Geochemistry (R.L., Holland, H.D., and Turekian, K.K. eds.), Elsevier- Pergamon, Oxford, 1−64.

Salnikova, E.B., Kozakov, I.K., Kotov, A.B., Kröner, A., Todt, W., Bibikova, E.V., Nutman, A., Yakovleva, S.Z., Kovach, V.P., 2001. Age of Palaeozoic granites and metamorphism in the Tuvino–Mongolian Massif of the Central Asian Mobile Belt: loss of a Precambrian microcontinent. Precambrian Research 110, 143–164.

Scherer, E., Munker, C., Mezger, K., 2001. Calibration of the Lutetium–Hafnium clock. Science 293, 683–687.

Sengör, A.M.C., Natal'in, B.A., 1996. Paleotectonics of Asia: fragments of a synthesis. In: Yin, A., Harrison, M. (Eds.), The tectonic evolution of Asia. Cambridge University Press, Cambridge, pp. 486–640.

Sengör, A.M.C., Natal'in, B.A., Burtman, V.S., 1993. Evolution of the Altaid tectonic collage and Paleozoic crustal growth in Asia. Nature 364, 299–307.

Sengör, A.M.C., Natal'in, B.A., Burtman, V.S., 2004. Phanerozoic analogues of Archean oceanic basement fragments: altaid ophiolites and ophirags. In: Kusky, T.M. (Ed.), Precambrian ophiolites and Related Rocks. Elsevier, Amsterdam, pp. 675–726.

Shan, Q., Niu, H.C., Yu, X.Y., Zhang, H.X., 2005. Geochemistry and zircon U–Pb age of volcanic rocks from the Hanasi basin in the northern Xinjiang and their tectonic significance. Geochimica 34, 315–327 (in Chinese).

Shaw, D.M., 1972. The origin of the Apsby gneiss, Ontario. Canadian Journal of Earth Sciences 9, 18–35.

Sun, S.S., McDonough, W.F., 1989. Chemical and isotopic systematics of oceanic basalts: implications for mantle composition and processes. In: Saunders, A.D., Norry, M.J. (Eds.), Magmatism in the Ocean Basins, vol. 42. Geological Society of London, Special Publication, pp. 315–345.

Tong, Y., Wang, T., Hong, D.W., 2005. Zircon U–Pb age of Tielike pluton in the western Altay orogen and its implications. Acta Geoscientia Sinica 26, 74–77 (in Chinese with English abstract).

Wan, Y.S., Wilde, S.A., Liu, D.Y., Yang, C.X., Song, B., Yin, X.Y., 2006. Further evidence for ~1.85 Ga metamorphism in the Central Zone of the North China Craton: SHRIMP U–Pb dating of zircon from metamorphic rocks in the Lushan area, Henan Province. Gondwana Research 9, 189–197.

Wang, Z.G., Zhao, Z.H., Zou, T.R., 1998. Geochemistry of the granitoids in Altay. Science Press, Beijing. 152 pp., (in Chinese with English abstract).

Wang, F.Z., Yang, M.Z., Zheng, J.P., 2002. Geochemical evidence of the basement assembled by island arc volcanic terranes in Junggar basin. Acta Petrologica et Mineralogica 21 (1), 1–10.

Wang, Z.S., Sun, J., Li, Q., Hou, K., Qin, W., Xiao, Hao, J., 2003. Paleozoic tectonic evolution of the northern Xinjiang, China: geochemical and geochronological constraints from the ophiolites. Tectonics 22, 1014.

Wang, T., Hong, D.W., Jahn, B.M., Tong, Y., Wang, Y.B., Han, B.F., Wang, X.X., 2006. Timing, petrogenesis, and setting of Paleozoic synorogenic intrusions from the Altai Mountains, Northwest China: implications for the tectonic evolution of an accretionary orogen. Journal of Geology 114, 735–751.

Wei, C., Clarke, G., Tian, W., Qiu, L., 2007. Transition of metamorphic series from the Kyanite-to andalusite-types in the Altai orogen, Xinjiang, China: evidence from petrography and calculated KMnFMASH and KFMASH phase relations. Lithos 96 (3–4), 353–374.

Wilde, S.A., Zhao, G.C., 2005. Archean to Paleoproterozoic evolution of the North China Craton. Journal of Asian Earth Sciences 24, 519–522.

Windley, B.F., Kröner, A., Guo, J., Qu, G., Li, Y., Zhang, C., 2002. Neoproterozoic to Paleozoic geology of the Altai orogen, NW China: new zircon age data and tectonic evolution. Journal of Geology 110, 719–739.

Windley, B.F., Alexeiev, D., Xiao, W., Kroner, A., Badarch, G., 2007. Tectonic models for accretion of the Central Asian Orogenic Belt. Journal of Geological Society London 164, 31–47.

Woodhead, J., Hergt, J., Shelley, M., Eggins, S., Kemp, R., 2004. Zircon Hf-isotope analysis with an excimer laser, depth profiling, ablation of complex geometries, and concomitant age estimation. Chemical Geology 209, 121–135.

Wu, F.Y., Sun, D.Y., Jahn, B.M., Wilde, S., 2004. A Jurassic garnet-bearing granitic pluton from NE China showing tetrad REE patterns. Journal of Asian Earth Sciences 23, 731–744.

Wu, F.Y., Yang, Y.H., Xie, L.W., Yang, J.H., Xu, P., 2006. Hf isotopic compositions of the standard zircons and baddeleyites used in U–Pb geochronology. Chemical Geology 234, 105–126.

Xia, X.P., Sun, M., Zhao, G.C., Li, H.M., Zhou, M.F., 2004. Spot zircon U–Pb isotope analysis by ICP–MS coupled with a frequency quintupled (213 nm) Nd–YAG laser system. Geochemical Journal 38, 191–200.

Xiao, X.C., Tang, Y.Q., Li, J.Y., Zhao, M., Feng, Y.M., Zhu, B.Q., 1990. On the tectonic evolution of the northern Xinjiang, Northwest China. Xinjiang Geology 1, 47–68 (in Chinese).

Xiao, X.C., Tang, Y.Q., Feng, Y.M., Zhu, B.Q., Li, J.Y., Zhao, M., 1992. Tectonics in northern Xinjiang and its neighbouring areas. Geological Publishing, Beijing, pp. 104–121 (in Chinese).

Xiao, W.J., Windley, B.F., Badararch, G., Sun, S., Li, J., Qin, K., Wang, Z., 2004. Paleozoic accretionary and convergent tectonics of the southern Altaids: implications for the growth of central Asia. Journal of Geological Society London 161, 1–4.

Xiao, W.J., Windley, B.F., Yan, Q.R., Qin, K.Z., Chen, H.L., Yuan, C., Sun, M., Li, J.L., 2006. SHRIMP Zircon Age of the Aermantai Ophiolite in the North Xinjiang Area, China and its tectonic implications. Acta Geologica Sinica 80 (1), 32–37.

Xu, B., Jian, P., Zheng, H.F., Zou, H.B., Zhang, L.F., Liu, D.Y., 2005. U–Pb zircon geochronology and creochemistry of Neoproterozoic volcanic rocks in the Tarim Block of northwest China: implications for the breakup of Rodinia supercontinent and Neoproterozoic glaciations. Precambrian Research 136, 107–123.

Yuan, X.C., 1995. Remark on structure of China continental basement. Acta Geophysica Sinica 38, 448–459 (in Chinese with English abstract).

Yuan, C., Xiao, W.J., Chen, H.L., Li, J.L., Sun, M., 2006. Zhaheba Potassic Basalt, Eastern Junggar (NW China): geochemical characteristics and tectonic implications. Acta Geologica Sinica 80, 254–263 (in Chinese).

Zhai, M.G., Liu, W.J., 2003. Palaeoproterozoic tectonic history of the North China craton: a review. Precambrian Research 122, 183–199.

Zhang, Z.Q., Shen, Q.H., Geng, Y.S., Tang, S.H., Wang, J.H., 1996. Geochemistry and ages of Archean metamorphic rocks in northwestern Hebei Province, China, and formation time of the paleocrust in the region. Acta Petrologica Sinica 12, 315–328.

Zhang, C.L., Li, Z.X., Li, X.H., Ye, H.M., Wang, A.G., Guo, K.Y., 2006. Neoproterozoic bimodal intrusive complex in the southwestern Tarim Block, Northwest China: age, geochemistry, and implications for the rifting of Rodinia. International Geology Review 48, 112–128.

Zhao, G.C., Cawood, P.A., Wilde, S.A., Sun, M., Lu, L., 2000. Metamorphism of basement rocks in the Central Zone of the North China craton: implications for Palaeoproterozoic tectonic evolution. Precambrian Research 103, 55–88.

Zheng, J., Sun, M., Zhao, G., Robinson, P.T., Wang, F., 2007. Elemental and Sr–Nd–Pb isotopic geochemistry of Late Paleozoic volcanic rocks beneath the Junggar basin, NW China: Implications for the formation and evolution of the basin basement. Journal of Asian Earth Sciences 9, 778–794.

Zhou, Y.Q., 1994. Discussion on the basement property of Junggar basin. Xinjiang Geology 5, 19–27 (in Chinese).

Zonenshain, L.P., Kuzmin, M.I., Natapov, L.M., 1990. Geology of the USSR: a plate tectonic synthesis. American Geophysical Union. Geodynamics Series monograph 21, 242 pp.